



Université de Sherbrooke

**DNA damage in TpT induced by very low energy electrons**

Par

Ghazal Khorsandgolchin

Department of Nuclear Medicine and Radiobiology

Mémoire présenté à la Faculté de médecine et des sciences de la santé  
en vue de l'obtention du grade de maître ès sciences (M. Sc.)  
en Sciences des radiations et imagerie biomédicales

Sherbrooke, Québec, Canada

June, 2019

Membres du jury d'évaluation

**J.Richard Wagner**, Co-director, Department of Nuclear Medicine and Radiobiology,  
Faculty of Medicine and health Sciences, Université de Sherbrooke

**Léon Sanche**, Co-director, Department of Nuclear Medicine and Radiobiology, Faculty  
of Medicine and health Sciences, Université de Sherbrooke

**Benoit Paquette**, internal evaluator of program, Department of Nuclear Medicine and  
Radiobiology, Faculty of Medicine and health Sciences, Université de Sherbrooke

**Yi Zheng**, external evaluator of program, Research Institute of Photocatalysis, State Key  
Laboratory of Photocatalysis on Energy and Environment, Fuzhou University

©Ghazal Khorsandgolchin, 2019



# RÉSUMÉ

## DNA damage in TpT induced by very low energy electrons

Par

Ghazal Khorsandgolchin

Department of Nuclear Medicine and Radiobiology

Mémoire présenté à la Faculté de médecine et des sciences de la santé en vue de l'obtention du grade de maître ès sciences (M. Sc.) en Sciences des radiations et imagerie biomédecinales, Faculté de médecine et des sciences de la santé, Université de Sherbrooke, Sherbrooke, Québec, Canada, J1H 5N4

Nous nous concentrons sur les dommages de l'ADN induits par les électrons de très basse énergie (VLEE  $\sim 1.8$  eV) en utilisant des méthodes d'irradiation à l'état solide et l'analyse LC-MS / MS des produits de dégradation. Trois principaux types de dommages sont produits lors de l'irradiation du TpT avec des VLEE : 1) clivage de la liaison C-O (similaire à une rupture de brin) ; 2) libération de thymine non modifiée ; et 3) réduction de la thymine en 5,6-dihydrothymine. La formation de chaque type de produit est linéaire en fonction de la dose et les rendements sont à peu près égaux, tel que déduit par les analyses LC-MS / MS. Le clivage de la liaison C-O peut se produire dans le TpT au niveau des terminaisons phosphodiester des extrémités 3' ou 5'. Lorsque la réaction se produit en position 3', les fragments sont la thymidine 5'-monophosphate et la 3', 2'- didésoxythymidine. Lorsque la réaction se produit en position 5', les fragments sont la thymidine 3'-monophosphate et la 5', 2'-didésoxythymidine. Il est intéressant de constater que le rendement en thymidine monophosphate est supérieur à celui du fragment didésoxythymidine correspondant, suggérant que d'autres réactions contribuent au clivage de la liaison phosphodiester. Sur la base du rendement des produits, le clivage C-O aux extrémités 3' est deux fois plus efficace que celui aux extrémités 5'. En ce qui concerne les autres types de dommages, la libération de thymine non modifiée peut s'expliquer soit par le clivage de la liaison N-glycosidique induite par le attachement dissociatif (DEA), soit par la formation de radicaux centrés sur le fragment 2-désoxyribose. Nous n'avons pas observé de rendements équivalents de sites abasiques (TpT sans résidu T) suggérant que le clivage N-glycosidique induit par DEA est indirect ou donne une chimie compliquée à l'état solide. Enfin, nous avons observé une quantité relativement importante de TpT contenant de la 5,6- dihydrothymine : le produit de réduction de la thymine. Cette réaction implique probablement l'addition de l'électron sur la double liaison 5,6 de la thymine. En variante, les atomes d'hydrogène générés par DEA au niveau d'autres sites de la molécule peuvent ensuite réagir avec la thymine pour produire la 5,6-dihydrothymine. En résumé, nous montrons que les électrons à très basse énergie (1.8 eV) induisent des dommages aux composés simples, constituants de l'ADN,

par des processus initiés par DEA.

Mots-clés: Analyse de produits, études mécanistiques, électrons, ADN, faible énergie

# SUMMARY

## **DNA damage in TpT induced by very low energy electrons**

By

Ghazal Khorsandgolchin

Program: Radiation sciences and biomedical imaging

Thesis presented at the Faculty of Medicine and Health Sciences for the obtention of Master degree diploma in Radiation sciences and biomedical imaging, Faculty of Medicine and Health Sciences, Université de Sherbrooke, Sherbrooke, Québec, Canada, J1H 5N4

We focus on DNA damage induced by very low energy electrons (VLEEs  $\sim 1.8$  eV) using solid-state irradiation methods and LC-MS/MS analysis of the degradation products. Three major types of damage are produced upon irradiation of TpT with vLEEs: 1) C-O bond cleavage (similar to a strand break); 2) release of non-modified thymine; and 3) reduction of thymine to 5,6-dihydrothymine. The formation of each type of product was linear as a function of dose and the yields were about equal as inferred by LC-MS/MS analyses. C-O bond cleavage can occur in TpT at either the 3' or 5' phosphodiester termini. When the reaction occurs at the 3' position, the fragments are thymidine 5'-monophosphate and 3',2'-dideoxythymidine. When the reaction occurs at the 5' position, the fragments are thymidine 3'-monophosphate and 5',2'-dideoxythymidine. Interestingly, the yield of thymidine monophosphate was higher than that of the corresponding dideoxythymidine fragment, suggesting other reactions contribute to phosphodiester bond cleavage. Based on the yield of products, C-O cleavage at 3' termini was two fold more efficient than that at 5' termini. As for the other types of damage, the release of non-modified thymine may be explained by either DEA-induced N-glycosidic bond cleavage or formation of C-centered radicals at the 2-deoxyribose moiety. We did not observe equivalent yields of abasic sites (TpT without a T residue) suggesting that DEA mediated N-glycosidic cleavage is indirect or gives complicated chemistry in the solid state. Lastly, we observed a relatively large amount of TpT containing 5,6-dihydrothymine: the reduction product of thymine. This reaction likely involves addition of the electron onto the 5,6-double bond of thymine. Alternatively, hydrogen atoms generated by DEA at other sites of the molecule may subsequently react with thymine to produce 5,6-dihydrothymine. In summary, we show that vLEEs induce damage to DNA model compounds by DEA-mediated processes.

Keywords: ionizing radiation, DNA damage, mass spectrometry, secondary electrons

## TABLE DES MATIÈRES

<b>Résumé</b>	<b>iii</b>
<b>Summary</b>	<b>v</b>
<b>Table des matières</b>	<b>vi</b>
<b>Liste des figures</b>	<b>viii</b>
<b>Liste des tableaux</b>	<b>xi</b>
<b>1 Introduction</b>	<b>1</b>
1.1 Is radiation necessary for life? . . . . .	1
1.2 Caution radiation area! . . . . .	1
1.3 Radiation exposure and health effects . . . . .	2
1.4 How cancer develops in the human body . . . . .	5
1.4.1 Types of DNA damage . . . . .	7
1.5 Why study low-energy electron-induced reactions . . . . .	7
1.6 Principles of the interaction of LEEs with molecules . . . . .	8
1.7 DNA damage induced by ionizing radiation . . . . .	10
1.7.1 Report of prior results by our group . . . . .	12
1.8 Our laboratory methods and LEE irradiator system . . . . .	14
1.8.1 Spin Coating System . . . . .	14
1.8.2 Apparatus for low energy electron production . . . . .	15
1.8.3 DNA damage detection by LC-MS/MS technique . . . . .	16
1.9 The brief explanation of the research project (Objective) . . . . .	18
<b>2 Article</b>	<b>19</b>
2.1 Résumé . . . . .	20
2.2 Abstract . . . . .	21
2.3 Introduction . . . . .	22
2.4 Methods and Materials . . . . .	24
2.5 Results and Discussion . . . . .	25
2.5.1 Analysis of products from vLEE-induced modification of TpT . .	25
2.5.2 DEA-mediated C-O bond cleavage of TpT . . . . .	27
2.5.3 DEA-mediated C-N bond cleavage of TpT . . . . .	31
2.5.4 Reduction of thymine to 5,6-dihydrothymine by vLEE . . . . .	33
2.6 Conclusions . . . . .	34
2.7 Acknowledgements . . . . .	34
2.8 Supplementary materials . . . . .	34

<b>3</b>	<b>Discussion</b>	<b>48</b>
3.1	Fragments and mechanisms induced by vLEE . . . . .	48
3.1.1	First part: N-glycosidic bond cleavage . . . . .	48
3.1.2	First part: Phosphodiester bond cleavage (at 3' C-O bond and 5' C-O bond) . . . . .	49
3.1.3	First part: Base damage (Conversion of thymine to 5,6-dihydrothymine moeity) . . . . .	51
3.1.4	Second part: Damage induced on monomers by vLEE . . . . .	52
3.1.5	Comparison of our findings to previous studies . . . . .	54
<b>4</b>	<b>Conclusions and Perspectives</b>	<b>57</b>
<b>5</b>	<b>Acknowledgment</b>	<b>59</b>



## LISTE DES FIGURES

1.1	Electromagnetic spectrum separating non-ionizing and ionizing radiation.	2
1.2	Direct and indirect action of radiation in biological systems . . . . .	3
1.3	Time scale of radiolysis of water (Alizadeh et Sanche, 2012) . . . . .	5
1.4	DNA forms a double stranded helix, and adenine pairs with thymine and cytosine pairs with guanine. . . . .	6
1.5	(a) Schematic energy distribution of secondary electrons generated during a primary ionizing event which means the energy distribution of the secondary electrons demonstrate that the majority of these electrons have energies below 10 eV. (b) cross section for electron-induced dissociation for a typical molecule; (c) dissociation yield as a function of electron energy for a typical molecule. . . . .	10
1.6	(reprinted from Kumar et Sevilla (2012)). Schematic diagram showing the electronic configuration of a neutral (a) and transient negative ion (TNI) (b, c). The interacting electron initially captures into the unoccupied MOs of the neutral molecule resulting in TNI formation via: (a) shape resonance or (c) core-excited resonance. . . . .	11
1.7	Effective cross sections ( $\sigma$ ) for the formation of SSB in plasmid DNA by 0.1– 4.7 eV electrons. The shaded portion corresponds to shape resonances at 1 eV and around 2.5 eV.(Reprinted from Panajotovic <i>et al.</i> (2006)).	12
1.8	Schematic diagram of the spin-coating system. I—vacuum chamber, J—tube holder, K— sample substrate, L1 and L2—ball-bearing shafts, M—magnetic coupling, N—electric motor, O—Teflon space. . . . .	14
1.9	I. The schematic diagram of the experimental setup for irradiating DNA. (A) electron gun, (B) linear drive, (C) rotatable disk used as cylinder support, (D) electron current detector, (E) cylindrical sample substrate, (F) quick access port, (G) glove box sealed under a N <sub>2</sub> atmosphere, (H) Tantalum Plate. IIa. Illustration of electron trajectories. IIb. Multi-detector. . .	15
1.10	Schematic design of LC-MS. This diagram demonstrates the technique that combines the physical separation capabilities of liquid chromatography (HPLC) with the mass analysis capabilities of the mass spectrometer.	17
1.11	Schematic of the multiple reaction monitoring (MRM) scanning technique on a triple quadrupole mass spectrometer. The targeted parent ion (shown in yellow) is selected in the first quadrupole (Q1) and enters the second quadrupole (Q2) where it undergoes collision induced dissociation (CID). The resulting “product ions” are mass analyzed using the third quadrupole (Q3) . . . . .	18

2.1	Structures of compounds under study. vLEEs irradiation of the parent compound (TpT) gave 2',3'-dideoxythymidine (ddT3'), thymidine 5'-monophosphate (TMP5'), 2',5'-dideoxy-thymidine (ddT5') thymidine 3' monophosphate (TMP3'), thymine (Thy) and 5,6-dihydro-2'-deoxythymidine (5,6-dhT). . . . .	26
2.2	LC-MS/MS analysis of products from C3'-O and C5'-O cleavage of TpT. The formation of ddT3' and ddT5' increased considerably from non-irradiated controls (a) to irradiated samples (c). Likewise, the formation of TMP5' and TMP3' increased upon irradiation with vLEEs (chromatograms b and d). . . . .	27
2.3	LC-MS/MS analysis of products from C1'-N1 cleavage and base reduction from TpT. The formation of thymine increased when comparing non-irradiated control to irradiated samples (chromatograms a and c) as indicated by the ratio of isotopically internal standard (red line) and natural product present in the sample (blue line). Likewise, the formation of TMP5' and TMP3' increased upon irradiation with vLEEs (chromatograms b and d). . . . .	28
2.4	Formation of major products as a function of electron fluence. Error bars show the standard deviation from five independent experiments. Data were fitted by linear regression analysis (red line). Regression coefficient ( $r^2$ ) was greater than 0.99 except for Thy ( $r^2=0.92$ ). Percent error in standard derivation of the slope was 5.1% for TMP5', 3.6% for ddT3', 4.0% for TMP3', 4.7% for ddT5', 2.0% for ddT5', and 13% for Thy. All slopes were statistically significant ( $P < 0.001$ ). . . . .	29
2.1	Proposed mechanism for the formation of C3'-O and C5'-O cleavage products. . . . .	30
2.2	Proposed mechanism for the release of non-altered thymine. . . . .	31
S1	Diagram depicting the irradiation of target molecules. A system used in numerous experiments for electrons with energies between 4-20 eV (Zheng <i>et al.</i> , 2004b) was modified for electrons with lower energies (1.8 eV) by placing an electrode at the exit of the cylinder to reflect vLEEs back toward the surface. Red lines emanating from the electron gun (top center) show the simulated trajectory of vLEEs. A multi-detector (shown on the right) was inserted in place of the cylinder to adjust the electron flux so that electrons were evenly distributed along the inside surface of the cylinder. . . . .	35
S2	Calibration curve for labeled ( $m/z + 4$ ) and non-labeled thymine. Linear regression of the data gave $y = 35.9 - 4.1$ ( $r^2 > 0.99$ ) for labeled Thymine (Thy) and $y = 25.4x - 2.0$ ( $r^2 > 0.99$ ) for non- labeled Thymine (Thy). . .	37
S3	Calibration of isotopic standard for the quantification of thymine. Linear regression gave: $y = 0.83x + 1.05$ ( $r^2 > 0.99$ ). . . . .	38
S4	Calibration curve for ddT5' and ddT3'. Linear regression of the data gave $y = 14.1x - 1.7$ ( $r^2 > 0.99$ ) for ddT5' and $10.6x - 1.2$ ( $r^2 > 0.99$ ) for ddT3'. . .	38
S5	Calibration curve for 5,6-dhT. Linear regression of the data gave $y = 1.33x - 0.06$ ( $r^2 > 0.99$ ). . . . .	39

S6	Calibration curve for TMP3' and TMP5'. Linear regression of the data gave $y = 1.76x - 0.68$ ( $r^2 > 0.99$ ) TMP3' and $0.86x - 0.3$ ( $r^2 > 0.99$ ) for TMP5'. . . . .	40
S7	Formation of 5'-X1pT-3' from irradiated 5'-TpT-3'. . . . .	41
S8	Formation of 5'-X2pT-3' from irradiated 5'-TpT-3'. . . . .	41
S9	Formation of ddT5' from irradiated TMP5'. . . . .	42
S10	Formation of 5,6-dhT from irradiated TMP5'. Note that the dinucleotide was enzymatically digested to the nucleoside before analysis. . . . .	43
S11	Formation of Thy from irradiated TMP5'. . . . .	43
S12	Formation of ddT3' from irradiated TMP3'. . . . .	44
S13	Formation of 5,6-dhT from irradiated TMP3'. . . . .	44
S14	Formation of Thy from irradiated TMP3'. . . . .	45
S15	Formation of ddT3' from irradiated thymidine. . . . .	46
S16	Formation of ddT5' from irradiated thymidine. . . . .	46
S17	Formation of 5,6-dhT from irradiated thymidine. . . . .	47
S18	Formation of Thy from irradiated thymidine. . . . .	47
D1	A proposed mechanism for thymidine N-glycosidic bond break by LEE bombardment . . . . .	49
D2	Proposed mechanism of C-O bond cleavage and released products by LEEs	51
D3	A proposed pathway for formation of 5,6-dihydrothymine (base damage).	52
D4	There are 3 main channels for TpT, II) For simpler molecule such as dThd (dT) fewer channels are available, thus, the electron has an increased probability to go to the other side. . . . .	54

## LISTE DES TABLEAUX

2.1	Summary of product yields for different molecular targets showing the efficiency of vLEE-induced damage in molecules of product per incident electrons ( $\times 10^{-4}$ ). The values were obtained from the slopes of a linear regression for the formation of each product as a function of fluence (Fig.2.4 for TpT; Figs. S9-S11 for TMP5'; Figs. S12-S14 for TMP3'; and Figs. S15-S18 for thymidine (dThd). All slopes were statistically significant ( $P < 0.05$ ). . . . .	30
S1	LC-MS/MS properties of vLEE-induced products of TpT, TMP3', TMP5' and thymidine. The products include thymine non labeled (NL), thymine labeled (L), 5,6-dihydro-2'- deoxythymidine (5,6-dhT), 2',3'-dideoxythymidine (ddT3'), 2',5'-dideoxythymidine (ddT5'), thymidine 5'-monophosphate (TMP5'), thymidine 3'-monophosphate (TMP3'), 5.-X1pT-3' where X1= 1',2'-dideoxyribose, and 5'-X2pT-3' where X2= 2'-deoxyribose. Products (a): LC separation was carried out with a Phenomenex Luna Omega 1.6 $\mu$ m Polar C18 100 x 2.1 mm (i.d.) column protected by a pre-column of the same material. The products were eluted with solvent A (0.05% formic acid) using a gradient of solvent B (90% acetonitrile) from an initial 1% to a final 30% in 8 min followed by a short wash (2 min) and re-equilibration (3 min). The nucleoside of 5,6-dhT was measured in separate runs after enzymatic digestion of the sample into its component nucleosides The analysis of TMP3' and TMP5' was also carried out in a separate run under the same conditions as above except the MS was operated in negative mode. The dwell time of the MS was 100 ms and the analytes were measured using unit resolution. The complete analysis of products was carried out in three stages. Products (b): LC separation was carried out with a Acquity UPLC HSS T3; 1.8 $\mu$ m particle size; 100 x 2.1 mm (i.d.) protected by a Van-Guard <sup>TM</sup> pre-column. The products were eluted with solvent A (5 mM formate buffer (pH 5.0) using a gradient of solvent B (80% acetonitrile) from an initial 1% to a final 12% in 8 min followed by a short wash (2 min) and re-equilibration (3 min). . . . .	36

## LISTE DES ABRÉVIATIONS

**Ade** *Adenine*

**C** *Cytosine*

**°C** *Degree celcius*

**C-O bond** *Sugar-phosphate bond*

**CI** *Collision Induced Dissociation*

**cm** *Centimeter*

**Cyt** *Cytosine*

**DEA** *Dissociative electron attachment*

**ddT3'** *2',3'-dideoxythymidine*

**ddT5'** *2' , 5'-dideoxythymidine*

**dTh** *deoxythymidine*

**DFT** *Density functional theory*

**5,6-dHT** *5,6-dihydro-2'-deoxythymidine*

**DNA** *Deoxyribonucleic acid*

**DSB** *Double strand break(s)*

**E** *Incident electron energy*

**ESI** *electrospray ionization*

**e<sup>-</sup>** *Electron*

**Ea** *Activation energy*

**EC** *electrochemical detection*

**e<sup>-</sup>(aq)** *Solvated electron/ hydrated electron*

**ec<sup>-</sup>** *Continuum electron*

**E. coli** *Escherichia coli*

**ESIMS** *Electrospray ionization mass spectrometry*

**et<sup>-</sup>** *Transfer electron*

**eV** *Electron volt*

**Fe<sup>2+</sup>** *Ferrous ion*

**Fe<sup>3+</sup>** *Ferric ion*

**FWHM** *Full width half maximum*

**G** *Guanine*

**GC/MS** *Gas chromatography/ mass spectrometry*

**Gua** *Guanine*

**h** *Hour(s)*

**•H** *Hydrogen radical*

**H<sup>-</sup>** *hydride anions*

**H<sub>2</sub>** *Hydrogen gas*

**H<sub>2</sub>O<sup>\*</sup>** *Excited water*

**H<sub>2</sub> O<sup>+</sup>** *Water cation*

**H<sub>2</sub>O<sub>2</sub>** *Hydrogen peroxide*

**H<sub>3</sub>O<sup>+</sup>** *Hydronium ion*

**HOMO** *Highest occupied molecular orbital*

**HPLC** *High performance liquid chromatography*

**IR** *Infrared*

**keV** *Kilo electron volt (10<sup>3</sup> electron volt)*

**LBL** *Layer-by-layer*

**LC/MS** *Liquid chromatography/ mass spectrometry*

**LC-MS/MS** *Liquid chromatography-mass spectrometry/ mass spectrometry*

**LEE(s)** *Low-energy electron(s)*

**LET** *Linear energy transfer*

**LUMO** *Lowest unoccupied molecular orbital*

**M** *Molar*

**MeV** *Mega electron volt (10<sup>6</sup> electron volts)*

**MRM** *Multiple reaction monitoring*

**min** *Minute(s)*

**N<sub>2</sub>** *Nitrogen gas*

**nm** *Nanometer(n) (10<sup>-9</sup> meter)*

**N<sub>2</sub>O** *Nitrous oxide*

**O<sub>2</sub>** *Oxygen gas*

**•OH** *Hydroxyl radical*

**O(3P)** *Oxygen atom in the triplet 3P ground state*

**P** *Phosphate group*

**pT** *Thymidine-5'-monophosphate*

**pTp** *Thymidine-3',5' -diphosphate*

**pTpTp** *5'-pTpTp-3'*

**QQQ** *Triple quadrupole in mass spectrometer*

**QTOF** *Quadrupole time-of-flight*

**R** *Deoxyribose sugar*

**ROS** *Radical oxidative species*

**RPM** *Revolutions per minute*

**SATP** *Standard ambient of temperature and pressure*

**SE** *Secondary electrons*

**SSB** *Single strand break(s)*

**Thy** *Thymine*

**TNI** *Transient negative ions*

**TMI** *Transient molecular anion*

**TMP5'** *thymidine 5'-monophosphate*

**TMP3'** *Thymidine-3' -monophosphate*

**TOF** *Time-of-flight*

**Tp** *Thymidine-3' -monophosphate*

**TpT** *Thymine-phosphate-thymine*

**TTT** *5'-TpTpT-3'*

**TXT** *5'-TpXpTp-3' (X= T, C, A, G)*

**UHV** *Ultra high vacuum*

**UMO** *unoccupied molecular orbital*

**UV** *Ultraviolet*

**vLEEs** *Very low-energy electron*



# 1 INTRODUCTION

## 1.1 Is radiation necessary for life?

These days, developments in science and technology are fundamentally altering the way people live and have increased the willingness of humans to know more and increase their understanding of the physical world. One of the most significant discoveries in the 19<sup>th</sup> century was radiation. At that time nobody thought that certain kinds of matter can emit radiation, especially when submitted to a high voltage, but in 1896 a German physics professor, Wilhelm Conrad Roentgen, discovered the main properties of X-rays. He found that the X-ray would pass through the tissue of humans leaving the bones and metals visible. This feature was enough to change the medical world forever. Soon afterward, the penetrating properties of the rays began to be exploited for medical purposes (Reed, 2011).

In the past few decades, many researchers and physicians have developed radiation science in a variety of different ways. It has been used for different reasons and applications. For example, some people used it wisely to produce positive outcomes in medical science, however, others utilized it for destructive purposes such as nuclear weapons like those used in the atomic bombings of Hiroshima and Nagasaki in 1945 that demonstrated the grave biological response to radiation. Therefore, it has both beneficial and harmful effects simultaneously. However, due to people's tendency to remember negative events or traumatic experiences they might have had, they face unnecessary or irrational fear. These are one of the reasons that some people are afraid of radiation, and we called this Radiophobia (Koslov, 1982).

## 1.2 Caution radiation area!

We live and breathe in a world that is like an invisible sea of radiation. In recent years, people have learned to fear the consequences of radiation. They do not want to live near nuclear reactors. They are shocked by reports of connections between excessive exposure to sunlight and skin cancer. They are worried about the leakage from microwave ovens or the radiation produced by their television sets but what is radiation and how hazardous is it? Radiation can be explained as energy or particles that travel through space or other mediums. Many types of interactions can take place when radiation strikes an object.

Overall, two things can occur if radiation is absorbed by matter: excitation or ionization.

We can generally classify radiation as either ionizing or non-ionizing based on whether it has sufficient energy to remove an electron from the atom that it interacts with. Ionizing radiation is mostly X-ray and Gamma-rays (Figure 1.1) that can remove tightly bound electrons from the orbit of an atom and cause the atom to become charged or ionized. The resulting secondary species can react with molecules, such as DNA inside the cells, along the radiation track, which can be applied for the treating human health problems. Non-ionizing radiation can be considered less dangerous than ionizing radiation. Overexposure to non-ionizing radiation can cause health issues, for instance, from power lines, microwaves, radio waves, infrared radiation, visible light, and lasers.

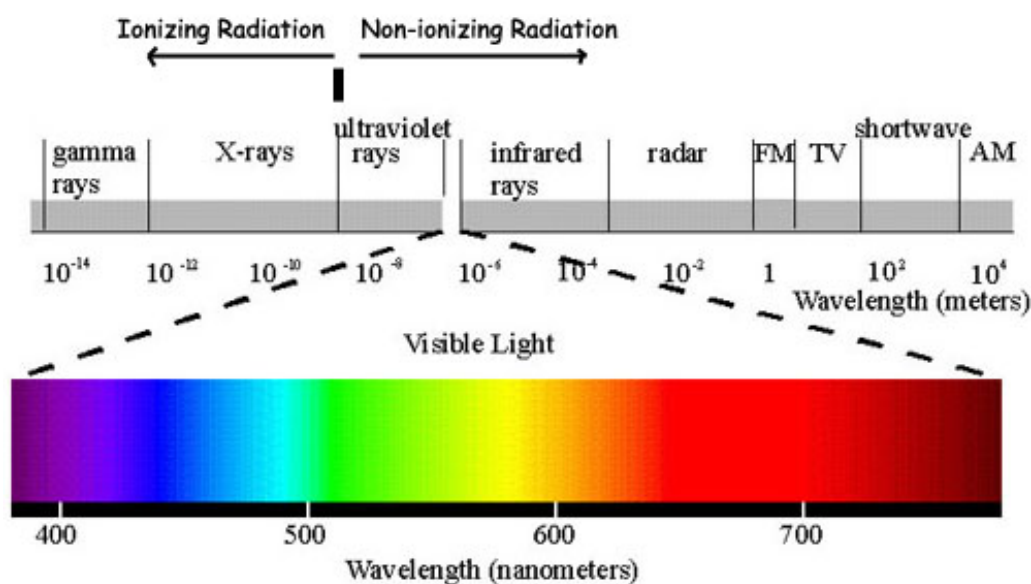


**Figure 1.1** – Electromagnetic spectrum separating non-ionizing and ionizing radiation.

Excitation is the transfer of an electron by absorbing energy from a lower electronic energy level to a higher energy level, thus, it causes an atom to move from a ground state to an excited state. The principal difference between excitation and ionization is that excitation illustrates the movement of an electron from a lower electronic energy level to a higher energy level while ionization involves the complete removal of an electron from the atom or molecule.

### 1.3 Radiation exposure and health effects

Ionizing radiation harms living things at the molecular level by ionizing molecules inside microscopic cells that make up the human body. The use of radiation, especially ionizing

radiation, is currently attracting considerable attention in the field of medical sciences, thus, it is essential to know and understand the role of ionizing radiation. The first way radiation affects our health is through the breakage of DNA molecules by direct or indirect effects. If an X-ray or ionizing radiation interacts with the DNA molecule, this is considered a direct effect, whereas, most of the damage to DNA molecules from X-ray is achieved through the indirect effect because when X-rays or ionizing radiation enter a cell, they are much more likely to ionize a water molecule because water is the most abundant molecule in cells; water consist of 70% or more of total cell mass (Frohlinde, 1986; O'Neill *et al.*, 2002).

Overall, ionization can happen in any molecule in the cell forming a radical cation and an ejected electron. The ejected electron can attack another molecule or it can become solvated before additional reactions. The radical fragment can be transferred to another nearby molecule. Simultaneously, the radical cations can react and become neutralized by giving up a proton, such is the case of the radical cation produced by ionization of water.  $H_2O^+$  reacts with an adjacent water molecule immediately (10-14s) to create the hydroxyl radical  $\bullet OH$ . As a consequence of these reactions, cellular DNA can be damaged in several ways, including direct ionization of the DNA, reactions between the DNA and electrons, or solvated electrons,  $\bullet OH$  or  $H_2O^+$ , or other radicals ( Figure 1.2 ) (Han et Yu, 2009).

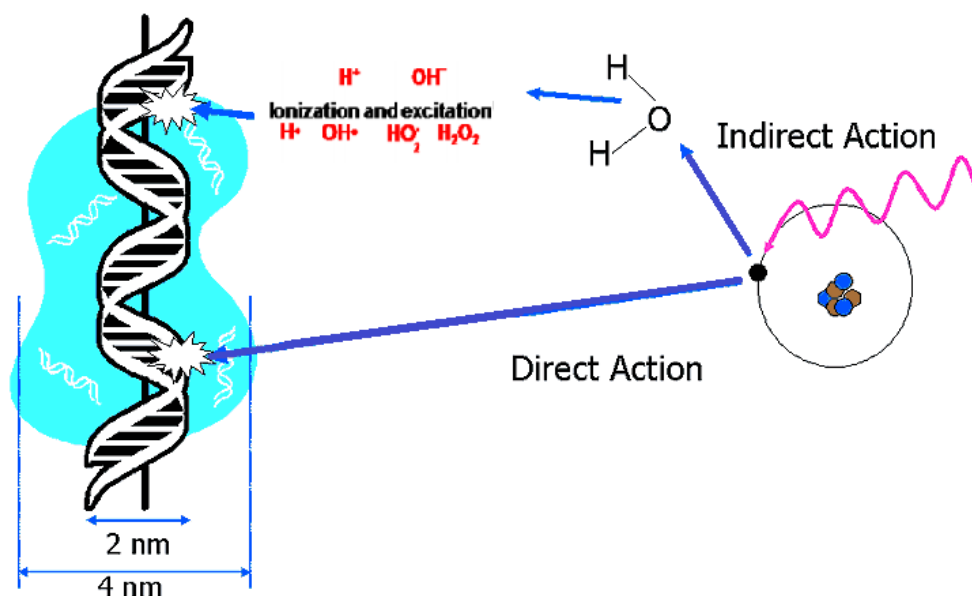


**Figure 1.2** – Direct and indirect action of radiation in biological systems

As mentioned above, ionizing radiation can induce many physical, chemical, and biolog-

ical changes. Therefore, it is vital to recognize whether the equal doses of different types of radiation provide the same effect when they are absorbed in biological material. For instance, the rate of ionizing particle energy loss along their tracks for X-ray and electrons is not the same, thus, it is necessary to compare the detected radiation effects with the rate of energy loss, the idea of linear energy transfer (LET) was proposed (Swiderek, 2006).

Each type of radiation has a specific structure and can be delivered over a range of different energies. When the radiation interacts with matter, it loses its energy through interactions with the atoms. The average amount of energy is spread over a determined distance, for example, the energy deposited in cells, tissues, and organs is known as the LET. The particular unit regularly used for this quantity is kilo electron volt per micrometer ( $\text{keV}/\mu\text{m}$ ) of unit density material. LET is used to classify radiation as High LET radiation and Low LET radiation. High LET radiation is a type of ionizing radiation that deposits a significant amount of energy in a small distance, e.g. neutrons and alpha particle, whereas Low LET radiation deposits less amount of energy along the track or has widely spaced ionizing events. e.g. X-rays and Gamma-rays. If we take water as an example, High LET radiation ionizes water into  $\text{OH}^\bullet$  and  $\text{H}^\bullet$  radicals over a very short track but Low LET radiation also ionizes water molecules over a much longer track giving a radiation-induced decomposition of water molecules by ionization and excitation. This pathway is called radiolysis of water which can also contribute to the destruction of cells.

For understanding the biological effects which are produced by ionizing radiation, it is better to understand the physical and chemical stages provided by ionizing radiation in liquid water since mammalian cells typically consist of  $\sim 70\text{-}85\%$  water,  $\sim 10\text{-}20\%$  proteins,  $\sim 10\%$  carbohydrates, and  $\sim 2\text{-}3\%$  lipids (Turner, 2008).

The physical stage is the initial phase that is produced by radiation in water and thereby forms the ionized and excited molecules, e.g.  $\text{H}_2\text{O}^+$ ,  $\text{H}_2\text{O}^*$  take place in less than  $10^{-15}$  s. After, the initial radicals such as  $\text{H}^-$ ,  $\text{OH}^-$ ,  $\text{H}_2\text{O}^{\bullet-}$ ,  $e^-$ ,  $\text{H}^\bullet$ ,  $\text{OH}^\bullet$  are generated by a physio-chemical process within  $10^{-15}$  to  $10^{-12}$  s. The radical-radical reaction of two  $\text{OH}^\bullet$  or  $\text{H}^\bullet$  give stable molecules ( $\text{H}_2\text{O}_2$  and  $\text{H}_2$ ). In the following stage which depends on LET, the radicals species which are produced in the last step begin to come adequately close to react with each other as their diffusion and distribution in water advance. Chemical changes due to bond breakage result from the reaction of those radicals with target molecules in the biological stage causing lots of damage in the cell at various times. That is how cancer develops over time in the human body, by acquiring more and more DNA mutations until they reach a hazardous point at which the cell eventually becomes cancerous in the human body (Figure 1.3).

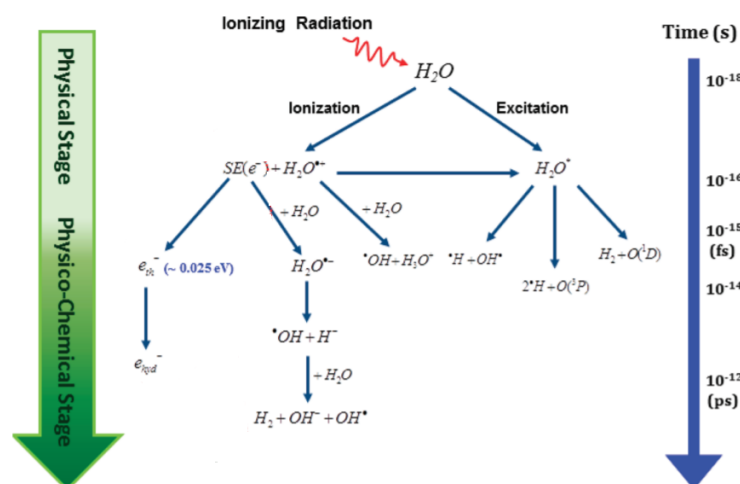


**Figure 1.3** – Time scale of radiolysis of water (Alizadeh et Sanche, 2012)

#### 1.4 How cancer develops in the human body

If radiation is absorbed in biological material, ionization and excitations will happen and is not distributed at random but favors localization along the tracks of single charged particles in a way that depends on the dose and type of radiation. Depending on the geometry of the tracks, the biological effects of radiation can vary widely. Some quickly occur while others may take years to become evident. DNA damage induced by radiation can cause critical health effects. Deoxyribonucleic acid, more generally known as DNA, is a complex molecule that contains all of the information required to build and maintain an organism. It consists of two long polymeric strands made of four types of nucleotide subunits which include five-carbon sugar attached to one or more phosphate groups and a nitrogen- containing base which includes purine ( guanine and adenine) and pyrimidine ( cytosine and thymine). Each of these chains is known as a DNA chain or a DNA strand. The sugar and phosphate groups, which build the backbone of each strand, are placed on the surface of DNA whereas the bases are on the inside of the helix (Fig. 1.4). Hydrogen bonds between the complementary base pairs of each strand, connect the two strands of the helix (i.e. between A and T and between C and G), and lead to the pairing of bases that holds the two strands together and gives stability to the DNA polymer (Alberts *et al.*, 2002).

If ionizing radiation interacts with a cell, it can break the DNA strands. In this situation, three things can happen:

- DNA repairs all the damage and the cell will survive without any changes to its

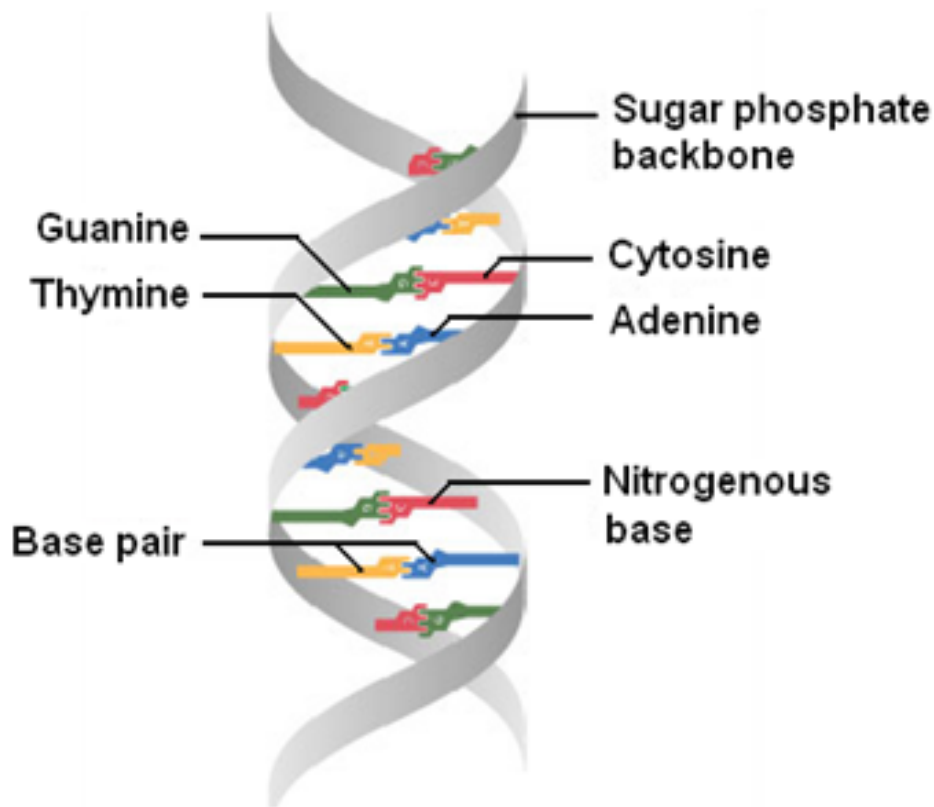


**Figure 1.4** – DNA forms a double stranded helix, and adenine pairs with thymine and cytosine pairs with guanine.

function or leave no damage

- DNA repair deficiency can lead to mutation. This indicates that cells can lose their ability to reproduce themselves correctly and then transfer the genetic abnormality on to other cells through reproduction, prompting the biophysical change in cells.
- Cell death occurs when the damaged on the cell cannot be repaired. In this case, cells permanently lose their proliferating ability and their functions. This process occurs all the time in everyone. In reality, people are exposed to nearly 10000 to 100000 toxic damage per cell every day due to thermal depurination, oxidation, and alkylation (Lindahl *et al.*, 1993) but the probability of this type of harmful effect is proportionate to the dose and it improves with increasing the radiation dose. If the cell structure changes because it repairs itself inappropriately, this modification could have no additional consequence or the effect could appear later in life. Thus, cancer and genetic defects may or may not succeed (Jackson et Bartek, 2009)

### 1.4.1 Types of DNA damage

It is accepted that radiation can create a significant amount of DNA lesions including damage to the nucleotide bases (Base damage) or DNA single and double-strand breaks. Base damage occurs via radiation when there is a chemical modification in one of the four base pairs or breakage in the inner rings of the DNA ladder due to several processes. One of them is oxidation by Reactive Oxygen Species (ROS) products. There are various sources of ROS that can cause the formation of oxidative damage. Radiolysis of water by ionizing radiation is one of the sources of ROS products involved in base damage mostly prompted by the reactive species formed from water radiolysis including hydroxyl radicals, solvated electrons, and H atoms (Bauer *et al.*, 2015). The damaged base can be repaired through various base excision repair pathways. Basically, it just removes the damaged nucleotide and replace it with a normal nucleotide. If the abstraction of a hydrogen atom from deoxyribose moiety occurs, a single strand break will be formed and the polymer is broken into two fragments after this interaction. Although most of this type of damage produced by radiation can easily and quickly be repaired, approximately in 5 minutes, while the other class is clustered lesions which includes DSBs and other multiple lesions involving strand breaks and base damages, are much more complicated to repair and also results in potentially dangerous DNA damage responses. DSBs induced by ionizing radiation can cause abnormality in the chromosomes. Chromosomes are found in the nucleus of most living cells, providing genetic information in the forms of genes. Therefore radiation can harm many genes causing failure and death in cells (Han et Yu, 2010). DSB is the common lesion produced by ionizing radiation where the phosphate backbone of two corresponding DNA strands are broken and generate very cytotoxic forms of damage (Mehta et Haber, 2014). Recently, another feature of radiation damage has been identified as clustered DNA damage which occurs when two or more lesions are formed within one or two helical turns of the DNA through the reactive species produced by the track of a charged particle via direct and indirect effects.

The LET of radiation defines the rate and complexity of clustered damages, in view of several modeling studies, as estimated to be about 30% and 70% of DSBs induced by low and high LET radiation respectively (Cannon, 2016).

## 1.5 Why study low-energy electron-induced reactions

When high energy radiation (such as X-rays and Gamma-rays) and fast charged particles interact with matter, copious numbers of electrons will be produced by the ejection of electrons from molecules during the initial ionization process. There are two processes

which dominate when the matter absorbs energetic photons. At low energies, typically the primary process is the photoelectric absorption ( $E < 0.5$  MeV), a photon transfers all its energy to an inner-shell electron in an atom resulting in the ejection of that electron from its shell. In turn, the electron can pass through the surrounding matter to cause additional ionization.

Briefly, photoelectric reactions are most probable to occur with low-energy photons and elements with high atomic numbers provided the photons have adequate energy to overcome the forces binding in electrons in their cells. Photoelectric absorption facilitates the measurement of the energy of a Gamma-ray photon and this interaction can also lead to the creation of X-ray fluorescence.

At higher energies (approximately 0.7-10 MeV), if the incident X-ray photon is deflected from its initial path by interaction with an electron, it will cause the ejection of that electron from its orbital position. Thus, the X-ray photon loses energy because of the interaction but continues to travel through the material along an altered path. It can subsequently be involved in further interactions leading to the production of a large number of relatively fast electrons because after scattering, the photon has less energy so it is more probable to produce the photoelectric effect which these fast electrons can further excite or ionize other atoms in the medium giving a large amount of the secondary LEE before the electron is thermalized. In both of these processes, nearly all of the absorbed photon energy turns into kinetic energy when an X-ray produces a photoelectron this electron is a primary electron and after secondary LEE.

The reason why these LEEs are so important is that they are produced in large amounts. Approximately  $4 \times 10^4$  per 1 MeV of the primary photon changes into many reactive species, e.g. radicals, ions, and excited molecules which were created through the ionizing radiation track. Since the optical oscillator strength for small (e.g.,  $H_2O$ ) and large (e.g., DNA) biomolecules is greatest at an energy of about 22 eV, when this primary interaction leads to ionization, the distribution of electrons has a maximum below 15 eV. The majority of the energy of LEEs is distributed below 30 eV with the most probable energy of around 9–10 eV. These electrons are referred to as secondary LEE (Sanche, 2003).

## 1.6 Principles of the interaction of LEEs with molecules

To get the idea that how LEEs induce damage to DNA and generate radiobiological damage such as strand breaks and other fragments, it is crucial to understand and precisely explain the detailed pathways of reactions and mechanisms involving low-energy electrons (LEEs) interaction with DNA.



Generally, low-energy electron collisions with molecules can be classified into two main types: elastic and inelastic. During elastic collisions, the loss of electron energy to the target is negligible, therefore, there is no loss of energy. In contrast, inelastic collisions lose a significant amount of electron energy to the target. Thus, it may create electronically excited states followed by other reactions. The elastic collisions are less significant as no energy is deposited, in contrast to the inelastic collision. The inelastic collisions of low-energy electrons with molecules and atoms lead to several energetic species that are the primary reasons for the wide variety of radiation-induced chemical reactions. Because of the numerous inelastic collisions, these secondary electrons become thermalized in nearly one picosecond.

There are several processes in this study initiated by electron interactions with matter and terminating with DNA damage by the initial formation of a transient molecular anion (TMA) or transient negative ion (TNI) of a DNA localized subunit. TMA is one of the most important features illustrating how LEEs induce DNA damage. TMA is formed by the initial capture of an electron by a molecule i.e. the incoming electron temporarily occupies a previously unfilled orbital of a molecule. Upon TMA formation, an extra electron is captured into the unoccupied molecular orbital (UMO) of the neutral molecule resulting in shape or core-excited resonance (Kumar et Sevilla, 2008). A shape resonance or a single-particle state occurs if the additional electron occupies a previously unfilled orbital (such as a lowest unoccupied molecular orbital or LUMO which is an electron in an excited state that skips from the ground state after the energy of a photon of sufficient energy is transferred to the electron in the HOMO) of a molecule in its ground state. Usually, this happens at low energies (0–4 eV) with lifetimes in the range  $10^{-15}$  to  $10^{-10}$  s. Core-excited resonance or two-particle states, formed when an interacting electron excites one of the core electrons of the molecule from the ground state (when the incident electron has higher energy, usually  $E > 3\text{eV}$ ) giving a configuration consisting of an electron in a LUMO and an electron-hole in HOMO. Core-excited resonances occur typically above 4 eV, are highly energetic, and have been suggested to play a role in double-strand breaks in DNA (Figure 1.6) (Alizadeh *et al.*, 2016).

The other process, which is also the most important process, is called dissociative electron attachment (DEA). In this process, if the TMA state is dissociative and the resonance lifetime is higher than about half of the vibration period of the anion, it can dissociate into neutral and anionic fragments. The dissociation possibility rises with increasing incident electron energy. The dissociation yield is highest at low incident electron energies ( $E > 10$  eV) owing to the abundance of secondary electrons at those energies. In contrast, electron

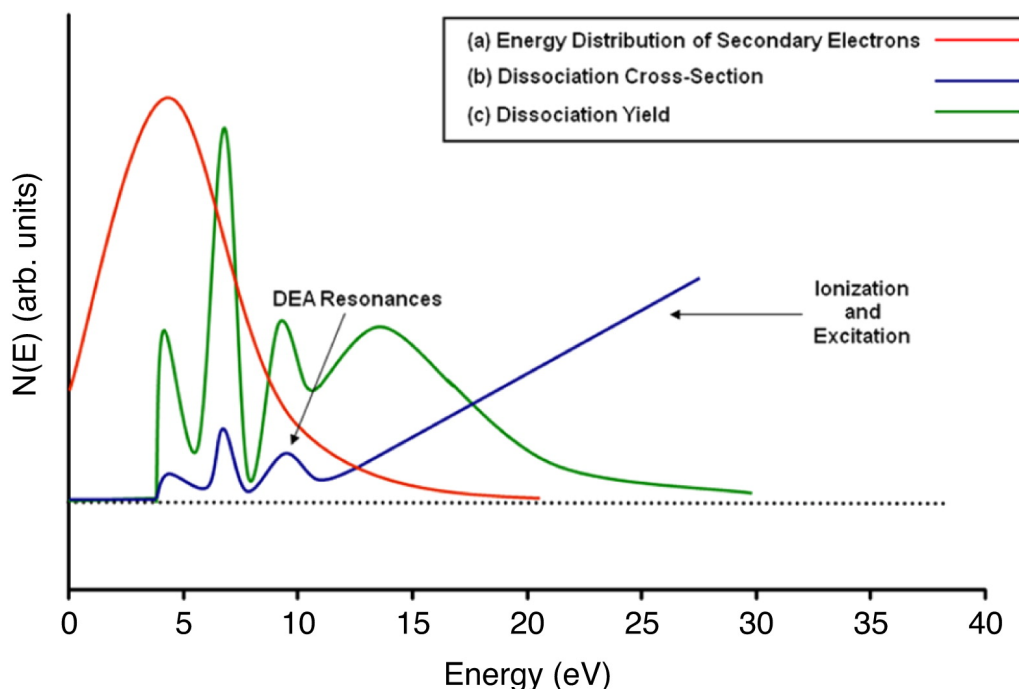


**Figure 1.5** – (a) Schematic energy distribution of secondary electrons generated during a primary ionizing event which means the energy distribution of the secondary electrons demonstrate that the majority of these electrons have energies below 10 eV. (b) cross section for electron-induced dissociation for a typical molecule; (c) dissociation yield as a function of electron energy for a typical molecule.

impact excitation and the electron impact ionization regularly take place at energies above 6 eV and 10 eV respectively (Figure 1.5)(Arumainayagam *et al.*, 2010)

### 1.7 DNA damage induced by ionizing radiation

As briefly described in Section 1.6, low-energy electrons (LEE) are produced copiously during high-radiation events and are increasingly being considered as important DNA-damaging agents. The primary series of experiments by Sanche and coworkers (Li *et al.*, 2008; Zheng *et al.*, 2004a; Abdoul-Carime *et al.*, 2001) determined that LEEs in the 0–10 eV range produce single- and double-strand breaks in DNA. Indeed, they found that LEEs are several times more damaging than photons of comparable energy.

In 2000, a key publication (Boudaïffa *et al.*, 2000) concerned the formation of resonances from the interreaction of DNA with low-energy electrons. In this study, plasmid DNA (pGEM 3Zf(-)) obtained from *E. coli* was irradiated with monoenergetic LEE beams (+/– 0.5 eV) with kinetic energies in the range between 3–20 eV. They found that electrons having energy below the ionization limit of DNA (ca. 7.5–10 eV (Hush et Cheung, 1975;

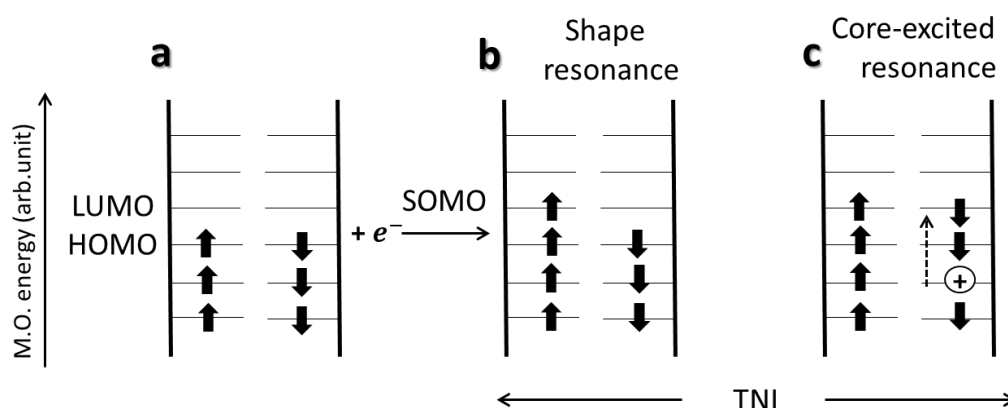


**Figure 1.6** – (reprinted from Kumar et Sevilla (2012)). Schematic diagram showing the electronic configuration of a neutral (a) and transient negative ion (TNI) (b, c). The interacting electron initially captures into the unoccupied MOs of the neutral molecule resulting in TNI formation via: (a) shape resonance or (c) core-excited resonance.

Orlov *et al.*, 1976) ) were able to create SSB and DSB. From these studies, the yield of damage was demonstrated for both SSB and DSB, and calculated as  $8.2 \times 10^{-4}$ , and  $2 \times 10^{-4}$  strand breaks per incident electron, respectively, for 10 eV electrons. The yields of SSB and DSB in DNA depended on the energy of the interacting electron and were proposed to be produced by the rapid fragmentation reactions of transient molecular resonances localized on DNA components i.e. base and sugar moieties, and the phosphate backbone.

Sanche and co-workers obtained further insights into the mechanisms of LEE-induced DNA damage (Panajotovic *et al.*, 2006). There are several key results shown in this study. The first one is that 0–4.7 eV electrons are able to generate SSB in plasmid DNA with related yields to those obtained at higher energies. The second key finding is that the cross-section for SSB formation at 1 eV is greater than that observed at 10 eV. The last main point that this group also found was that 0.1–4.5 eV electrons induce only SSB by the involvement of resonances for causing damage at 0.8 and 2.2 eV. Due to the low electron energies, these resonances were defined as shape resonances (Figure 1.7).

The findings from strand breaks in plasmid DNA induced by 3–100 eV electrons and correlation with shape resonances of the bases identified by Burrow *et al* in the gas phase indicated that, below 5 eV, LEE-induced SSB takes place through dissociative electron attachment (DEA) via shape resonances (Boudaïffa *et al.*, 2000; Huels *et al.*, 2003; Martin *et al.*, 2004; Panajotovic *et al.*, 2006; Brun *et al.*, 2009) whereas, between 5 and 15 eV, the core-excited resonances induce SSB and DSB. Also, several theoretical studies were

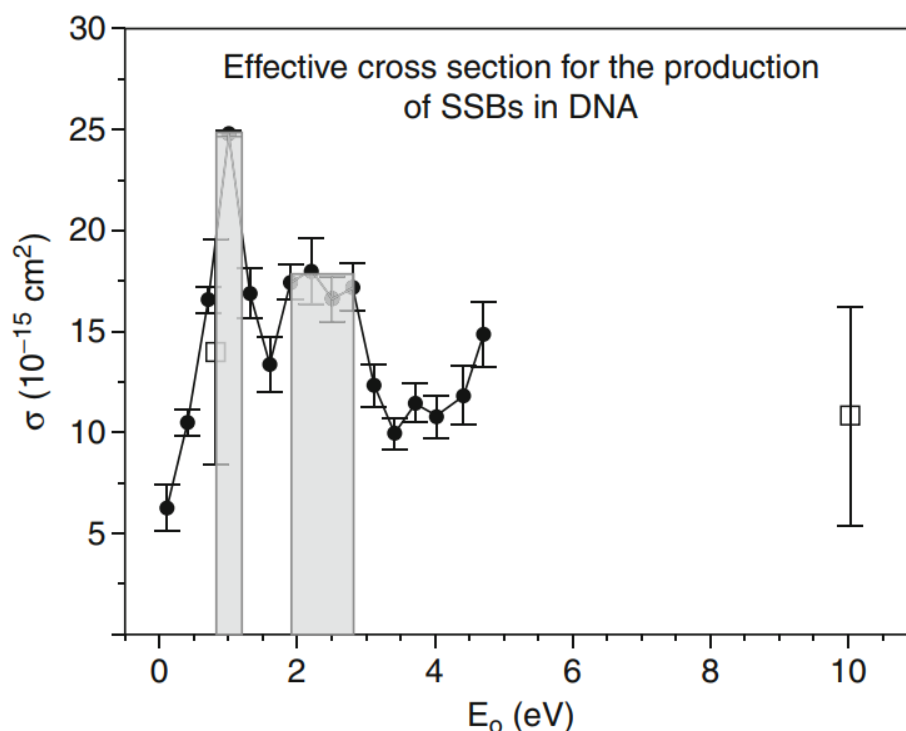


**Figure 1.7** – Effective cross sections ( $\sigma$ ) for the formation of SSB in plasmid DNA by 0.1– 4.7 eV electrons. The shaded portion corresponds to shape resonances at 1 eV and around 2.5 eV.(Reprinted from Panajotovic *et al.* (2006)).

undertaken to explain the mechanism of LEE induction of DNA strand breaks soon after the discovery that low- energy (3–20 eV) electrons caused both single- and double-strand breaks in plasmid DNA (Boudaïffa *et al.*, 2000). The authors used density functional theory (DFT) and theoretical simulations to predict LEEs interactions with DNA (Bao *et al.*, 2006; Berdys *et al.*, 2004; Gu *et al.*, 2005; Kumar et Sevilla, 2007; Simons, 2007). Since the calculation of the complete DNA molecule at the ab initio or DFT level is presently restricted to small molecule size, fragments of DNA structure were usually modeled including a base, sugar, and phosphate moieties attached at 3'- and 5'- ends of the sugar ring.

### 1.7.1 Report of prior results by our group

DNA damage induced by irradiation has been studied for many decades. Such studies enable us to have a better understanding of the dangers caused by radiation and to improve the efficiency of the radiotherapies that are used to combat cancer. Regarding this idea, the fundamental interactions of LEEs with nucleobases, 2-deoxyribose derivatives, oligonucleotides, and plasmid DNA have been investigated (Ptasińska *et al.*, 2005; Huels *et al.*,

1998; Abdoul-Carime *et al.*, 2001; Breton *et al.*, 2004; Huels *et al.*, 2004; Lepage *et al.*, 1998; Ptasińska *et al.*, 2004; Park *et al.*, 2006; Ray *et al.*, 2005; Martin *et al.*, 2004).

First, in 2004, Zheng *et al.* studied the interaction of thymidine with LEEs. They showed that cleavage of the N-glycosidic bond of thymidine leading to the release of thymine was a significant product (Zheng *et al.*, 2004a). This means that glycosidic bond cleavage created within the formation of a transient anion state is formed by low-energy electrons localizing in the antibonding orbitals of the glycosidic bond. Hence, the conclusion was that LEEs are involved in glycosidic bond cleavage. Later, this group focused on the formation of products by monoenergetic LEEs from bigger molecules: two tetramers (CGTA and GCAT) (Zheng *et al.*, 2005). They observed the formation of numerous products including non-modified nucleobase, nucleoside, and nucleotide fragments associated with the cleavage of the phosphodiester C–O bonds between the sugar and phosphate bonds together with the N-glycosidic bond between the base and sugar group within each tetramer.

These results demonstrate the pathway of bond breaking via electron promotion into an antibonding orbital of the phosphate group or an antibonding orbital of the DNA base, from where the electron can be transferred to the phosphate group through bond transfer followed by cleavage of the C–O bond. The breaking of the C–O bond is preferred owing to the very high electron affinity of the phosphate group (Swiderek, 2006). This hypothesis was further supported by Simon and co-workers who showed, using theoretical calculations, that the excess electron is initially captured in an orbital located in the nucleobase and then transferred remotely to the phosphodiester bond (Simons, 2006). Such experiments play a significant role in obtaining a fundamental understanding of radiation-induced DNA damage in a living cell.

There are several investigations about the effect of the phosphate group reported by Li and co-workers. First, they focus on the effect of the terminal phosphate group using different sizes of DNA model compounds including monomers (pT, Tp, pTp), dinucleotides (pTpT, TpTp, pTpTp), and trinucleotides (TpTpT). Based on their experiments, the presence of terminal phosphate groups dramatically affected the distribution of low-energy electron-induced damage in DNA model compounds. In addition, Li and co-workers studied the effect of base sequences in a series of oligonucleotide trimers including TXT where X can be one of four standard DNA bases (C, T, A, G). The analysis of damage remaining within the nonvolatile condensed phase was determined following irradiation by the low-energy electron (10 eV). They found that the initial low-energy electron capture and subsequent bond breaking within the transient negative anion depended on the sequence and electron affinity of the bases, with the highest damage attributed to the most electronegative base,

thymine (Li *et al.*, 2010).

In later years, different experiments have led to a better understanding of the effects of low-energy electrons. Surakan and co-workers investigated the products induced by both LEE and ionization. They deposited prepared dry films of linear double-stranded DNA on glass and tantalum substrates and then, after LEE bombardment, they measured damage as base modification and non-modification. Their results indicated the formation of both base release and base modification products by LEE-induced, DEA-mediated processes. The nature and yields of products were very similar, but not identical to, those arising from ionization. The yield of non-modified bases, as well as base modifications, increased by 20- 30% when DNA was deposited on a tantalum substrate which generated low-energy electrons compared to that on a glass substrate which mimicked direct ionization (Choo-fong *et al.*, 2016).

## 1.8 Our laboratory methods and LEE irradiator system

### 1.8.1 Spin Coating System

In order to prepare samples for bombardment with LEE, a spin-coating system was developed in our lab several years ago (Zheng *et al.*, 2004a). The biomolecules were spin-coated onto the inner surface of the tantalum cylinders (Figure 1.8). Seven tantalum cylinders were bound together with Teflon spacers, and they can contain a certain amount of the solution individually onto the inner surface of each cylinder. The cylinders were installed into a UHV chamber and rotated magnetically outside the chamber to an angular velocity up to around 1500 rpm under low pressure. Through this method, the sample can be expected to be distributed uniformly onto the inner surface of the cylinders resulting in a thin coat of controllable thickness depending on the initial amount of molecules added.

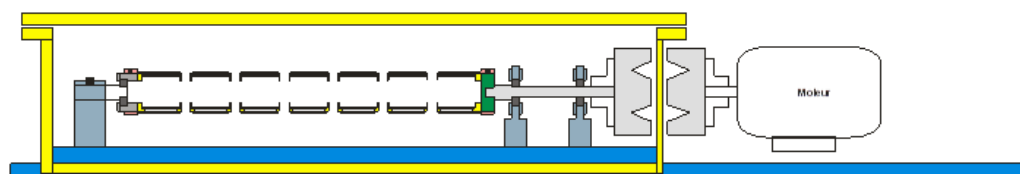


**Figure 1.8** – Schematic diagram of the spin-coating system. I—vacuum chamber, J—tube holder, K— sample substrate, L1 and L2—ball-bearing shafts, M—magnetic coupling, N—electric motor, O—Teflon space.

### 1.8.2 Apparatus for low energy electron production

Irradiation with a low-energy electron is accomplished using an electron gun apparatus. Our group developed this novel system several years ago. The LEE gun irradiator was set in an ultra-high vacuum (UHV) chamber driven by an oil-free turbo molecular pump enabling the chamber to be evacuated rapidly from atmospheric pressure to the  $10^9$  Torr range (Figure 1.9). The assembly includes the electron gun (A) fixed on a linear drive (B) and a rotatable circular platform (C) such that rotation of this platform enables the sample to be bombarded individually through the electron gun at precise energy and current for a given time. A cylindrical multiple-electrode detector can support the energy distribution of an electron (D) in the inner surface of seven tantalum cylinders (E). The port is used for quick access to the UHV chamber (F) from the inside of a glove box (G) which is kept under a dry  $N_2$  atmosphere. Therefore, using this equipment, the gun can irradiate the inner surface ( $26\text{ cm}^2$ ) of a tantalum cylinder with 3-130 eV electrons having an entire energy spread of 0.5 eV full width at half maximum.

Lately, our group modified this system to produce electrons below an energy of 3 eV by placing a tantalum plate (H) directly below the cylindrical sample substrate to repel the incident electron toward the inner surface of tantalum cylinders (Figure 1.9).

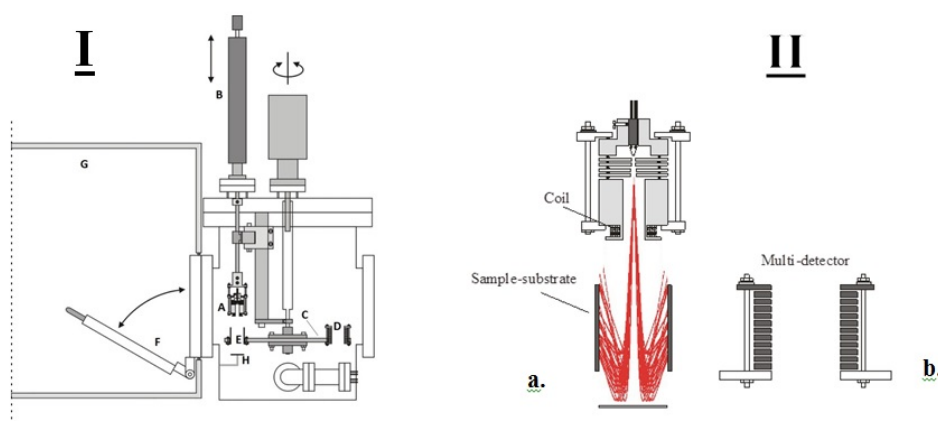


**Figure 1.9** – I. The schematic diagram of the experimental setup for irradiating DNA. (A) electron gun, (B) linear drive, (C) rotatable disk used as cylinder support, (D) electron current detector, (E) cylindrical sample substrate, (F) quick access port, (G) glove box sealed under a  $N_2$  atmosphere, (H) Tantalum Plate. IIa. Illustration of electron trajectories. IIb. Multi-detector.

### 1.8.3 DNA damage detection by LC-MS/MS technique

In the past, numerous analytical techniques were used to measure and detect DNA damage. These included acid hydrolysis of DNA, comet assay, enzymatic digestion of DNA, high-performance liquid chromatography (HPLC) with electrochemical detection (ECD), GC/MS, and LC/MS.

These days, among all these techniques, LC-Mass spectrometry (LC-MS) has become the most popular technology compared to others due to its ability for sensitivity and specificity but, with growing experience, researchers improved this technique as a significant discovery in the field of clinical research. Instruments have been transformed from complicated, high-cost, highly advanced research tools to robust, easy-to-use routine detectors.

Moreover, as the instruments have been improved, more applications have been developed. The progress of tandem MS or MS/MS in this field is mainly because of its higher sensitivity (up to the ppt range) which is suitable for the accurate detection of a variety of reductively and oxidatively modified bases of DNA.

The LC-MS/MS performs with a combination of chromatography (LC) and multiple quadrupole mass spectrometers (MS). The chromatographic system first separates the various components, concentrating the amount of each single component entering the mass spectrometer. Division of the sample components is achieved through an HPLC column where the analytes display differential separation between the mobile phase (eluent) and the stationary phase (coated onto a support material and packed into the column). The principle of mass spectrometry, which is directly connected to electrospray, is the alteration of the separated analyte molecules to a charged (ionized) state following the analysis of the ions and any fragment ions that are formed through the electrospray ionization (ESI) process. Because the ions travel through a magnetic or electrical field, their movement is determined by their  $m/z$  ratio, therefore, ions are separated based on their  $m/z$  ratio in the MS analyzer (Gross, 2006). In this system,  $m$  and  $z$  stand for mass and charge of the detected ions respectively (Figure 1.10).

There are several very popular mass analyzers used for LC-MS and they differ in the primary way in which they separate species on a mass-to-charge basis (Tretyakova *et al.*, 2013). The first one is the Quadrupole Mass Analyzer. The ions are first filtered by the electrostatic potentials applied to the elements of the mass analyzers and then they focus ions for analysis depending on their mass to charge ratio. The second one is the Time of Flight (TOF) Mass Analyzer. Ion filtration can be done by the time it takes for a flight from one point (start) to another point (end) because higher  $m/z$  ions require more time to



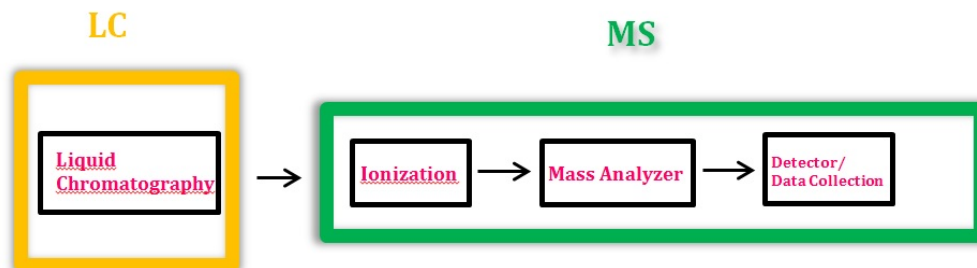


**Figure 1.10** – Schematic design of LC-MS. This diagram demonstrates the technique that combines the physical separation capabilities of liquid chromatography (HPLC) with the mass analysis capabilities of the mass spectrometer.

flight compared to the low  $m/z$  ions. The last one is the Trapped-Ion Mass Analyzer which operates by sorting ions using direct current (DC) and radio frequency (RF) electric field to trap ions. The ions can be collected or manipulated in various ways, such as isolation or fragmentation, and are then driven from the cell in  $m/z$  sequence. Ion traps are available in linear and 3-D configurations. This gives some unique capabilities such as extended MS/MS experiments, very high resolution, and high sensitivity.

In this section, I will focus on the Triple Quadrupole Mass Analyzer and will describe it for a better understanding of my project. Triple Quadrupole Mass Spectrometer (QQQ) Analyzers are often used when higher sensitivity and specificity is needed. They consist of a series of three quadrupoles (Q1-Q3) together with several modes of operation resulting in different information. Therefore, the first quadrupole (Q1) selects ions of interest that were generated in the ion source. The second quadrupole (Q2) is typically filled with nitrogen and is used as a collision chamber to create fragment or daughter ions by a process called Collision Induced Dissociation (CID). The third quadrupole (Q3) is used to monitor the specified fragment ions which are related to the molecular structure of analyte ions and, thus, provides the characteristic structural information of the molecule.

Triple Quadrupole MS systems can be performed in a tandem MS/MS called Selected Multiple Reaction Monitoring (MRM) mode which is the most common method for quantitation of analytes by LC/MS/MS (Dass, 2007). In our experiment, we detect DNA damage products with this method. MRM mode acts like a double mass filter which drastically reduces noise and increases selectivity. The first quadrupole filters a particular precursor ion of interest (Q1) and then enters the second quadrupole (Q2) known as a collision cell. The parameters are optimized to produce fragments from the neutral collision gas, such as nitrogen, and create product ions that are transferred into the third quadrupole where

only a specific  $m/z$  is permitted to pass (Q3) This is a very sensitive method and used for quantitation (Keshishian *et al.*, 2007)(Figure 1.11).

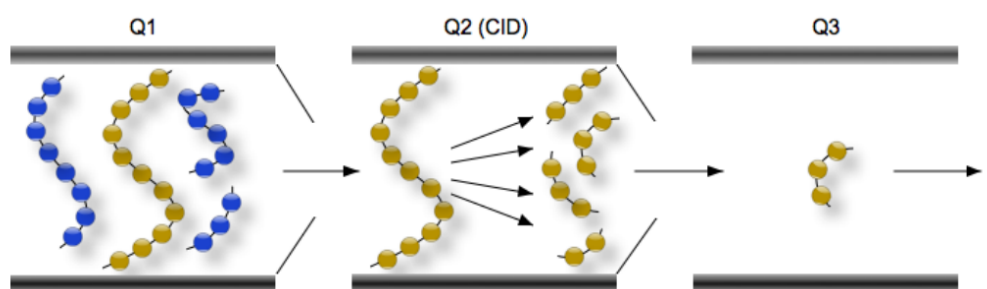


**Figure 1.11** – Schematic of the multiple reaction monitoring (MRM) scanning technique on a triple quadrupole mass spectrometer. The targeted parent ion (shown in yellow) is selected in the first quadrupole (Q1) and enters the second quadrupole (Q2) where it undergoes collision induced dissociation (CID). The resulting “product ions” are mass analyzed using the third quadrupole (Q3)

### 1.9 The brief explanation of the research project (Objective)

With the purpose of better understanding the mutagenic and lethal effects of ionizing radiation, Our group has recently begun studying the low-energy electron induced process in biomolecular films. Our recent studies have shown that low-energy secondary electrons produced in biological tissues through high-energy radiation therapy can create single- and double-strand DNA breaks and site-specific cleavage of DNA bases.

Our main goal for the present project is to understand the chemical mechanism of damage by a very low-energy electron (below 5 eV) using chemical analyses of damaged molecules and model compounds of DNA in particular dinucleotides. We chose to study thymidine dinucleotide (TpT) as a simple model of DNA because we have much experience with thymine decomposition and because previous studies suggested that it was the most sensitive of DNA bases to low-energy electron induced damage. For experiments, we deposited the thin film of TpT into the inner surface of tantalum cylinders to be exposed to a very low- energy electron ( $\sim 1.8$  eV) under SATP (Standard Ambient Temperature and Pressure) surrounded by the  $N_2$  atmosphere. The DNA damage such as single-strand breaks, base release (Thy), and base modification of Thy caused by vLEE are detected by LC-MSMS by MRM mode.

## 2 ARTICLE

### **Strand breaks induced by very low energy electrons: Product analysis and mechanistic insight into the reaction with TpT**

**Authors:** Ghazal Khorsandgolchin, Léon Sanche, Pierre Cloutier, J. Richard Wagner.

**Article status:** Submitted to *Journal of the American Chemical Society*, March 26, 2019.

I did most of the experiments and all the calculation regarding the final results in this paper. Prof. J. Richard Wagner and Mr. Pierre Cloutier did the optimization and calibration of products as given in part in the supplementary information of the paper. Alos, Prof. J. Richard Wagner taught me how to use the instruments of HPLC and LC-MS/MS. Mr. Pierre Cloutier helped me to work with the LEE irradiation source and repaired it when it had problems. Prof. Wanger and Sanche wrote the manuscript. I helped in preparing the methods, materials and the results sections.

## 2.1 Résumé

De nombreuses études expérimentales montrent que les électrons de 5-15 eV induisent des ruptures de brin dans l'ADN même à des énergies inférieures au seuil d'ionisation des composants de l'ADN. Dans cette gamme d'énergie, les dommages à l'ADN résultent principalement de la formation d'ions négatifs transitoires et dissociatifs (attachement dissociatif d'électron, DEA) et d'excitation électronique d'états dissociatifs. Ici, nous avons effectué une analyse LC-MS / MS des produits de dégradation résultant de l'irradiation de TpT, un composé modèle de l'ADN, bombardé avec des électrons de très basse énergie ( $1,8 \pm 0,3$  eV). La formation de thymidine 5'-monophosphate (TMP5') avec la 2', 3'-didésoxythymidine (ddT3') peut être expliquée par le clivage direct de la liaison C3'-O de TpT, alors que la thymidine 3'-monophosphate (TMP3') et la 2', 5'-didésoxythymidine (ddT5') sont formées par clivage de la liaison C5'-O. La formation de ddT3' et de ddT5' diminue lors de l'irradiation de TMP5' ou de TMP3', et même plus dans le cas de la thymidine, soulignant le rôle critique du groupe phosphate. Il est intéressant de noter que les rendements en TMP5' et TMP3' étaient supérieurs à ceux des produits correspondants ddT3' et ddT5', suggérant des destins alternatifs pour les radicaux sucre centré C3' et C5'. En revanche, la libération de thymine était faible (<20%) et n'a pas entraîné la formation de produits attendus à partir du clivage induit par la DEA au niveau de la liaison N-glycosidique. Enfin, les électrons de 1,8 eV ont induit la conversion de la thymine en 5,6-dihydrothymine (5,6-dhT) au sein de TpT, une réaction impliquant vraisemblablement des radicaux anions thymine. En résumé, nous montrons qu'une des voies majeures de dégradation implique le clivage, induit par la DEA, des liaisons C3'-O et C5'-O de TpT, ce qui entraîne la formation de fragments spécifiques, qui représentent une rupture d'un seul brin de l'ADN.

**Mots clés:** rayonnements ionisants, lésions de l'ADN, la spectrométrie de masse, électrons secondaires

## 2.2 Abstract

Numerous experimental studies show that 5-15 eV electrons induce strand breaks in DNA at energies below the ionization threshold of DNA components. In this energy range, DNA damage arises principally by the formation of transient negative ions, decaying into dissociative electron attachment (DEA) and electronic excitation of dissociative states. Here, we carried out LC- MS/MS analysis of the degradation products arising from bombardment of TpT, a DNA model compound, irradiated with very low energy electrons (vLEEs;  $\sim 1.8$  eV). The formation of thymidine 5'-monophosphate (TMP5') together with 2',3'-dideoxythymidine (ddT3') can be explained by direct cleavage of the C3'-O bond of TpT, whereas thymidine 3'-monophosphate (TMP3') and 2',5'-dideoxythymidine (ddT5') are formed by cleavage of the C5'-O and bond. The formation of ddT3' and ddT5' decreased upon irradiation of either TMP5' or TMP3', and even further in the case of thymidine, underlining the critical role of the phosphate group. Interestingly, the yield of TMP5' and TMP3' was higher than that of the corresponding ddT3' and ddT5' products, suggesting alternative fates of C3' and C5'-centered sugar radicals. In contrast, the release of thymine was minor (<20%) and did not result in the formation of expected products from DEA-mediated cleavage at the N-glycosidic bond. Lastly, vLEE induced the conversion of thymine to 5,6-dihydrothymine (5,6-dhT) within TpT, a reaction likely involving thymine anion radicals. In summary, we show that a major pathway of vLEEs involves DEA-mediated cleavage of the C3'-O and C5'-O bonds of TpT resulting in the formation of specific fragments, which represent a single strand break in DNA.

**Keywords:** ionizing radiation, DNA damage, mass spectrometry, secondary electrons

## 2.3 Introduction

The genotoxic effects of ionizing radiation have largely been attributed to the reaction of hydroxyl radicals with DNA (the indirect effect) and the direct ionization of DNA components, both giving oxidative DNA modifications, including base damage and strand breaks (Sonntag, 2006; Cadet et Wagner, 2014). In contrast, the effects of electrons that are ejected during the ionization process have been neglected because they are believed to either ionize the medium further or rapidly undergo hydration to solvated electrons. The latter species react with oxygen to give unreactive superoxide anions, or react with DNA to give base damage but no direct strand breaks (Nabben *et al.*, 1982). There is overwhelming evidence today that a third process also contributes to DNA damage, namely the reaction of low energy electrons (LEEs; 0-20 eV). About  $3 \times 10^4$  LEEs are released during the ionization process for every MeV absorbed along a radiation track (Pimblott et LaVerne, 2007). Numerous experiments demonstrate the ability of LEEs to break valence bonds in model compounds and isolated DNA under a variety of conditions (Sanche, 2009; Alizadeh et Sanche, 2012; Alizadeh *et al.*, 2015). LEE bombardment stimulates the desorption of various ionic fragments ( $\text{H}^-$ ,  $\text{O}^-$ ,  $\text{CN}^-$ ) from solid films of DNA model compounds below the ionization threshold (Ptasińska et Sanche, 2006). Upon LEE impact with solid films of plasmid DNA, numerous types of macromolecular damage are produced, such as strand breaks and DNA crosslinks, as inferred by the analysis of DNA fragments by gel electrophoresis (Brodeur *et al.*, 2018; Luo *et al.*, 2014). In the condensed phase, the maximum yield of ion desorption as well as strand breaks occurs in the region between 5-12 eV. Similar results with a maximum around 7 eV for strand breaks were also observed in oligonucleotides using a novel DNA origami platform approach (Schürmann *et al.*, 2017). Although it is clear that LEEs induce strand breaks in condensed films of oligonucleotides and plasmid DNA, there is a paucity of information about the chemical steps from initial bond cleavage to the formation of stable products. It is important to clarify these chemical steps and the corresponding intermediate and final products, because the structure of the final products ultimately dictates the biochemical consequences of damage in cellular DNA.

Previously, our approach has been to irradiate short oligonucleotides (e.g., GpCpApT, TpTpT, TpT) with monoenergetic LEEs (5-15 eV) as a dry condensed film under ultra-high vacuum (Zheng *et al.*, 2005, 2006a,b; Li *et al.*, 2011, 2010, 2008; Park *et al.*, 2011, 2013). The non-volatile products are recovered from the surface and subsequently subjected to LC-MS/MS analysis. Using this approach, the main products of DNA model targets were identified as non-altered nucleobases; 2) nucleotide fragments bearing a

terminal phosphate group; and 3) base modifications (e.g., 5,6-dihydrothymine and 5-hydroxymethyluracil). The formation of these products is explained by LEE-mediated dissociative electron attachment (DEA) involving C1'-N1 bond cleavage (nucleobase release); phosphodiester C-O bond cleavage (fragments bearing a terminal phosphate group), and either C-H or N-H bond cleavage (base modifications). Recently, we extended these studies to longer oligonucleotides and purified DNA exposed to LEEs with an average energy of 5.8 eV under standard temperature and pressure (Choofong *et al.*, 2016). Experimentally, the mechanism of strand break formation is mainly based on the appearance of fragments bearing a terminal phosphate; for example, Tp and pT from the irradiation of TpTpT with 10 eV electrons (Li *et al.*, 2010, 2008; Park *et al.*, 2011, 2013). However, various reactions of the sugar moiety result in the formation of fragments bearing a terminal phosphate group, such as the direct ionization of sugar moieties, photoexcitation of base cation radicals and others (Adhikary *et al.*, 2014). Thus, one of the goals in the present study is to confirm the mechanism of C-O cleavage by obtaining a more complete balance sheet of associated stable fragments using a relatively simple target, TpT.

Cleavage of the C1'-N1, C3'-O and C5'-O bonds in DNA has been extensively examined by molecular computational methods (Carsky et Curik, 2011; Gu *et al.*, 2012; Kumar et Sevilla, 2017; Kohanoff *et al.*, 2017). Although theory and experiment are largely in agreement, there is still much debate concerning the nature of the shape and core-excited resonances and in particular, the sites of initial electron capture and cleavage. The energy range between 0-4 eV is very interesting, since available reaction channels are limited to specific shape resonances decaying exclusively into DEA. This condition eliminates other more complex pathways arising from the attachment of 4-12 eV electrons. These include the mixed possibility of decay of core-excited resonances via DEA or autoionization leading to dissociation of electronically excited states. Core-excited resonances as well as some high-energy shape resonances are excluded for vLEEs in the 0-4 eV regime. Many theoretical investigations predict that the most favorable pathway to strand break in the vLEE regime involves the initial capture of electrons by the base moiety followed by transfer to an antibonding orbital and cleavage of the C3'-O3' bond as part of the sugar phosphate backbone (Aflatooni *et al.*, 1998; Simons, 2006; Bao *et al.*, 2006; Wang *et al.*, 2010; Smyth et Kohanoff, 2012; Chen *et al.*, 2014). In contrast, there is considerable theoretical support for DEA occurring via initial capture of vLEEs by the phosphate group, leading directly to strand breaks (Li *et al.*, 2003; Kumar et Sevilla, 2007, 2008, 2009; Bhaskaran et Sarma, 2014; Cauët *et al.*, 2013). Notwithstanding, there have been only a few experiments providing evidence for strand cleavage in this low energy regime (Martin *et al.*, 2004; Liu *et al.*, 2016; Solomun *et al.*, 2009; Kočišek *et al.*, 2018). To clarify the

chemical steps in the mechanism of formation of DNA strand breaks, we have examined in greater detail the formation of products from TpT upon impact with vLEE ( $\sim 1.8$  eV).

## 2.4 Methods and Materials

The irradiation system and protocol has been employed in numerous experiments with electrons of energies between 4-20 eV, as previously described in detail (Zheng *et al.*, 2004b). The target molecules are uniformly deposited by spin-coating on the inside surface of tantalum cylinders using a rotary device under reduced pressure. The system holds seven cylinders for individual irradiation with 11  $\mu\text{g}$  of target molecules per cylinder, which corresponds to approximately 5 monolayers taking the average density of DNA ( $1.7 \text{ g cm}^{-3}$ ). The advantage of this technique is that relatively large quantities of target molecules can be irradiated, permitting a more comprehensive chemical analysis of the stable products. Utilization of this apparatus for electrons below 4 eV, however, was not efficient because most electrons in this energy range were deflected away from the target due to space charges. To remedy this situation, an additional electrode was placed at the exit of the cylinder to reflect vLEEs back toward the irradiation surface (Fig. S1). By choosing the right distance between the cylinder and the electrode and by adjusting the magnitude of the magnetic field collimating the electron beam, the system was now able to efficiently irradiate the inside surface of the cylinder with vLEEs ( $\sim 1.8$  eV). The dispersion of electrons was adjusted with the aid of a multi-array charge detector to assure that the beam was uniform over the entire inner surface of the cylinder as described previously (Zheng *et al.*, 2004b).

The analysis of DNA modifications was carried out by ultra-high-performance liquid chromatography (LC) on line with tandem mass spectrometry (LC-MS/MS). The LC system (Nexera X2, Shimadzu) consisted of dual pumps (Model 30AD), an autosampler (SIL 30AC), a column oven (CTO-10AC) and an UV/Vis detector (SPD-20A). The products were separated using a Phenomenex Luna Omega 1.6  $\mu\text{m}$  Polar C18  $100 \times 2.1 \text{ mm}$  (i.d.) column protected by a pre-column of the same material. The temperature of the column was maintained at  $30^\circ\text{C}$ . For product separation, the mobile phase consisted of a gradient of 0.05% (v/v) formic acid in water (pH 3.5; solvent A) and 90% acetonitrile in water (solvent B). The mobile phase composition increased from 2% to 20% of solvent B in 10 min followed by a 2 min wash cycle with 100% of solvent B and a 3 min equilibration back to the initial conditions of 2% solvent B. For the detection of products, the eluent from the LC was first directed into a UV detector for quantification of the parent compound at 260 nm and then into the tandem mass spectrometer system (API 3000, AB-Sciex, Concord,



Canada). The products were detected in multiple reaction monitoring (MRM) mode taking preselected molecular and fragment ions. The key parameters for LC-MS/MS measurements, including MRM transitions, retention times and collision energies are summarized in Table S1.

Immediately following irradiation of the targets (TpT, TMP5', TMP3' and thymidine) with vLEEs, the target compound and the corresponding products remaining on the surface of the cylinders were recovered by carefully and repeatedly washing ( $3 \times 4$  mL) with a solution of aqueous methanol (50:50; v/v). The solutions were pooled and concentrated on a rotary evaporator to dryness in a 20 mL scintillation glass vial. Before analysis, the residue was dissolved in 80  $\mu$ L of water. The sample was first injected onto LC-MS/MS for the analysis of thymine, ddT3', and ddT5' with the MS operating in positive mode, and subsequently, injected for the analysis of TMP3' and TMP5' with the MS operating in negative ionization. An aliquot of the remaining solution was treated with either P1 nuclease and alkaline phosphatase for TpT or with only alkaline phosphatase for TMP5' and TMP3' to digest the nucleotides containing 5,6-dhT to the corresponding nucleosides for quantification by LC-MS/MS. The quantity of product was determined from the integrated peak areas obtained for each product in comparison to authentic standards, which were injected between 3-4 samples. The standards were purified by HPLC and calibrated for quantification by LC-MS/MS (SI, Supplementary Materials and Figs. S2-S6). The product peaks during a chromatographic run were normalized to the amount of parent molecules as recorded by UV detection at 260 nm on line with MS analysis. In the case of thymine, a known quantity of isotopically labeled thymine ( $m/z + 4$ ) was added to the solution used to recovery products from the cylinders. The formation of thymine induced by vLEEs was calculated from comparison of the natural and isotopic signals on the same chromatographic run. The yield of LEE-induced products was determined from the slope of a linear regression of the total moles of product versus moles of incident electrons (fluence). The moles of incident electrons was calculated from the current ( $\mu$ A) arriving at the inner surface of the cylinder multiplied by the time of irradiation (min), i.e.,  $1\mu\text{A} \times \text{min} = 0.6219 \times 10^{-9}$  moles of electrons.

## 2.5 Results and Discussion

### 2.5.1 Analysis of products from vLEE-induced modification of TpT

Six main products were observed upon irradiation of TpT with vLEEs (Figure 2.1). The analysis of products was carried out by LC-MS/MS as depicted for ddT3', TMP5', ddT5' and TMP3' (Fig. 2.2) and for Thy and 5,6-dhT (Fig. 2.3). The presence of thymine

(Thy) and thymidine mononucleotides (TMP5' and TMP3') in non-irradiated samples (Fig. 2.2b and 2.3a) can be attributed to low and unavoidable thermal instability of the target compound during sample manipulation. Because of the relatively high and variable background level of thymine, it was necessary to include an isotopically labeled standard of thymine ( $m/z + 4$ ) in the sample before irradiation (i.e., added during the spin coating step) to correct for variations in deposition and recovery (compare Figs 2a and 2.3c). The formation of products followed a linear relationship as a function of electron fluence (Figs. 2.4a-2.4d), indicating that each product arises from a single reaction of incident vLEE with target molecules. It was not possible to estimate the loss of TpT as a function of fluence due to variation in the recovery of TpT from the surface of the cylinders ( $\pm 10\%$ ). Based on the yield of observed products, the conversion of TpT by vLEEs at the highest fluence may be estimated to be about 0.1% of the initial amount of TpT deposited for irradiation. The amount deposited was 20 nmol while the total amount of products formed at the highest dose was only 0.2 nmol ( $\sim 1\%$ ). Thus, one can rule out the reaction of vLEEs with primary products of TpT as a source of measurable damage. In addition to the above products, we detected minor amounts of X1pT, where X1 represents 1',2'-dideoxyribose, and X2pT, where X2 represents 2'-deoxyribose ( $<1\%$  of the total yield of products, Figs S7 and S8).

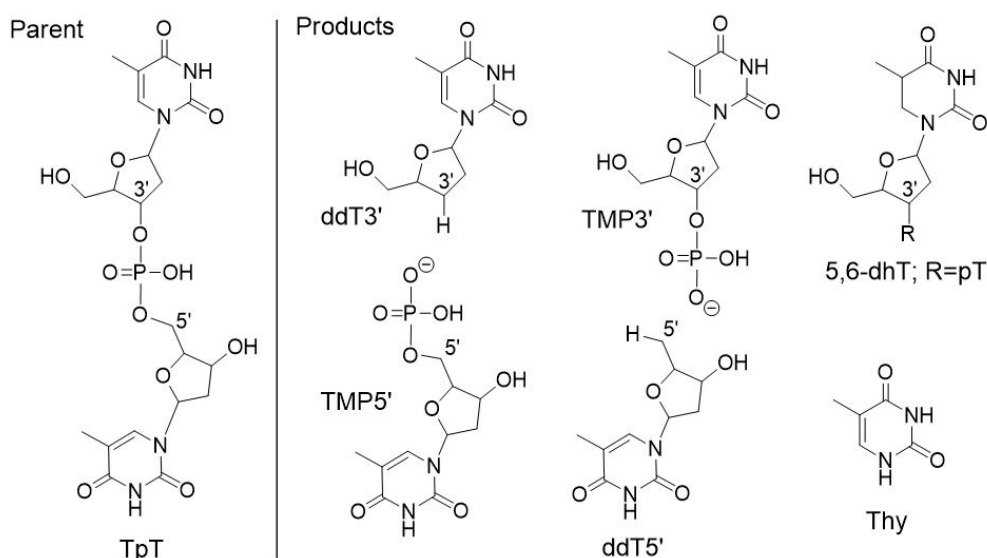


**Figure 2.1** – Structures of compounds under study. vLEEs irradiation of the parent compound (TpT) gave 2',3'-dideoxythymidine (ddT3'), thymidine 5'-monophosphate (TMP5'), 2',5'-dideoxy-thymidine (ddT5') thymidine 3' monophosphate (TMP3'), thymine (Thy) and 5,6-dihydro-2'-deoxythymidine (5,6-dhT).

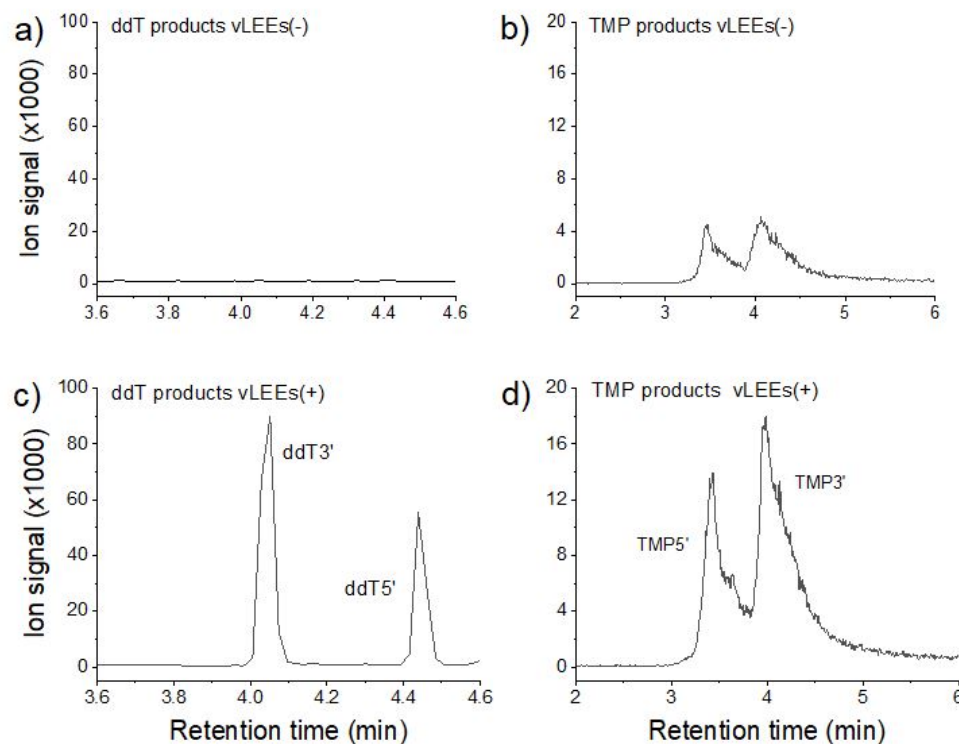


**Figure 2.2** – LC-MS/MS analysis of products from C3'-O and C5'-O cleavage of TpT. The formation of ddT3' and ddT5' increased considerably from non-irradiated controls (a) to irradiated samples (c). Likewise, the formation of TMP5' and TMP3' increased upon irradiation with vLEEs (chromatograms b and d).

### 2.5.2 DEA-mediated C-O bond cleavage of TpT

Four of the six main products can be attributed to DEA mediated C-O bond cleavage (Scheme 2.1 ). DEA at the phosphodiester C-O bonds likely involves heterolytic cleavage in which the negative charge transfers to the phosphate group, while the radical site localizes on the carbon atom. The alternative arrangement in which the radical species settles on the phosphate group with the anion at the carbon atom is much less favorable on the basis of energetic considerations (Simons, 2006; Bao *et al.*, 2006; Wang *et al.*, 2010). C-O bond cleavage within TpT may occur at either the C3' or C5' positions of the central phosphate. Cleavage at C3'-O results in the formation of TMP5' together with a C3'-centered sugar radical, whereas cleavage at C5'-O gives TMP3' together with a C5'-centered sugar radical (Scheme 1). The presence of dideoxyribose products (ddT3' and ddT5') together with the corresponding thymidine monophosphate products (TMP5' and TMP3') provides strong evidence for the above mechanism of phosphodiester C-O bond cleavage. The formation of ddT3' and ddT5' from the corresponding C3'- and C5'-centered radicals may

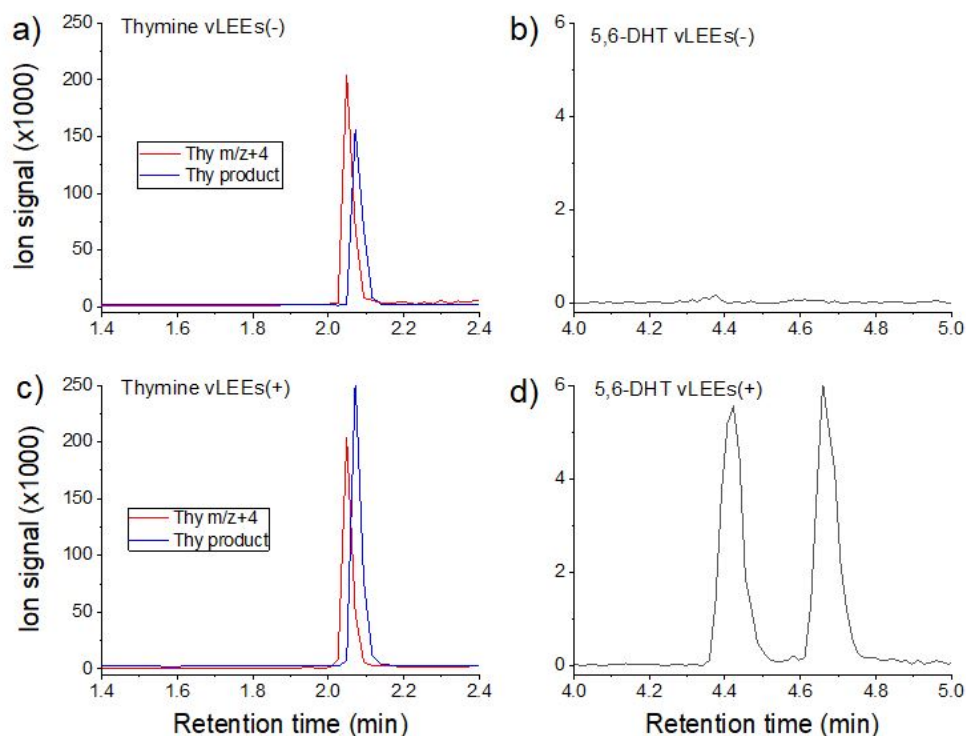


**Figure 2.3** – LC-MS/MS analysis of products from C1'-N1 cleavage and base reduction from TpT. The formation of thymine increased when comparing non-irradiated control to irradiated samples (chromatograms a and c) as indicated by the ratio of isotopically internal standard (red line) and natural product present in the sample (blue line). Likewise, the formation of TMP5' and TMP3' increased upon irradiation with vLEEs (chromatograms b and d).

be explained by either a reduction (+e) followed by protonation (+H<sup>+</sup>) or a single step H-atom abstraction (Scheme 2.1, Pathways a and b). C3'-centered radicals have been previously characterized by electron spin resonance spectroscopy at 77°K upon irradiation of hydrated DNA with argon and krypton ion beams (Becker *et al.*, 2003; Sevilla *et al.*, 2016). In addition, the same species were independently generated in aqueous solution by photo-induced cleavage of a C3'-substituted tert-butyl ketone derivative (Audat *et al.*, 2012). The latter study indicated that C3'-centered radicals efficiently convert into ddT3' in the presence of a reducing agent. Similarly, intermediate C3'-and C5'-centered sugar radicals may undergo reduction in our system by trapping thermalized electrons within the film during irradiation (Scheme 1, pathways a and b). Subsequently, protonation of ddT3' and ddT5' anions may occur with available protons in the system, i.e., residual water or basic protons of target molecules. As an alternative pathway to reduction followed by protonation, C3'-and C5'-centered radicals may undergo H-atom abstraction from neighboring

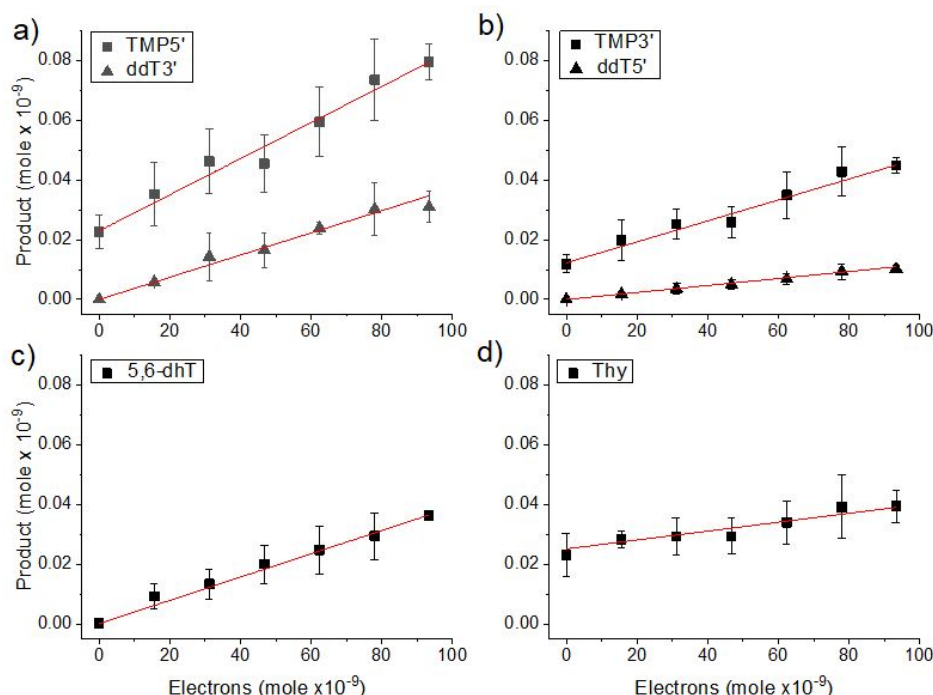


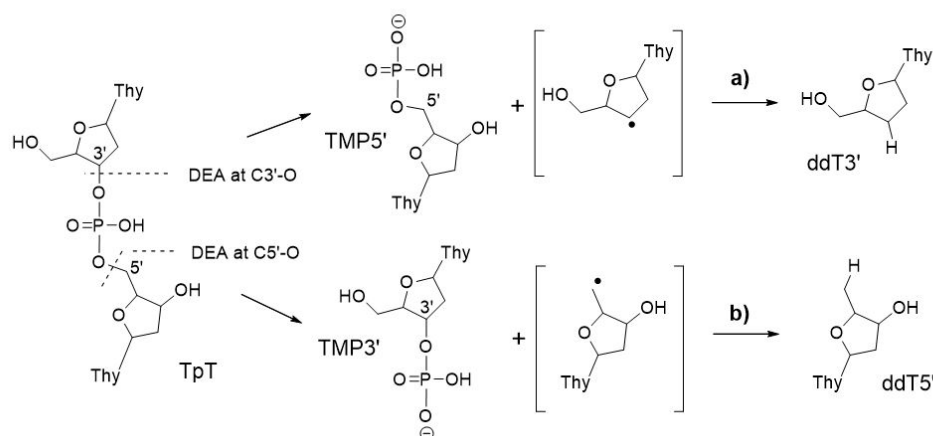
**Figure 2.4** – Formation of major products as a function of electron fluence. Error bars show the standard deviation from five independent experiments. Data were fitted by linear regression analysis (red line). Regression coefficient ( $r^2$ ) was greater than 0.99 except for Thy ( $r^2=0.92$ ). Percent error in standard derivation of the slope was 5.1% for TMP5', 3.6% for ddT3', 4.0% for TMP3', 4.7% for ddT5', 2.0% for ddT5', and 13% for Thy. All slopes were statistically significant ( $P < 0.001$ ).

molecules. It was not possible to distinguish between reduction followed by protonation versus H-atom abstraction without a more thorough investigation of minor products. Thus, we conclude that the conversion of C3'- and C5'-centered radicals to ddT3' and ddT5', respectively, occurs by either reduction followed by protonation or H-atom abstraction from neighboring target molecules.

From extensive theoretical studies, the mechanism of phosphodiester C-O bond cleavage by vLEEs is believed to involve initial capture of a vLEEs in the lowest unoccupied  $\pi^*$  orbital of the base accompanied with crossover of the electron into a  $\sigma^*$  orbital of the C-O bond of the sugar-phosphate backbone leading to cleavage (Zheng *et al.*, 2006b; Simons, 2006; Smyth et Kohanoff, 2012; Kumar et Sevilla, 2008; Bhaskaran et Sarma, 2015b). The driving force of this reaction, which occurs at very low energies ( $< 2.0$  eV), is attributed to the large electron affinity of the departing phosphate radical that attracts the electron to this site (Simons, 2006; Wang *et al.*, 2010). In the present study, the importance of the phosphate substituent is supported by comparison of the yield of products from TpT

**Table 2.1** – Summary of product yields for different molecular targets showing the efficiency of vLEE-induced damage in molecules of product per incident electrons ( $\times 10^{-4}$ ). The values were obtained from the slopes of a linear regression for the formation of each product as a function of fluence (Fig.2.4 for TpT; Figs. S9-S11 for TMP5'; Figs. S12-S14 for TMP3'; and Figs. S15-S18 for thymidine (dThd). All slopes were statistically significant ( $P < 0.05$ ).

Target	TMP5'	ddT3'	TMP3'	ddT5'	5,6-dhT	Thymine
TpT	6.0	3.7	3.5	1.2	3.9	1.5
TMP5'	—	—	—	0.6	6.9	4.4
TMP3'	—	3.1	—	—	7.2	5.8
dThd	—	0.4	—	0.2	15.2	12.1



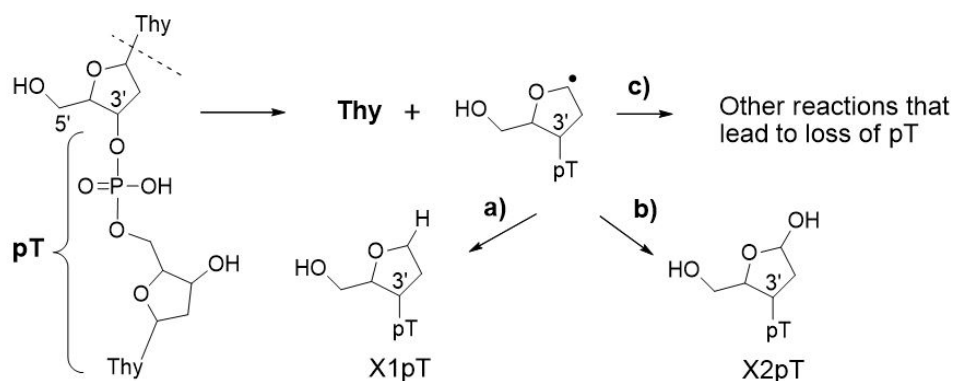
**Schematic 2.1** – Proposed mechanism for the formation of C3'-O and C5'-O cleavage products.

with corresponding yields from other targets with and without phosphate groups (TMP5', TMP3' and thymidine). The presence of a phosphate group at C5' enhanced the formation of ddT5' from TMP5' while a phosphate group at C3' enhanced the formation of ddT3' from TMP3' (Table 2.1). The lack of a phosphate group all together with thymidine as a target reduced the formation of either ddT3' or ddT5' by at least 4-fold. From the yields of ddT3' to ddT5', one can estimate the ratio of C-O cleavage at the C3' position to be 3-fold greater than that at the C5' position (0.35:0.12; Table 2.1). Such a bias toward C-O cleavage at the C3' position is also in agreement with theoretical predictions (Wang *et al.*, 2010; Chen *et al.*, 2014; Gu *et al.*, 2011). In sharp contrast, a theoretical investigation proposing direct attachment of vLEE to the phosphate group ( $P=O$   $\pi^*$  orbital) reported greater cleavage at C5'-O compared to C3'-O (Bhaskaran et Sarma, 2015a).

Interestingly, the yield of dideoxythymidine products (ddT3' and ddT5') was lower than the yield of thymidine monophosphate products (TMP3' and TMP5'; Table 2.1). This suggests that C3'- and C5'-centered sugar radicals arising from phosphodiester C-O bond cleavage do not quantitatively convert to ddT3' and ddT5' respectively, under our conditions. Other possible reactions of C5'-centered radicals may include cyclization with the base moiety and ring opening accompanied with base release as reported for similar sugar radicals (Shaik *et al.*, 2015; Shaw et Cadet, 1988). In addition, TMP3' and TMP5' may arise from alternative sources. For example, H-atom abstraction reactions from target molecules will create additional carbon-centered radicals possibly at the sugar moiety that are known to lead to phosphodiester bond cleavage as exemplified in the reactions of hydroxyl radicals with nucleotides and DNA (Sonntag, 2006; Raleigh *et al.*, 1974; Dedon, 2008).

### 2.5.3 DEA-mediated C-N bond cleavage of TpT

In addition to products arising from phosphodiester C-O cleavage, we observed the formation of non-altered thymine base release, indicating cleavage of the C1'-N1 bond, when TpT was bombarded with vLEEs (Table 2.1). During DEA at C1'-N1, the electron most likely transfers to N1 of the base moiety because the nitrogen radical is more electronegative than the carbon radical; hence, the C1'-centered radical is likely produced (Scheme 2.2) (Gu *et al.*, 2005; Li *et al.*, 2006). This radical is unique in comparison to radicals produced by H-atom abstraction at C1' of the sugar moiety and it has not previously been characterized in radiation studies. To understand the possible fate of putative C1'-centered radicals, we investigated the formation of X1pT, where X represents



**Schematic 2.2** – Proposed mechanism for the release of non-altered thymine.

1',2'-dideoxyribose, resulting from reduction followed by protonation of C1' centered radicals or H-atom abstraction (Scheme aSc2, pathway a). Because C1'-centered radical are

potentially oxidizing, i.e., being next to an oxygen atom, we also investigated the formation of X2pT, where X2 is equal to 2-deoxyribose (Scheme 2, pathway b). Surprisingly, the yield of either X1pT or X2pT was much less than that expected from the release of non-altered thymine (< 1%, Figs. S7 and S8). On one hand, the discrepancy between the yields of thymine and its fragment partners (X1pT or X2pT) suggest that there are alternative fates of C1'-centered radicals arising from DEA-mediated C1'-N1 cleavage. A possibility that has been proposed from theoretical studies involves the transfer of a proton from either the sugar or phosphate moiety to a nascent thymine anion, which significantly reduces the barrier for C1'-N1 cleavage (Kočišek *et al.*, 2018; Gu *et al.*, 2007; Dąbkowska *et al.*, 2005; Rak *et al.*, 2011). The transfer of a proton to a thymine anion during vLEE mediated C1'-N1 cleavage within TpT may lead to other products that were not detected in this work, such as further breakdown or modifications of X1pT and X2pT. Nevertheless, the low yield of non-altered thymine release relative to other products suggest that DEA-mediated C1'-N1 bond cleavage is a minor process when TpT is bombarded with vLEEs.

Although DEA-mediated cleavage of the C1'-N1 bond of DNA is supported by numerous experimental studies (Zheng *et al.*, 2005, 2006a,b; Li *et al.*, 2011, 2010, 2008; Park *et al.*, 2011, 2013; Choofong *et al.*, 2016), the majority of these studies has been performed with relatively high energy LEEs (10 eV). A striking difference in going from high (10 eV) to low (1.8 eV) electron energies is the lack of products arising from C1'-N1 bond cleavage products (i.e., thymine) accompanied with an increase in phosphodiester C-O cleavage (i.e., TMP5' and TMP3'). For example, the yield of thymine was remarkably 6.4-fold lower than the yield of TMP5' plus TMP3' upon exposure of TpT to vLEE (Table 2.1). In contrast, the opposite trend was observed with a 1.3 to 3-fold higher yield of thymine release compared to the formation of fragments with a terminal phosphate group when similar targets, e.g. TpT and TpTpT, were bombarded with electrons of higher energy (10 eV) (Li *et al.*, 2010, 2008; Park *et al.*, 2013). These results indicate that the C3'-O and C5'-O cleavage pathways gain importance at the expense of the C1'-N1 cleavage for the reaction of vLEE (1.8 eV) with TpT in comparison to LEEs with higher energy (10 eV). Our experimental observations are supported by theoretical predictions, which indicate that the energy barrier for C1'-N1 bond cleavage is higher than that for either C3' or C5' bond cleavage (Wang *et al.*, 2010; Chen *et al.*, 2014; Bhaskaran et Sarma, 2014). Thus, lowering the electron energy from 10 eV to 1.8 eV greatly reduces C1'-N1 bond cleavage and release of unaltered thymine.



#### 2.5.4 Reduction of thymine to 5,6-dihydrothymine by *v*LEE

A major product from *v*LEE irradiation of TpT was 5,6-dhT, observed as two isomers in equal amount after enzymatic digestion of TpT to its component nucleosides (Fig. 2d, Table 2.1). The same base modifications were observed in previous studies using similar reaction conditions except with electrons of higher energy (Park *et al.*, 2011). Previously, we attributed the formation of 5,6-dhT to the reaction of either hydride anions ( $\text{H}^-$ ) or hydrogen atoms ( $\text{H}\bullet$ ), which are by-products of initial DEA-mediated C-H bond cleavage reactions of high-energy LEEs (10 eV) (Alizadeh *et al.*, 2014). In the present study, however, the involvement of  $\text{H}^-$  may be excluded because their yield becomes negligible for electrons of energies lower than about 4 eV (Antic *et al.*, 1999; Ptasińska *et al.*, 2005; Ptasińska et Sanche, 2007). Similarly, the generation of  $\text{H}\bullet$  from large molecules has not been shown in the condensed phase although the reaction occurs in the gas phase as inferred by the desorption of  $(\text{B-H})^-$  from nucleobases (B) in the range of 1.1 to 2.4 eV (Denifl *et al.*, 2004). To explain the formation of 5,6-dhT, we propose an alternative pathway in which the reaction of *v*LEEs with TpT leads to transient negative ions of thymine, which subsequently lose their energy to the surroundings to form stable thymine radical anions. This is a reasonable hypothesis in view of the similarities in electronic structure between the electronic excited state of thymine radical anions and transient negative ions of thymine (Adhikary *et al.*, 2014; Carsky et Curik, 2011; Gu *et al.*, 2012; Kumar et Sevilla, 2017; Kohanoff *et al.*, 2017; Aflatooni *et al.*, 1998; Simons, 2006; Bao *et al.*, 2006; Wang *et al.*, 2010; Smyth et Kohanoff, 2012; Chen *et al.*, 2014; Li *et al.*, 2003; Kumar et Sevilla, 2007, 2008). The formation of 5,6-dhT is the primary diamagnetic product of thymine radical anions in both solid and aqueous environments in the absence of oxygen (Sonntag, 2006; Shaw *et al.*, 1988).

Interestingly, changing the target from TpT to thymidine monophosphates (TMP5' or TMP3') and finally to dThd reveals a marked increase in the formation of both 5,6-dhT and Thy (Table 2.1). The increase of 5,6-dhT and Thy is correlated with a decrease in products arising from phosphodiester C-O cleavage reactions (ddT3' or ddT5'), suggesting that all three pathways are in competition for individual reaction channels. This implies that the major products of *v*LEE-induced degradation of TpT may have a common precursor in their formation, i.e., the same transient negative ion that decays via the following DEA channels: phosphodiester C-O cleavage, C1'-N1 cleavage, and electron stabilization on thymine. Such modulation of the relative amount of product is similar to the end effect observed in previous studies with high LEEs (10 eV) in which base release from the termini is enhanced compared to base release from center positions of tetra- and trinucleotides.

cleotides (Zheng *et al.*, 2005; Li *et al.*, 2010). An explanation for the end effect is that internal bases can transfer to two C-O bonds for cleavage, whereas terminal bases can only transfer to a single C-O bond. The same phenomenon appears in TpT, which shows an increase in the yield of 5,6-dhT and Thy of two-fold upon removing one phosphodiester bond (i.e., with TMP5' or TMP3') and approximately another doubling of the latter products upon removal of a second phosphodiester bond (i.e, with dThd; Table 2.1).

## 2.6 Conclusions

When ionizing radiation interacts with DNA components, initial electrons with an average energy of 10 eV can break bonds in the target through dissociative excited states and core-excited and shape resonances. Examining the behavior of electrons near the lowest energy limit enables the observation of damage created only by shape resonances. This work demonstrates the ability of vLEEs ( $\sim 1.8$  eV) to break C-O bonds of the sugar-phosphate group of TpT based on chemical analysis of partner fragments, which include a thymidine monophosphates (TMP5' or TMP3') together with a dideoxythymidine product ((2',3'-dideoxythymidine (ddT3') or 2',5'-dideoxythymidine (ddT5')). The mechanism of DEA-mediated C-O bond cleavage is in close agreement with numerous theoretical studies, which predict that the electron is initially captured by the base moiety and transferred to either the C3' or to a lesser extent, the C5'-O position, of the phosphate-sugar backbone where DEA occurs. This reaction exemplifies the formation of prompt strand breaks in polymeric DNA. The chemistry of vLEEs ( $\sim 1.8$  eV) is different from that of higher energy electrons (10 eV) in that the C3'-O and C5'-O bond cleavage pathways are enhanced while the C1'-N1 bond cleavage pathway is reduced.

## 2.7 Acknowledgements

This work was supported by grants from the Natural Science and Engineering Research Council of Canada (NSERC) and the Canadian Institutes of Health Research (CIHR; grant no. PJT-162325).

## 2.8 Supplementary materials

5'-TpT-3' and 5'-X1pT-3', where X1 is equal to 1',2'-dideoxyribose, were purchased from AlphaDNA (Montreal), purified by reverse phase HPLC using 20 mM formate buffer in water, and desalted using reverse phase solid phase separation cartridges and water as the eluent. The purity of dinucleotides was greater than 99%, as estimated by HPLC analysis and UV detection at 220 nm. Thymine and the corresponding labeled compound (Thymine- $\alpha,\alpha,\alpha$ ,d4) were purchased from Sigma-Aldrich (T0376) and Cambridge

Isotope Laboratories (DLM-1089), respectively. Thymidine 5'-monophosphate was purchased from Alfa Aesar (J60747). Thymidine 3'-monophosphate was produced by treating TpT with an excess of bovine phosphodiesterase I (Sigma-Aldrich), which cleaves the phosphodiester bond to give thymidine 3'-monophosphate (TMP3') as the main product. The resulting compound was purified by reversed phase HPLC before doing the experiments. Thymidine (PY7727), 5,6-dihydrothymidine (PY7340), and 2',3'-dideoxythymidine (PY7277) were purchased from Berry and Associates Inc. 2',5'-Dideoxythymidine was purchased from Santa Cruz biotechnologies (SC256957A). 5'-X2pT-3', where X2 is equal to 2'-deoxyribose, was produced by acid hydrolysis of 5'-GpT-3' in 50 mM HCl at 37°C for 2 h, and the product was purified by reverse phase HPLC. Lastly, P1 nuclease (N8630) was purchased from Sigma-Aldrich and alkaline phosphatase (M0290S) from New England Biolabs.

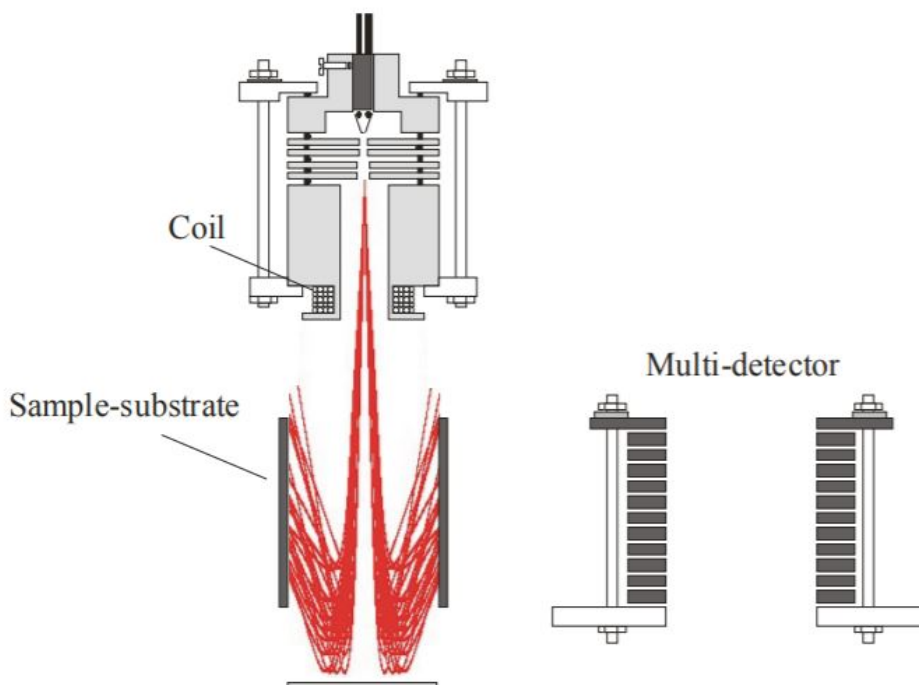


**Figure S1** – Diagram depicting the irradiation of target molecules. A system used in numerous experiments for electrons with energies between 4-20 eV (Zheng *et al.*, 2004b) was modified for electrons with lower energies (1.8 eV) by placing an electrode at the exit of the cylinder to reflect vLEEs back toward the surface. Red lines emanating from the electron gun (top center) show the simulated trajectory of vLEEs. A multi-detector (shown on the right) was inserted in place of the cylinder to adjust the electron flux so that electrons were evenly distributed along the inside surface of the cylinder.

**Table S1** – LC-MS/MS properties of vLEE-induced products of TpT, TMP3', TMP5' and thymidine. The products include thymine non labeled (NL), thymine labeled (L), 5,6-dihydro-2'- deoxythymidine (5,6-dhT), 2',3'-dideoxythymidine (ddT3'), 2',5'-dideoxythymidine (ddT5'), thymidine 5'-monophosphate (TMP5'), thymidine 3'-monophosphate (TMP3'), 5'-X1pT-3' where X1= 1',2'-dideoxyribose, and 5'-X2pT-3' where X2= 2'-deoxyribose. Products (a): LC separation was carried out with a Phenomenex Luna Omega 1.6  $\mu$ m Polar C18 100 x 2.1 mm (i.d.) column protected by a pre-column of the same material. The products were eluted with solvent A (0.05% formic acid) using a gradient of solvent B (90% acetonitrile) from an initial 1% to a final 30% in 8 min followed by a short wash (2 min) and re-equilibration (3 min). The nucleoside of 5,6-dhT was measured in separate runs after enzymatic digestion of the sample into its component nucleosides. The analysis of TMP3' and TMP5' was also carried out in a separate run under the same conditions as above except the MS was operated in negative mode. The dwell time of the MS was 100 ms and the analytes were measured using unit resolution. The complete analysis of products was carried out in three stages. Products (b): LC separation was carried out with a Acquity UPLC HSS T3; 1.8  $\mu$ m particle size; 100 x 2.1 mm (i.d.) protected by a VanGuard<sup>TM</sup> pre-column. The products were eluted with solvent A (5 mM formate buffer (pH 5.0) using a gradient of solvent B (80% acetonitrile) from an initial 1% to a final 12% in 8 min followed by a short wash (2 min) and re-equilibration (3 min).

	Detection mode	MS/MS Transition	Collision Energy	Retention time (min)	Ion Signal ( $\times 1000$ ) 1pmol	Signal/ Noise 1 pmol
Thymine NL <sup>a</sup>	Positive	127 to 110	25.0	2.05	25	65
Thymine L <sup>a</sup>	Positive	131 to 114	25.0	2.03	36	50
5,6-dhT <sup>a</sup>	Positive	245 to 117	20.0	4.42	15	350
ddT3' <sup>a</sup>	Positive	227 to 127	25.0	4.05	106	290
ddT5' <sup>a</sup>	Positive	227 to 127	25.0	4.40	141	430
TMP3' <sup>a</sup>	Negative	321 to 195	-22.5	4.00	18	70
TMP5' <sup>a</sup>	Negative	321 to 195	-22.5	3.40	9	57
5'-X1pT-3' <sup>b</sup>	Positive	423 to 181	20.0	4.50	3.7	30
5'-X2pT-3' <sup>b</sup>	Positive	456 to 421	12.5	3.85	2.7	22

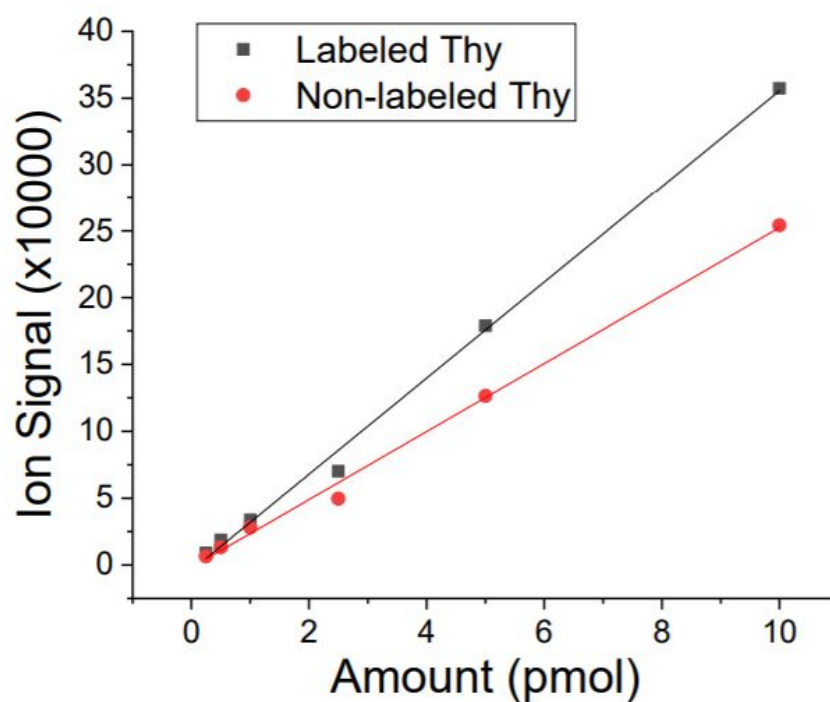


**Figure S2** – Calibration curve for labeled ( $m/z + 4$ ) and non-labeled thymine. Linear regression of the data gave  $y = 35.9x - 4.1$  ( $r^2 > 0.99$ ) for labeled Thymine (Thy) and  $y = 25.4x - 2.0$  ( $r^2 > 0.99$ ) for non-labeled Thymine (Thy).

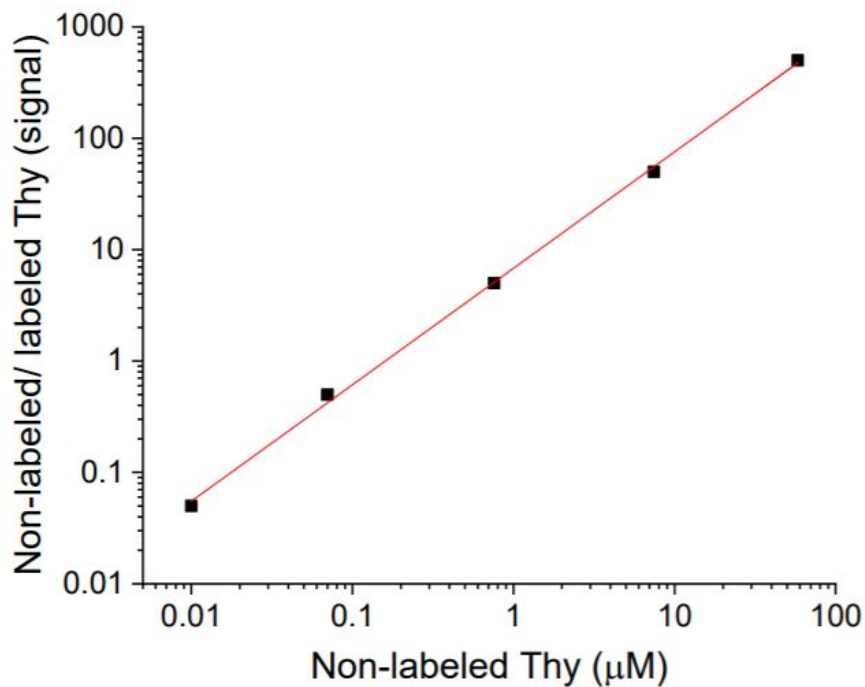


**Figure S3** – Calibration of isotopic standard for the quantification of thymine. Linear regression gave:  $y = 0.83x + 1.05$  ( $r^2 > 0.99$ ).

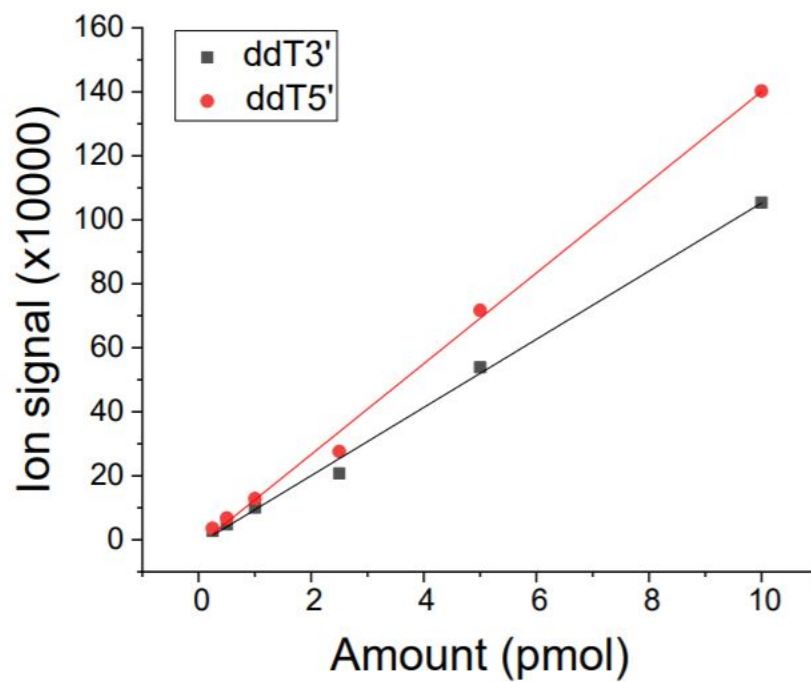


**Figure S4** – Calibration curve for ddT5' and ddT3'. Linear regression of the data gave  $y = 14.1x - 1.7$  ( $r^2 > 0.99$ ) for ddT5' and  $y = 10.6x - 1.2$  ( $r^2 > 0.99$ ) for ddT3'.

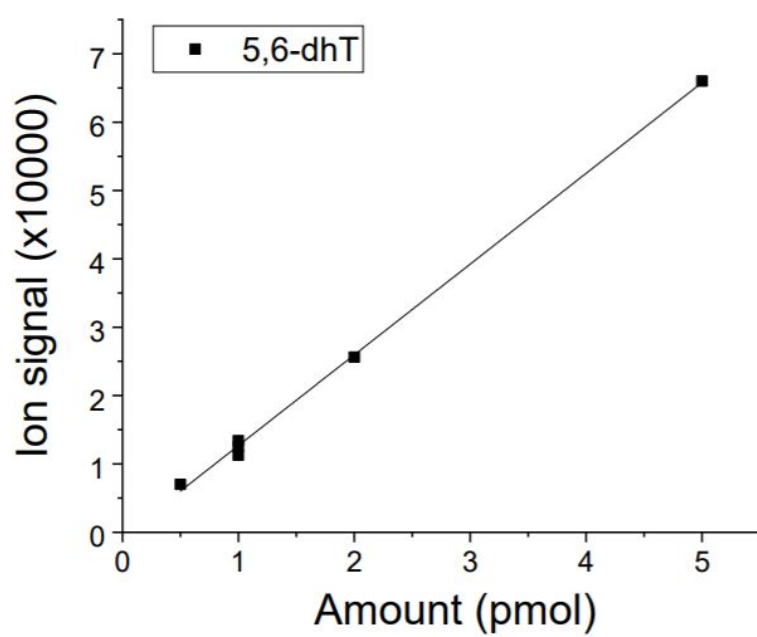


**Figure S5** – Calibration curve for 5,6-dhT. Linear regression of the data gave  $y = 1.33x - 0.06$  ( $r^2 > 0.99$ ).

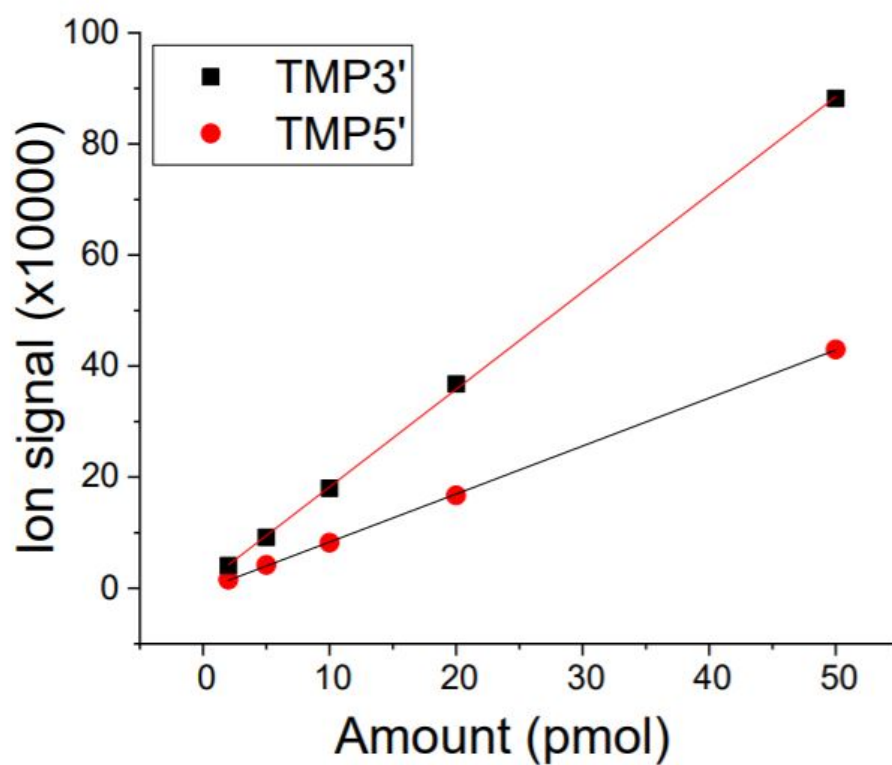


**Figure S6** – Calibration curve for TMP3' and TMP5'. Linear regression of the data gave  $y = 1.76x - 0.68$  ( $r^2 > 0.99$ ) TMP3' and  $0.86x - 0.3$  ( $r^2 > 0.99$ ) for TMP5'.



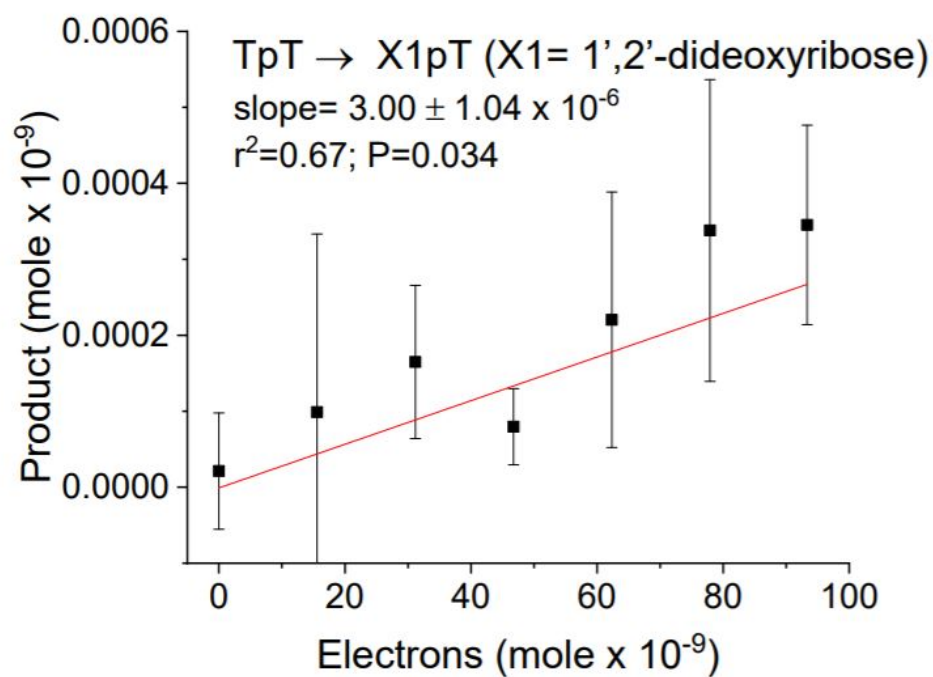


**Figure S7** – Formation of 5'-X1pT-3' from irradiated 5'-TpT-3'.

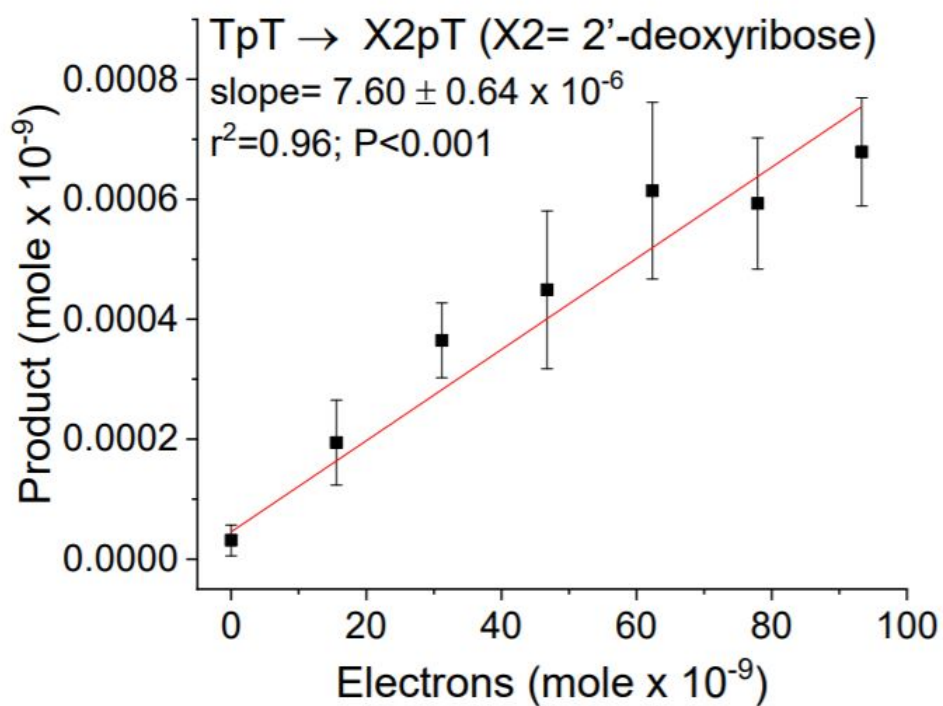


**Figure S8** – Formation of 5'-X2pT-3' from irradiated 5'-TpT-3'.

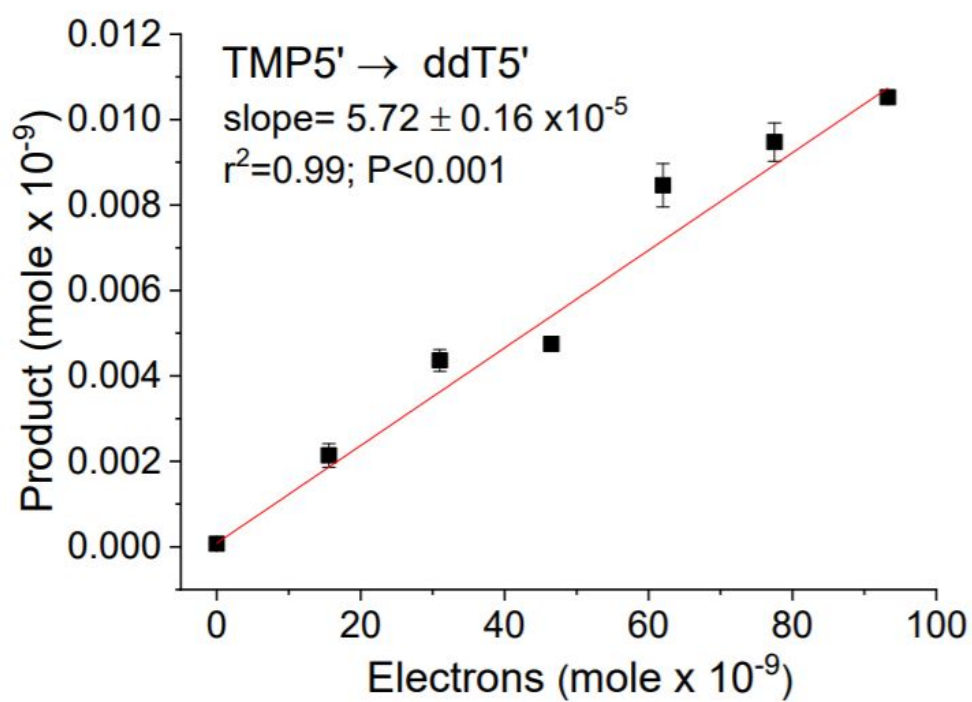


**Figure S9** – Formation of ddT5' from irradiated TMP5'.

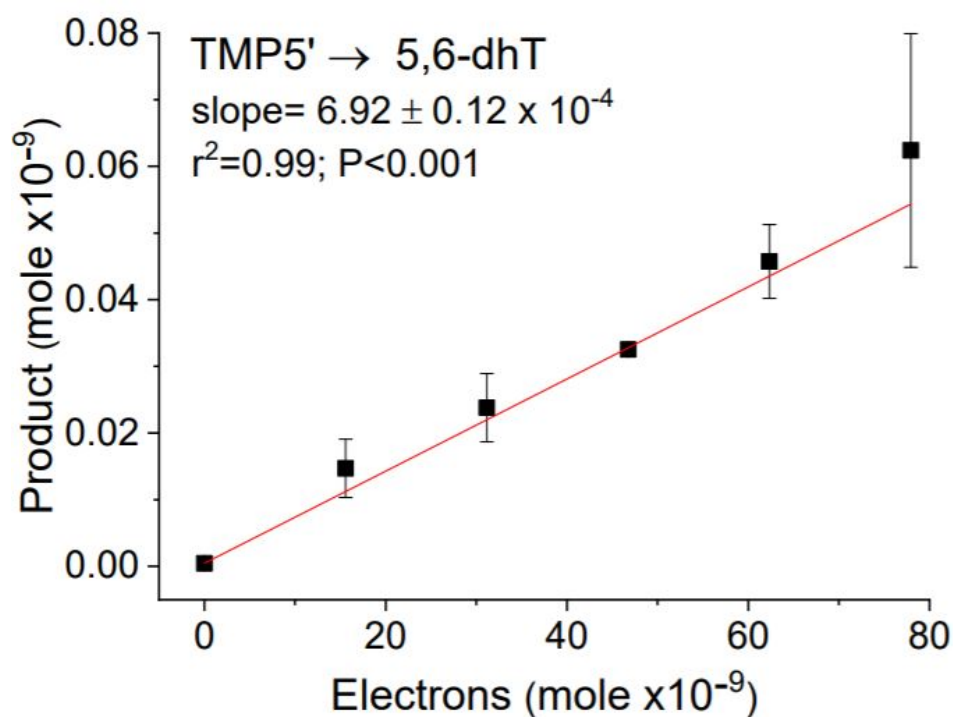


**Figure S10** – Formation of 5,6-dhT from irradiated TMP5'. Note that the dinucleotide was enzymatically digested to the nucleoside before analysis.

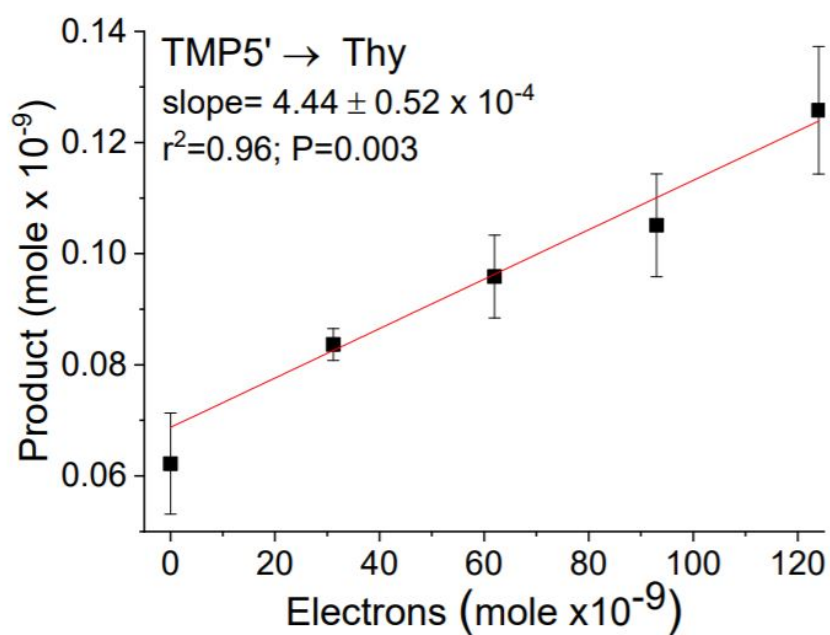


**Figure S11** – Formation of Thy from irradiated TMP5'.

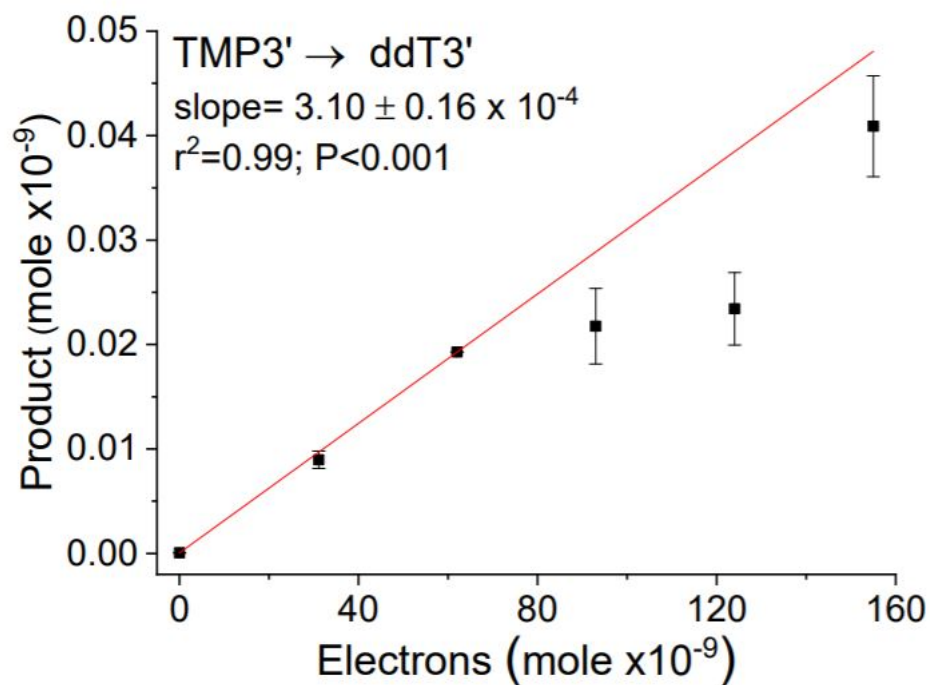


**Figure S12** – Formation of ddT3' from irradiated TMP3'.

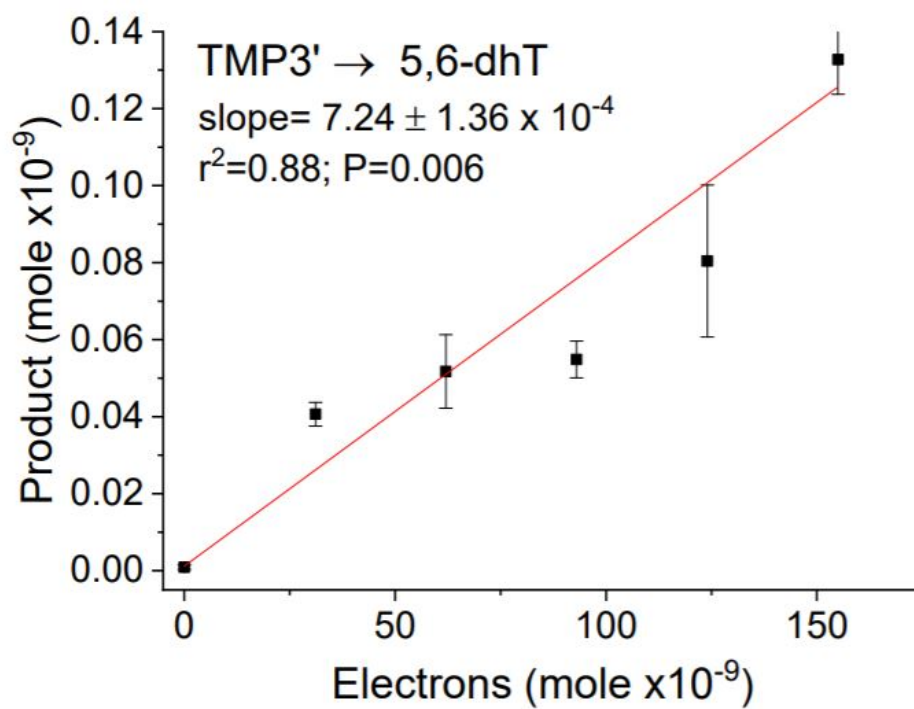


**Figure S13** – Formation of 5,6-dhT from irradiated TMP3'.

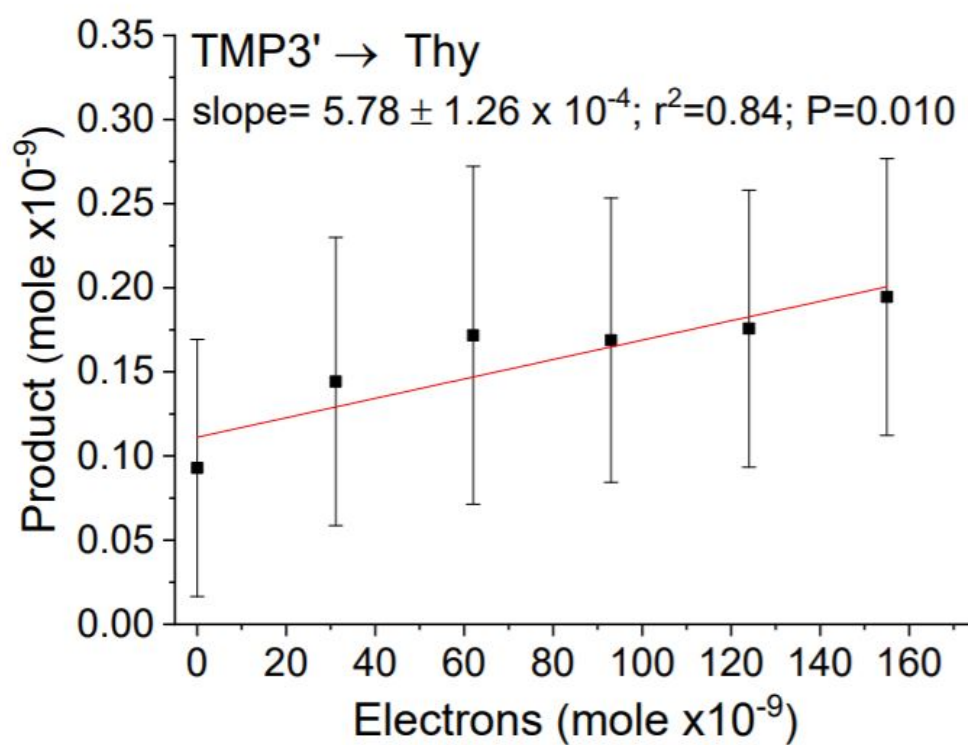


**Figure S14** – Formation of Thy from irradiated TMP3'.

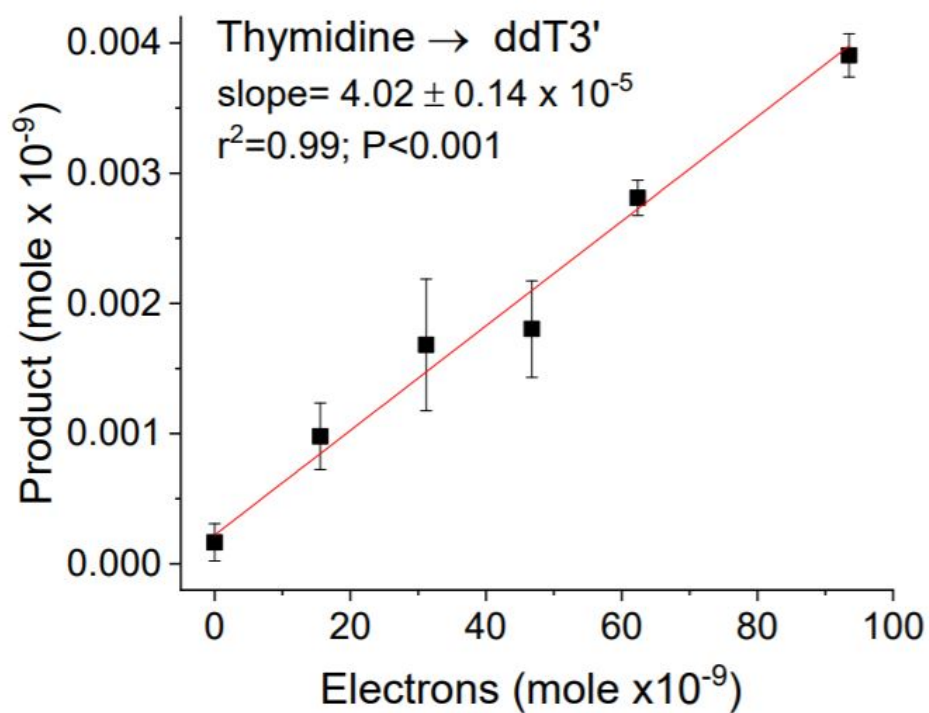


**Figure S15** – Formation of ddT3' from irradiated thymidine.

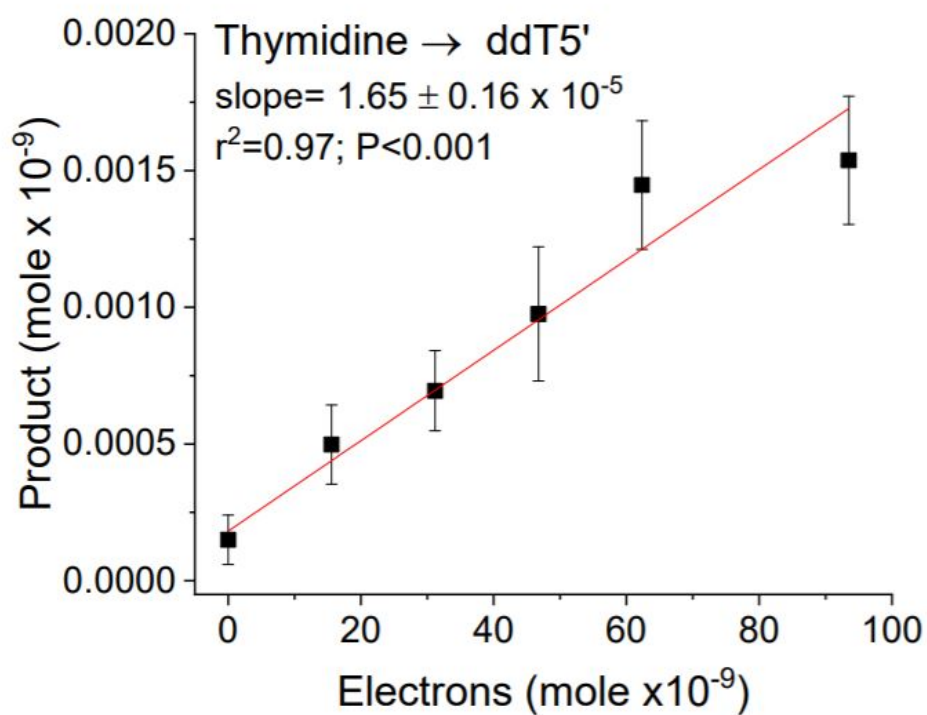


**Figure S16** – Formation of ddT5' from irradiated thymidine.

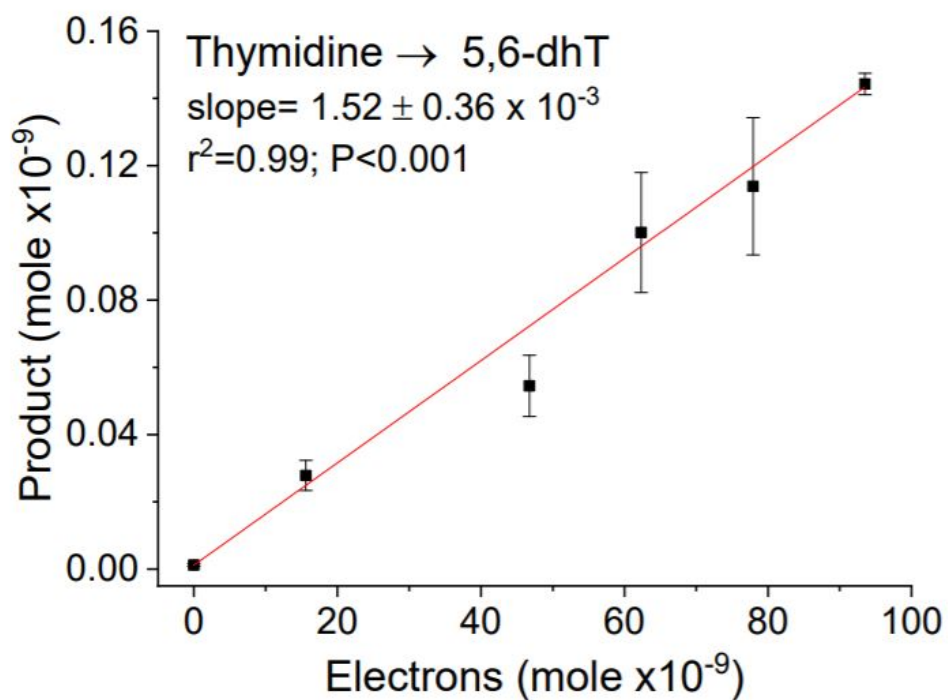


**Figure S17** – Formation of 5,6-dhT from irradiated thymidine.

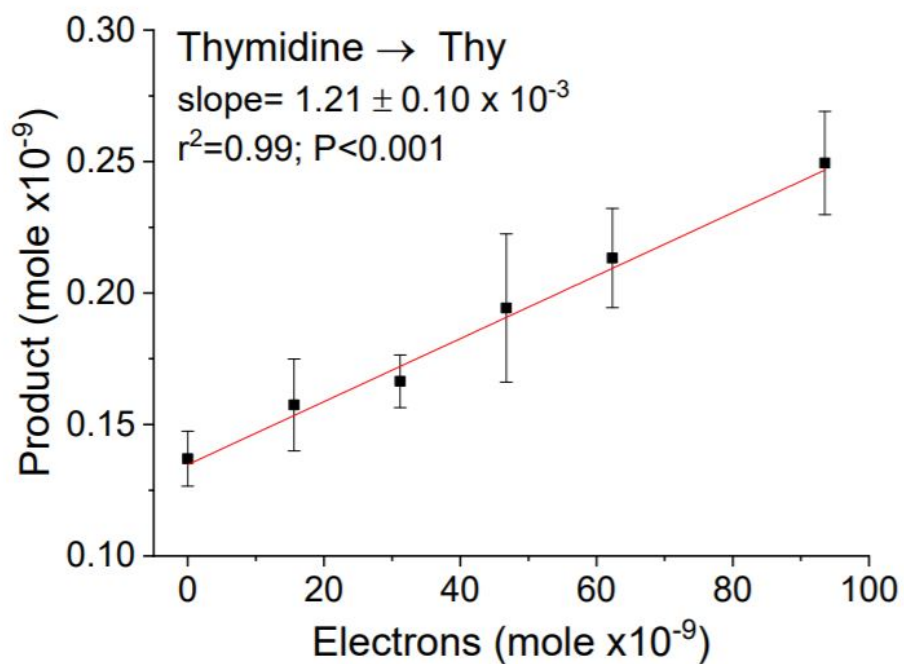


**Figure S18** – Formation of Thy from irradiated thymidine.

## 3 DISCUSSION

### 3.1 Fragments and mechanisms induced by vLEE

By using the spin coating system and modified LEE gun irradiator that is capable of producing the electrons below 3 eV which is described in the introduction and also utilizing TpT molecule as a small, simple model of DNA, sufficient amounts of degraded compound can be provided and prepared for chemical analysis by LC-MS/MS. This experiment is divided into two parts, in the first part we detected the mechanism of damage and calculated the yield of products in TpT model and in the second section we focused on LEE induced damage within a series of TpT model compounds (dThd, pT, Tp). Our result demonstrated that three mechanisms are involved in causing damage to TpT molecule and its fragments, N-glycosidic bond cleavage, Phosphodiester bond cleavage, base damage. These mechanisms can explain the formation of several fragments produced by vLEE bombardment.

#### 3.1.1 *First part: N-glycosidic bond cleavage*

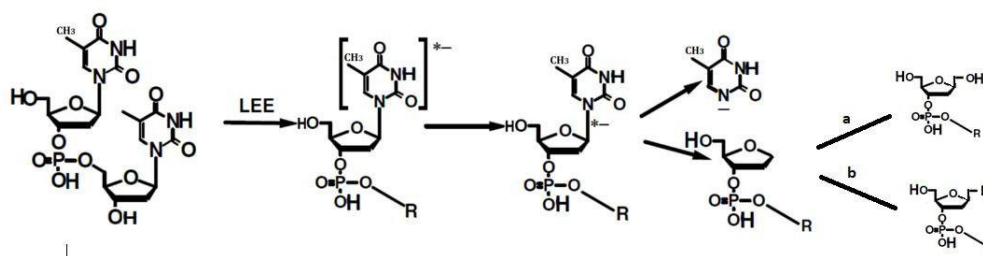
First, Zheng et al. reported that a Low-energy electron with a broad resonance centered near 11- 12 eV efficiently broke the N1-glycosidic bond of thymidine (dThd) and separated the base and sugar moieties. These analyses revealed the formation of thymine as the most abundant product suggesting that, at this energy, thymine was produced mainly via the formation of core-excited resonances located near 11-12 eV energy range (Zheng *et al.*, 2004b) involving dissociative attachment process (<15 eV). Several theoretical studies, such as density functional theory, also showed that an electron captured by the base and, after that, base release are preliminary processes in the mechanism of N-glycosidic bond cleavage.

Along the same line of work, we investigated the fragmentation and yield of damage of thymine dinucleotide by a very low energy electron ( $\sim 1.8$  eV). Our results indicated that the N-C cleavage by vLEE occurred mainly by the formation of shape resonances followed by the electron captured by the base and subsequent base release, for example, at the beginning, an electron attached to the thymine moiety and the transient negative thymine anion was created. Then, the N-glycosidic bond ruptured by a dissociative electron attachment releasing a thymine anion and a 2-deoxyribose radical. The proposed mechanism is supported by several theoretical studies such as density functional theory which shows



that an electron captured by the base and, after that, base release are preliminary processes in the mechanism of N-glycosidic bond cleavage. Gu et al. calculated the bond- breaking activation energy in the dT anion and also the electron detachment energy for dT anion as 18kcal/mol and 22 kcal/mol respectively (Gu *et al.*, 2005). Their results confirmed that separating the electron from dT anion requires more energy than breaking the N-glycosidic bond; therefore, the cleavage of N-glycosidic bond dominates when an electron is attached to thymidine. The proposed mechanism is shown in Scheme. D1.

Along the same line of work, we investigated the fragmentation and yield of damage of thymine dinucleotide by a very low energy electron ( $\sim 1.8$  eV). Our results indicated that the C-N cleavage by vLEE occurred by DEA mediated cleavage of the C-N bond, producing a thymine anion and a sugar fragment, with a radical site at C1'. Consequently, the C1' centered radical undergoes reduction followed by protonation, releasing the 1',2'-deoxyribose products (Scheme D1, a and b). we measured the yield of these products and found that the yield of non-modified thymine was much higher than the expected from the 1',2'-deoxyribose products. From this, we can infer that DEA-mediated C1'-N1 bond cleavage is a minor process when TpT is bombarded with vLEEs, In conclusion, we suggested that the release of thymine does not involve DEA at the C-N bond but rather another reaction that leads to the release of thymine.



**Schematic D1** – A proposed mechanism for thymidine N-glycosidic bond break by LEE bombardment

The formation of the thymine was identified by LC-MS/MS with authentic compounds for TpT, and then the yield of the product was calculated and estimated.

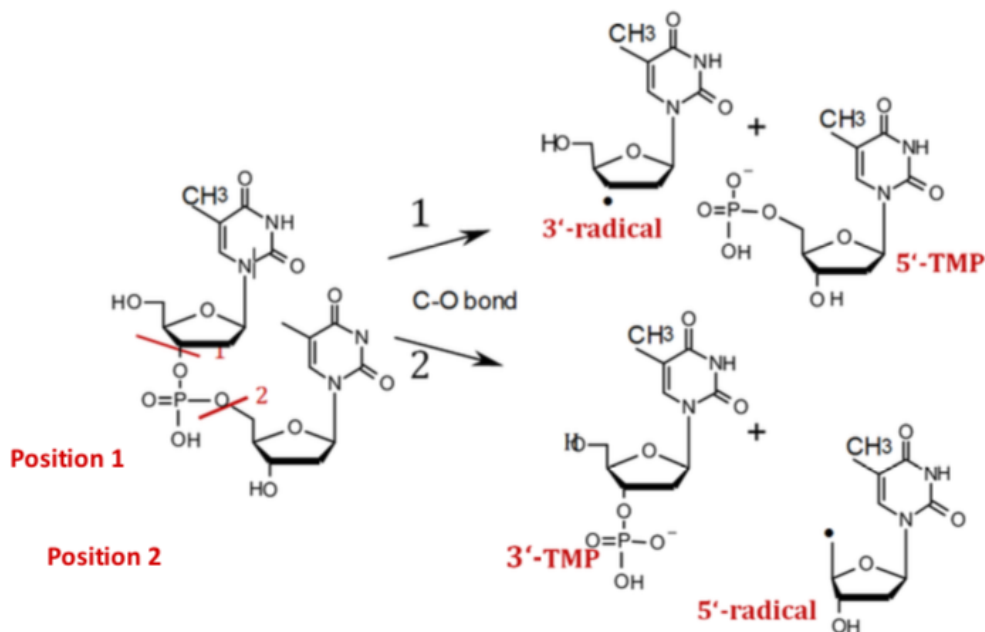
### 3.1.2 First part: Phosphodiester bond cleavage (at 3' C-O bond and 5' C-O bond)

In the present study, by our analysis of fragments and investigation of the mechanism from oligonucleotide dimer, we showed that cleavage of the phosphodiester bond primarily takes place via the formation of TNI followed by an electron transfer from the base to a phosphate group with a  $\sim 1.8$  eV low energy electron (Scheme. D2). Several theoretical

and experimental investigations inspired our work in this area, one of them which was done by our group several years ago was focused on the C-O bond cleavage with an 11 eV low energy electron (Zheng *et al.*, 2006a). They found that at 11 eV, an electron can be localized on the phosphate group of the DNA by two processes, the first one is a direct capture of the electron by the phosphate group of DNA and the second one is the initial capture of the electron by the base and then transferred to the sugar-phosphate C-O bond. (Zheng *et al.*, 2006a; Berdys *et al.*, 2004; Pan et Sanche, 2005, 2006) During an electron transfer, the base goes from a ground state to an excited state (Ptasińska et Sanche, 2007), therefore, the electron has adequately low energy to fill the P=O  $\pi^*$  orbital which can pass within the dissociative  $\sigma^*$  orbital causing the C-O bond rupture (Berdys *et al.*, 2004). This idea can be represented by the release of thymine from thymidine by a non-ionizing resonance process involving DEA as shown in Scheme. D1 (Zheng *et al.*, 2004b). Also, Simons et al. calculations demonstrated that, for electrons in the 0.1-2 eV range, C-O bond cleavage is most probably created if an electron enters a low-lying  $\pi^*$  orbital of a DNA base to form a shape resonance before an electron transfer event. (Simons, 2006).

There are several theoretical studies focused on the behavior of the phosphate group in DNA towards the attack of low energy electrons under 10 eV; Gu et al. and Bao et al. investigated the LEE-induced phosphodiester C-O bond cleavage by using density functional theory (DFT) at 3' and 5' positions respectively. Their results revealed that first, a stable thymidine anion is formed followed by an electron transfer to the phosphate group C-O bond and then, when the phosphodiester C3'-O3' bond breaks, it will release the Thymidine 5'-monophosphate (5'-dTMP), and a 2-3'-deoxyribose radical (2,3'-ddT)(Position 2, Scheme. D2) and, in the case of the phosphodiester C5'-O5' bond cleavage, the products will be the thymidine 3'-monophosphate (3'- dTMP) and a 2-5'-deoxyribose radical (2,5'-ddT) (Position 1, Scheme. D2).

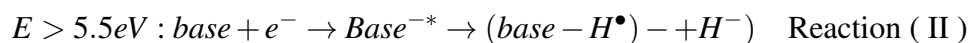
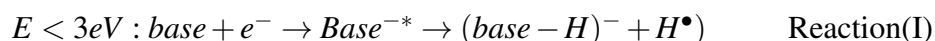
It is remarkable that the yield of products resulting from 3' C-O (Tp, 2.32) (Position 1, Scheme. 2) bond cleavage was higher than those from 5' C-O (pT 1.37) (Position 2, Scheme. 2) bond cleavage in TT. These results are in good agreement with the theoretical studies which calculated the energy barrier for C3'-O3' and C5'-O5' (Anusiewicz *et al.*, 2004). These studies reported that the energy barrier for C3'-O3' in the gas phase and the aqueous solution are 7.06 kcal/mol and 13.73 kcal/mol respectively whereas they reported the energy barrier for the C5'- O5' in the gas phase and the aqueous solution are 13.84 kcal/mol and 17.86 kcal/mol respectively. Therefore, they concluded that the C3'-O3' a-bond rupture dominates the LEE-induced SSB of DNA.



**Schematic D2** – Proposed mechanism of C-O bond cleavage and released products by LEEs

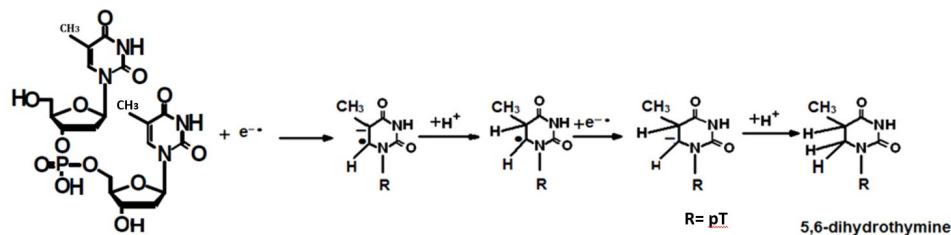
### 3.1.3 First part: Base damage (Conversion of thymine to 5,6-dihydrothymine moiety)

Earlier, in our results of oligo analysis, we identified LEE-induced modifications of thymine within TpT by two possible pathways: 1) addition of hydride anions or 2) addition of neutral hydrogen atoms ( $H^\bullet$ ) to the 5,6-double bond of Thy which becomes attached to the double bond of the thymine ring at C5-C6 site resulting in 5,6-dihydrothymine-5(or 6)-yl radicals that subsequently transform into 5,6-dHT by reduction. It is proven that DEA processes for thymine derivatives in the gas phase involve the loss of  $H^\bullet$  if electrons have subexcitation energies (i.e.,  $E < 3\text{eV}$ )(Reaction I) and loss of  $H^-$  if electrons have energy above 5.5 eV (Reaction II) (Ptasińska et Sanche, 2006; Alizadeh *et al.*, 2014; Abdoul-Carime *et al.*, 2004).



Generally, these processes depend on the energy of the incoming electron to cause the ejection of a hydrogen atom or a hydride anion (Denifl *et al.*, 2004). Since we were dealing with 1.8 eV electrons, hydride anions were not included in our experiment which is the target bombardment with electrons of energies lower than about 4 eV. Therefore, we introduce another pathway which is the reaction of vLEEs with TpT creates transient

negative ions of thymine, leads to forming stable thymine radical anions. This fragment is the strong base; thus, it will get protonate and form the 5,6-dihydrothymine (5,6-DHT) (Scheme. D3)



**Schematic D3** – A proposed pathway for formation of 5,6-dihydrothymine (base damage).

### 3.1.4 Second part: Damage induced on monomers by *vLEE*

In the second part of this project, we focused on the effect of a low energy electron on uncomplicated molecules. Three mononucleotides: thymidine 3'-monophosphate (Tp, 3'-dTMP), thymidine 5'-monophosphate (pT, 5'-dTMP), and thymidine (dThd) were bombarded with LEE individually under the same LEE irradiation conditions. The principal purpose of this part of our project is to investigate the effect of a phosphate group and also to have better knowledge of the LEE mechanism and electron transfer process under the same LEE irradiation conditions. Based on our results of product identification and investigation, we can divide our conclusion into two sections: 1) increased N-C cleavage in monomers 2) decreased C-O bond cleavage in monomers.

#### 1) Increased N-C cleavage in monomers (Release of thymine)

Our results demonstrated that (Table, Chapter 2) removing the phosphate group from monomers caused the release of more thymine. Generally, we can say that as a complexity increases, N-C cleavage will decrease. The electron transfer process can explain this idea supported by theoretical studies which indicate the energy barrier is much higher for N-C cleavage than both C-O bond, C5'-O5' bond, and C3'-O3' bond cleavage (Gu *et al.*, 2010). According to these results, when an electron is attached to the nucleobase, the N-glycosidic bond is more difficult to break and an electron transfer to the phosphate C-O bond is more accessible, hence, C-O bond cleavage will dominate. This means that, in the loss of a phosphate group, the yield of base release is increased because, when there is no phosphate, none of the electrons can transfer to that unite. Therefore, they only can focus on breaking the N1-C glycosidic bond and releasing more thymine and, consequently,

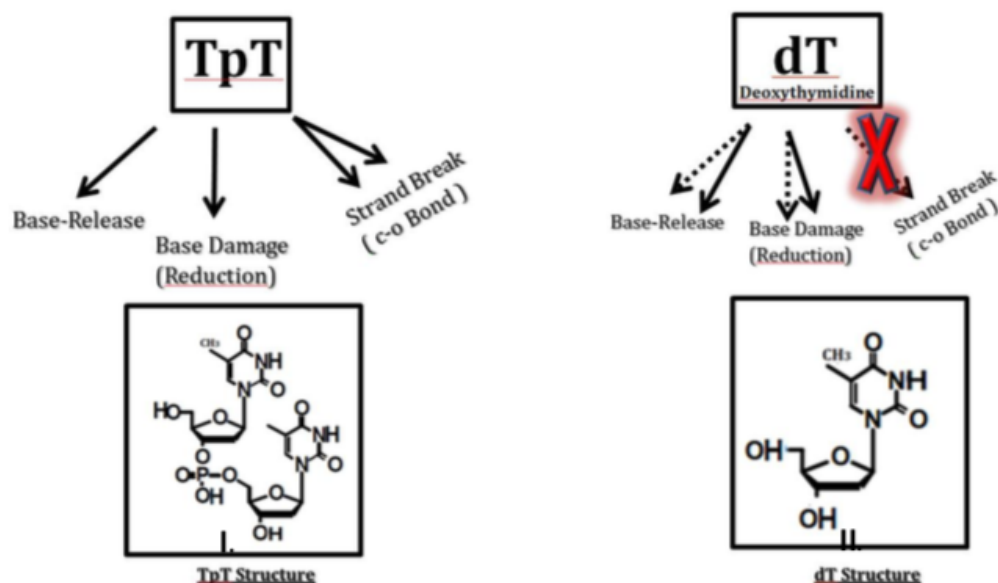
more base is released (5,6-DHT) as is shown in Table 2.1 in Chapter 2. Also, Something to check in future experiments is whether the expected products of DEA-mediated C-N cleavage arise in substrates that lack the phosphate group. This may suggest that as we eliminate a low-lying pathway, i.e., C-O cleavage, a higher lying pathway (i.e., C-N cleavage) is enhanced.

## 2) Decreased 3' C-O bond and 5' C-O bond cleavage in monomers

Our results demonstrated that (Table 2.1, Chapter 2) the yield of products released from a single- strand break or C-O bond cleavage is larger for TpT (5.19) than Tp (0.7), pT (0.3), or dThd (0.1). This indicates that all of the processes leading to damage involve DEA. The total yield stays about the same while the importance (i.e., the yield) of each of the individual pathways is different in the more complex molecule than the simpler one due to the base stacking effect which enhances overlap of  $\pi$  orbitals and ,therefore, results in greater delocalization of the initial electron wave (Caron et Sanche, 2005) enabling more thermodynamically acceptable and particular pathways (Ptasińska et Sanche, 2007) for the formation and decay of transient anions of the subunit.

These studies have several conclusions and implications for LEE induced DNA damage. First, based on our results, we cannot deny the fact that the phosphate group is needed to have DEA and then, induce a single-strand break because the electron affinity of phosphate drives the C-O bond cleavage and it is favorable to induce a single-strand break (Barrios *et al.*, 2002).

Second, from the comparison between the yield of products released from monomers and TpT dimer, we can conclude that the lower yield for Thy and DHT products is due to the availability of more decay channel for the complex molecule. Generally, the main point is when there is a phosphate group between the two bases and, therefore, increased complexity, the yield of N-C cleavage products and base damage decreases while the yield of C-O bond breakage products increases, thus, these two processes are related to each other. For instance, the yield of thymine release is lower than the dThd. In other words, there are more low-energy channels for more complicated molecules like TpT and, then, TMP and dThd. In the reverse effect, the yield of C-O bond cleavage products are much higher for TpT than dThd. This shows that electron transfer is sensitive to the structure of the molecule and will change with more complexity and orbital configuration (Scheme. D4).



**Schematic D4** – There are 3 main channels for TpT, II) For simpler molecule such as dThd (dT) fewer channels are available, thus, the electron has an increased probability to go to the other side.

### 3.1.5 Comparison of our findings to previous studies

Over the past few years, our group focused on monoenergetic LEEs (5-15 eV) induced damage by using short oligonucleotides (e.g., GpCpApT, TpTpT, TpT) as target. (Zheng *et al.*, 2004b, 2006a; Li *et al.*, 2011, 2008; Park *et al.*, 2011, 2013).

The main products of DNA model targets classified as (1) cleavage of the N-glycosidic bond leading to the release of nonmodified nucleobases (e.g., release of thymine from thymidine) and (2) cleavage of the phosphodiester C-O bond leading to the formation of a fragment with an intact terminal phosphate group; and 3) base modifications ( C-H or N-H bond cleavage). Li *et al.*, focused on the effect of terminal phosphate and base moieties on LEE ( 5-15 eV)-induced DNA damage (Li *et al.*, 2008). First they found that, the presence of terminal phosphate groups in monomers (pT, Tp, pTp) and dimers (pTpT, TpTp, pTpTp) increases overall damage by 2-3-fold while it decreases N-C and C-O bond cleavage by 2-10 fold. Furthermore, they showed that the yield of damage channeled to N-C and C-O cleavage in monomers (pT, Tp, pTp) , dimers (pTpT, TpTp, pTpTp) and a trimer TpTpT will increases with the number of nucleotides in the molecule thus, they concluded that phosphate appears to be an essential factor to induce DNA damage. We cannot ignore the fact that the phosphate group also captures electrons, i.e., especially 10

eV electrons, and this gives additional products that we did not identify in previous studies. Therefore, one of our goals in the present study is to prove the C-O cleavage mechanism through the bombardment of the DNA component TpT,pT,Tp, dT, using vLEE (  $\sim 1.8$  eV ).

The vLEE (0-4 eV) mechanism of damage (0-4 eV) is different than the higher energy. For instance, there are less pathways available for vLEE ( $\sim 1.8$  eV ) compare to complex channels which are resulting from the attachment of 4-12 eV electrons. The reason for this situation is possible reaction channels for vLEE are restricted to specific shape resonances decaying into DEA, and therefore Core-excited resonances are not involved in 0-4 eV electron energy range. Our results confirm that first, the mechanism of C-O cleavage and creation of strand breaks in DNA induced by vLEE occur by the formation of a transient anion, localized on the base moiety. Second, the significance of the phosphate group is determined by comparing our target with and without phosphate groups, we showed that there is a decrease in the yield of products such as thymidine, which the absence of a phosphate group reduces the production of both ddT3' or ddT5' by at least 4-fold compared to the thymidine monophosphate 3' or 5'.

On the other hand, we demonstrated the release of thymine for TpT which were bombarded with electrons of 1.8 eV electrons was 1.3 to 3-fold lower than the yield of TpT and TpTpT after bombardment with LEEs of 10 eV. Thus our experiments confirm that C-O cleavage pathway is more preferred than the C-N cleavage pathway for the reaction of vLEE (1.8 eV) with TpT in comparison to LEEs with higher energy.

There are other studies which investigate reactions of water radiolysis products such as solvated electrons and hydroxyl radical with DNA (Alizadeh et Sanche, 2012; Alizadeh *et al.*, 2015). A significant proportion to primary radiation energy transferred in the cells is absorbed in the cellular water since  $\sim 80\%$  of the mass of living cells is water. Also, because DNA is concentrated in the nucleus, the contribution of water radiolysis is less than the whole cell. In cellular environment, SE produced by a primary ionizing particles can effectively induced DNA damages through direct or indirect effects.

Several groups studied biomolecular films irradiated with different electron-beam current densities and fluencies and analyzed by various methods (Solomun et Skalický, 2008; Falk *et al.*, 1963; Orlando *et al.*, 2008). For instance in water-DNA situation which caused the formation of transient negative anion located on the phosphate group followed by decaying via autoionization, releasing a LEE, for instance  $<1$  eV and an electronically exciting site in the nearness of a base or sugar. These electrons can form a shape resonance

and causing the strand break while the electronically excited target can dissociate into reactive radicals, such as, O or OH. Also, these slow electrons can scatter inelastically and excite a particular resonance on a base on the different side of the strand. The sequence and joining these two channels can generate the DSB which requires the presence of water and is difficult to repair because of the proximity of damage sites (Ptasińska et Sanche, 2007).

Micheals et al. measured the direct effect and indirect effect contribution percentage values  $\sim 45\%$  and  $69\%$  respectively. Also, several other groups investigated the OH radical initiated the strand breaks in DNA, and they found that this situation can increase the direct effect contribution to  $50\%$ . LEEs have an essential role in the generation of the large amounts of longer-lived species such as free radicals, cations, and anions in a small volume even though they do not travel very far before thermalization. Those reactive species can react in the cell to create a wide variety of radiation- induced chemical reactions.



## 4 CONCLUSIONS AND PERSPECTIVES

For more than five decades a considerable number of experiments have been completed to explain the interaction of low energy electrons (LEEs, 0–30 eV) with simple molecules and small biomolecules, although, LEE interactions with large biomolecules have been investigated only during the last two decades. The production of a low energy electron initiated with interactions of high energy photons which produced a large number of secondary low energy electrons (LEE) with most probable energy around 10 eV. Lately, the mechanism of LEE, which introduces a large percentage of the total energy deposited by ionizing radiation, is highlighted due to the ability to cause damage on DNA components (bases, nucleosides, nucleotides), oligonucleotides, and, plasmid DNA. Several studies have been done during recent years to investigate the damage on DNA induced by a low energy electron with 10 eV energy range. This study, for the first time, experimentally focused on damage caused by below 2 eV LEEs using a novel modified electron gun irradiation system that was able to produce LEEs below ( $< 2$  eV). The obtained results showed that the low energy electron ( $< 2$  eV) could cause a single-strand break followed by the formation of stable anions and radical fragments within DNA through DEA processes. For this purpose, thin films of TpT dinucleotide, as a simple model of DNA, are deposited on tantalum substrates, surrounded by an  $N_2$  atmosphere, and irradiated with LEE with  $\sim 1.8$  eV. LC-MS/MS detected the damage caused by vLEE.

We found three significant pathways of damage for the reaction of vLEE with TpT: N-C glycosidic cleavage, phosphodiester bond cleavage, and conversion of thymine to 5,6-dihydrothymine (base damage). Cleavage of the glycosidic bond separating the base moiety and sugar-phosphate group lead to the base release (Thy). Cleavage of the phosphodiester bond leads to the release of four types of products, thymidine 3'-monophosphate, 2',5'-dideoxythymidine, thymidine 5'-monophosphate, and 2',3'-dideoxythymidine. Conversion of thymine to 5,6-dihydrothymine involves the addition of a hydrogen atom or solvated electron to the 5,6-thymine double bond which can lead to the formation of 5,6-DHT.

The above mechanisms of cleavage are supported in further studies of monomers to have a better knowledge of LEE mechanism. By our analysis of TpT fragments such as pT, Tp, and dThd, We showed that the addition of a phosphate group to monomers resulted in a considerable increase in C-O bond cleavage, while, it caused a marked decrease in the

release of non-modified thymine. As an example, the formation of C-O bond products in TpT dimer was higher compared to the yield of C-O bond breakage in monomers (pT, Tp, dThd) whereas the creation of both 5,6-dhT and Thy was lower for TpT compared to pT, Tp, and dThd (Table1, chapter 2). This suggests that these two processes are associated with each other, as the complexity of the molecule, decreases from TpT dimer to pT, Tp, dThd monomers, there are fewer available channels for an electron involved in reactions to induce damage and breaking bonds. It is worth mentioning that the electron transfer process is completely related to the molecular structure and it will change the damage distribution. These results can be explained by the electron capture by a base, formation of the transient negative ions (TNI) and then, due to the electronegativity of the phosphate group, it will transfer to this unit and cause the single-strand break via DEA.

In the future, a better understanding of DNA damage mechanism is essential in order to help with the improvement of new modalities for cancer therapy such as new drugs for different types of cancer and optimizing and developing various devices and techniques or clinical protocols for chemo-radiation therapy. One of the recent techniques, which is done in our lab, is using gold nanoparticles to enhance radiotherapy due to the ability to produce large amounts of LEEs when these particles are exposed to ionizing radiation. Hence, combining the gold nanoparticles in a chemotherapeutic agent can increase the effect of radiation therapy during the same period of time for cancer treatment.

It should be noted that there is no chemical evidence showing a contribution of LEE when cells are irradiated with ionizing radiation. Thus, a greater understanding of the chemical reactions and products permits to characterize the initial reactions. For example, 3',5'-dideoxyribose is not a product from the reaction of radicals from water radiolysis with DNA, and thus, one could use this molecule as a specific marker of LEE-mediated reactions. In contrast, we cannot estimate the contribution of LEE to other pathways of damage by measuring strand breaks because they are formed by reaction of DNA with LEEs as well as by reaction of DNA with radicals from water radiolysis.

## **5 ACKNOWLEDGMENT**

First and foremost, I would like to thank my supervisors Prof. Leon Sanche and Prof. Richard Wagner for giving me the opportunity to work in their research group. I am also grateful for their continuous support, patience and caring that provided me with an excellent atmosphere for doing my research.

I wish to express my sincere thanks to Mr. Pierre Cloutier who supported me in all the experimental procedure, methodology and technique. Special thanks to Dr. Andrew Bass, who was always willing to help and give his best advice. I also take this opportunity to express my thankfulness to all my colleagues in the lab who lent a hand in helping me through this project.

I appreciate the friendship and kindness of all the professors in the Department of Nuclear Medicine and Radiobiology.

I thank all the reviewers of this manuscript for their time and concern.

Last but not least, I would like to express my appreciation and gratefulness to my husband, Omid, for his unconditional support and consistent encouragement. I would like to thank every member of my family, whose love and guidance are with me in whatever I pursue.

## BIBLIOGRAPHY

- Abdoul-Carime, H., Cloutier, P., et Sanche, L. (2001) Low-energy (5–40 eV) electron-stimulated desorption of anions from physisorbed DNA bases. *Radiation research*, 155(4): 625–633.
- Abdoul-Carime, H., Gohlke, S., Fischbach, E., Scheike, J., et Illenberge, E. (2004) Thymine excision from DNA by subexcitation electrons. *Chemical Physics Letters*, 387(4): 267–270.
- Adhikary, A., Becker, D., et Sevilla, M. D. (2014) *Electron Spin Resonance of Radicals in Irradiated DNA*, pages 299–352. Springer International Publishing.
- Aflatooni, K., Gallup, G. A., et Burrow, P. D. (1998) Electron attachment energies of the DNA bases. *The Journal of Physical Chemistry A*, 102(31): 6205–6207.
- Alberts, B., Johnson, A., Lewis, J., Raff, M., Roberts, K., et Walter, P. (2002) *Cell junctions*. Garland Science.
- Alizadeh, E., Orlando, T. M., et Sanche, L. (2015) Biomolecular damage induced by ionizing radiation: the direct and indirect effects of low-energy electrons on DNA. *Annual review of physical chemistry*, 66: 379–398.
- Alizadeh, E., Ptasíńska, S., et Sanche, L. (2016) Transient anions in radiobiology and radiotherapy: From gaseous biomolecules to condensed organic and biomolecular solids. In *Radiation Effects in Materials*. InTech.
- Alizadeh, E. et Sanche, L. (2012) Precursors of solvated electrons in radiobiological physics and chemistry. *Chemical reviews*, 112(11): 5578–5602.
- Alizadeh, E., Sanz, A. G., Madugundu, G. S., García, G., Wagner, J. R., et Sanche, L. (2014) Thymidine decomposition induced by low-energy electrons and soft X rays under N<sub>2</sub> and O<sub>2</sub> atmospheres. *Radiation Research*, 181(6): 629–640.
- Antic, D., Parenteau, L., Lepage, M., et Sanche, L. (1999) Low-energy electron damage to condensed-phase deoxyribose analogues investigated by electron stimulated desorption of H- and electron energy loss spectroscopy. *The Journal of Physical Chemistry B*, 103(31): 6611–6619.
- Anusiewicz, I., Berdys, J., Sobczyk, M., Skurski, P., et Simons, J. (2004) Effects of base  $\pi$ -stacking on damage to DNA by low-energy electrons. *The Journal of Physical Chemistry A*, 108(51): 11381–11387.

- Arumainayagam, C. R., Lee, H.-L., Nelson, R. B., Haines, D. R., et Gunawardane, R. P. (2010) Low-energy electron-induced reactions in condensed matter. *Surface Science Reports*, 65(1): 1–44.
- Audat, S. A. S., Trzasko Love, C., Al-Oudat, B. A. S., et Bryant-Friedrich, A. C. (2012) Synthesis of c3' modified nucleosides for selective generation of the c3'-deoxy-3'-thymidinyl radical: A proposed intermediate in lee induced DNA damage. *The Journal of Organic Chemistry*, 77(8): 3829–3837.
- Bao, X., Wang, J., Gu, J., et Leszczynski, J. (2006) DNA strand breaks induced by near-zero-electronvolt electron attachment to pyrimidine nucleotides. *Proceedings of the National Academy of Sciences*, 103(15): 5658–5663.
- Barrios, R., Skurski, P., et Simons, J. (2002) Mechanism for damage to dna by low-energy electrons. *The Journal of Physical Chemistry B*, 106(33): 7991–7994.
- Bauer, N. C., Corbett, A. H., et Doetsch, P. W. (2015) The current state of eukaryotic dna base damage and repair. *Nucleic acids research*, 43(21): 10083–10101.
- Becker, D., Bryant-Friedrich, A., Trzasko, C., et Sevilla, M. D. (2003) Electron spin resonance study of DNA irradiated with an argon-ion beam: Evidence for formation of sugar phosphate backbone radicals. *Radiation Research*, 160(2): 174–185.
- Berdys, J., Anusiewicz, I., Skurski, P., et Simons, J. (2004) Damage to model dna fragments from very low-energy (< 1 ev) electrons. *Journal of the American Chemical Society*, 126(20): 6441–6447.
- Bhaskaran, R. et Sarma, M. (2014) Low energy electron induced cytosine base release in 2'-deoxycytidine-3'-monophosphate via glycosidic bond cleavage: A time-dependent wavepacket study. *The Journal of Chemical Physics*, 141(10): 104309.
- Bhaskaran, R. et Sarma, M. (2015a) Low-energy electron interaction with the phosphate group in DNA molecule and the characteristics of single-strand break pathways. *The Journal of Physical Chemistry A*, 119(40): 10130–10136.
- Bhaskaran, R. et Sarma, M. (2015b) The role of the shape resonance state in low energy electron induced single strand break in 2'-deoxycytidine-5'-monophosphate. *Phys. Chem. Chem. Phys.*, 17: 15250–15257.
- Boudaïffa, B., Hunting, D., Cloutier, P., Huels, M., et Sanche, L. (2000) Induction of single-and double-strand breaks in plasmid dna by 100–1500 ev electrons. *International journal of radiation biology*, 76(9): 1209–1221.
- Breton, S.-P., Michaud, M., Jäggle, C., Swiderek, P., et Sanche, L. (2004) Damage induced by low-energy electrons in solid films of tetrahydrofuran. *The Journal of chemical physics*, 121(22): 11240–11249.

- Brodeur, N., Cloutier, P., Bass, A., Bertrand, G., Hunting, D., Grandbois, M., et Sanche, L. (2018) Absolute cross section for DNA damage induced by low-energy (10 eV) electrons: Experimental refinements and sample characterization by AFM. *The Journal of chemical physics*, 149(16): 164904.
- Brun, e., Cloutier, P., Sicard-Roselli, C., Fromm, M., et Sanche, L. (2009) Damage induced to dna by low-energy (0-30 eV) electrons under vacuum and atmospheric conditions. *The journal of physical chemistry. B*, 113: 10008–13.
- Cadet, J. et Wagner, J. R. (2014) Oxidatively generated base damage to cellular DNA by hydroxyl radical and one-electron oxidants: similarities and differences. *Archives of biochemistry and biophysics*, 557: 47–54.
- Cannon, R. D. (2016) *Electron transfer reactions*. Butterworth-Heinemann.
- Caron, L. et Sanche, L. (2005) Diffraction in resonant electron scattering from helical macromolecules: Effects of the dna backbone. *Phys. Rev. A*, 72: 032726.
- Carsky, P. et Curik, R. (2011) *Low-energy electron scattering from molecules, biomolecules and surfaces*. CRC Press.
- Cauët, E., Bogatko, S., Liévin, J., De Proft, F., et Geerlings, P. (2013) Electron-attachment-induced DNA damage: Instantaneous strand breaks. *The Journal of Physical Chemistry B*, 117(33): 9669–9676.
- Chen, H.-Y., Yang, P.-Y., Chen, H.-F., Kao, C.-L., et Liao, L.-W. (2014) DFT reinvestigation of DNA strand breaks induced by electron attachment. *The Journal of Physical Chemistry B*, 118(38): 11137–11144.
- Choofong, S., Cloutier, P., Sanche, L., et Wagner, J. R. (2016) Base release and modification in solid-phase DNA exposed to low-energy electrons. *Radiation Research*, 186(5): 520–530.
- Dąbkowska, I., Rak, J., et Gutowski, M. (2005) DNA strand breaks induced by concerted interaction of H radicals and low-energy electrons. *The European Physical Journal D - Atomic, Molecular, Optical and Plasma Physics*, 35(2): 429–435.
- Dass, C. (2007) *Fundamentals of contemporary mass spectrometry*, volume 16. John Wiley & Sons.
- Dedon, P. C. (2008) The chemical toxicology of 2-deoxyribose oxidation in DNA. *Chemical Research in Toxicology*, 21(1): 206–219.
- Denifl, S., Ptasíńska, S., Probst, M., Hrušák, J., Scheier, P., et Märk, T. D. (2004) Electron attachment to the gas-phase DNA bases cytosine and thymine. *The Journal of Physical Chemistry A*, 108(31): 6562–6569.
- Falk, M., Hartman, K. A., et Lord, R. C. (1963) Hydration of deoxyribonucleic acid. ii. an infrared study. *Journal of the American Chemical Society*, 85(4): 387–391.

- Frohlinde, D. S. (1986) Comparison of mechanisms for dna strand break formation by the direct and indirect effect of radiation. In *Mechanisms of DNA damage and repair*, pages 19–27. Springer.
- Gross, J. H. (2006) *Mass spectrometry: a textbook*. Springer Science & Business Media.
- Gu, J., Leszczynski, J., et Schaefer, H. F. (2012) Interactions of electrons with bare and hydrated biomolecules: From nucleic acid bases to DNA segments. *Chemical Reviews*, 112(11): 5603–5640.
- Gu, J., Wang, J., et Leszczynski, J. (2010) Comprehensive analysis of dna strand breaks at the guanosine site induced by low-energy electron attachment. *ChemPhysChem*, 11(1): 175–181.
- Gu, J., Wang, J., et Leszczynski, J. (2011) Low energy electron attachment to the adenosine site of DNA. *The Journal of Physical Chemistry B*, 115(49): 14831–14837.
- Gu, J., Wang, J., Rak, J., et Leszczynski, J. (2007) Findings on the electron-attachment-induced abasic site in a DNA double helix. *Angewandte Chemie International Edition*, 46(19): 3479–3481.
- Gu, J., Xie, Y., et Schaefer, H. F. (2005) Glycosidic bond cleavage of pyrimidine nucleosides by low-energy electrons: A theoretical rationale. *Journal of the American Chemical Society*, 127(3): 1053–1057.
- Han, W. et Yu, K. (2010) Ionizing radiation, dna double strand break and mutation. *Advances in Genetics research*, 4: 197–210.
- Han, W. et Yu, K. N. (2009) Response of cells to ionizing radiation. *Adv Biomed Sci Eng*, pages 204–62.
- Huels, M. A., Boudaïffa, B., Cloutier, P., Hunting, D., et Sanche, L. (2003) Single, double, and multiple double strand breaks induced in dna by 3– 100 ev electrons. *Journal of the American Chemical Society*, 125(15): 4467–4477.
- Huels, M. A., Hahndorf, I., Illenberger, E., et Sanche, L. (1998) Resonant dissociation of dna bases by subionization electrons. *The Journal of chemical physics*, 108(4): 1309–1312.
- Huels, M. A., Parenteau, L., et Sanche, L. (2004) Reactive scattering of 1– 5 ev o-in films of tetrahydrofuran. *The Journal of Physical Chemistry B*, 108(41): 16303–16312.
- Hush, N. et Cheung, A. S. (1975) Ionization potentials and donor properties of nucleic acid bases and related compounds. *Chemical Physics Letters*, 34(1): 11–13.
- Jackson, S. P. et Bartek, J. (2009) The dna-damage response in human biology and disease. *Nature*, 461(7267): 1071.

- Keshishian, H., Addona, T., Burgess, M., Kuhn, E., et Carr, S. A. (2007) Quantitative, multiplexed assays for low abundance proteins in plasma by targeted mass spectrometry and stable isotope dilution. *Molecular & Cellular Proteomics*, 6(12): 2212–2229.
- Kohanoff, J., McAllister, M., Tribello, G. A., et Gu, B. (2017) Interactions between low energy electrons and DNA: a perspective from first-principles simulations. *Journal of Physics: Condensed Matter*, 29(38): 383001.
- Koslov, S. (1982) Radiophobia: The great american syndrome. *The Johns Hopkins Applied Physics Laboratory Technical Digest*, 2.
- Kočišek, J., Sedmidubská, B., Indrajith, S., Fárník, M., et Fedor, J. (2018) Electron attachment to microhydrated deoxycytidine monophosphate. *The Journal of Physical Chemistry B*, 122(20): 5212–5217.
- Kumar, A. et Sevilla, M. D. (2007) Low-energy electron attachment to 5'-thymidine monophosphate: Modeling single strand breaks through dissociative electron attachment. *The Journal of Physical Chemistry B*, 111(19): 5464–5474.
- Kumar, A. et Sevilla, M. D. (2008) The role of  $\pi\sigma^*$  excited states in electron-induced DNA strand break formation: A time-dependent density functional theory study. *Journal of the American Chemical Society*, 130(7): 2130–2131.
- Kumar, A. et Sevilla, M. D. (2009) Role of excited states in low-energy electron (LEE) induced strand breaks in DNA model systems: Influence of aqueous environment. *ChemPhysChem*, 10(9-10): 1426–1430.
- Kumar, A. et Sevilla, M. D. (2017) *Low-Energy Electron (LEE)-Induced DNA Damage: Theoretical Approaches to Modeling Experiment*, pages 1741–1802. Springer International Publishing, Cham.
- Lepage, M., Letarte, S., Michaud, M., Motte-Tollet, F., Hubin-Franskin, M.-J., Roy, D., et Sanche, L. (1998) Electron spectroscopy of resonance-enhanced vibrational excitations of gaseous and solid tetrahydrofuran. *The Journal of chemical physics*, 109(14): 5980–5986.
- Li, X., Sanche, L., et Sevilla, M. D. (2006) Base release in nucleosides induced by low-energy electrons: A DFT study. *Radiation Research*, 165(6): 721–729.
- Li, X., Sevilla, M. D., et Sanche, L. (2003) Density functional theory studies of electron interaction with DNA: Can zero eV electrons induce strand breaks? *Journal of the American Chemical Society*, 125(45): 13668–13669.
- Li, Z., Cloutier, P., Sanche, L., et Wagner, J. R. (2010) Low-energy electron-induced DNA damage: Effect of base sequence in oligonucleotide trimers. *Journal of the American Chemical Society*, 132(15): 5422–5427.
- Li, Z., Cloutier, P., Sanche, L., et Wagner, J. R. (2011) Low-energy electron-induced damage in a Trinucleotide containing 5-Bromouracil. *The Journal of Physical Chemistry B*, 115(46): 13668–13673.



- Li, Z., Zheng, Y., Cloutier, P., Sanche, L., et Wagner, J. R. (2008) Low energy electron induced DNA damage: Effects of terminal phosphate and base moieties on the distribution of damage. *Journal of the American Chemical Society*, 130(17): 5612–5613.
- Lindh, T. *et al.* (1993) Instability and decay of the primary structure of DNA. *nature*, 362(6422): 709–715.
- Liu, J., Yao, X., Cloutier, P., Zheng, Y., et Sanche, L. (2016) DNA strand breaks induced by 0–1.5 eV UV photoelectrons under atmospheric pressure. *The Journal of Physical Chemistry C*, 120(1): 487–495.
- Luo, X., Zheng, Y., et Sanche, L. (2014) DNA strand breaks and crosslinks induced by transient anions in the range 2–20 eV. *The Journal of Chemical Physics*, 140(15): 155101.
- Martin, F., Burrow, P. D., Cai, Z., Cloutier, P., Hunting, D., et Sanche, L. (2004) DNA strand breaks induced by 0–4 eV electrons: The role of shape resonances. *Phys. Rev. Lett.*, 93: 068101.
- Mehta, A. et Haber, J. E. (2014) Sources of DNA double-strand breaks and models of recombinational DNA repair. *Cold Spring Harbor perspectives in biology*, page a016428.
- Nabben, F. J., Karman, J. P., et Loman, H. (1982) Inactivation of biologically active DNA by hydrated electrons. *International Journal of Radiation Biology and Related Studies in Physics, Chemistry and Medicine*, 42(1): 23–30.
- O'Neill, P., Stevens, D. L., et Garman, E. (2002) Physical and chemical considerations of damage induced in protein crystals by synchrotron radiation: a radiation chemical perspective. *Journal of synchrotron radiation*, 9(6): 329–332.
- Orlando, T. M., Oh, D., Chen, Y., et Aleksandrov, A. B. (2008) Low-energy electron diffraction and induced damage in hydrated DNA. *The Journal of Chemical Physics*, 128(19): 195102.
- Orlov, V., Smirnov, A., et Varshavsky, Y. M. (1976) Ionization potentials and electron-donor ability of nucleic acid bases and their analogues. *Tetrahedron Letters*, 17(48): 4377–4378.
- Pan, X. et Sanche, L. (2005) Mechanism and site of attack for direct damage to DNA by low-energy electrons. *Phys. Rev. Lett.*, 94: 198104.
- Pan, X. et Sanche, L. (2006) Dissociative electron attachment to DNA basic constituents: The phosphate group. *Chemical Physics Letters*, 421(4): 404–408.
- Panajotovic, R., Martin, F., Cloutier, P., Hunting, D., et Sanche, L. (2006) Effective cross sections for production of single-strand breaks in plasmid DNA by 0.1 to 4.7 eV electrons. *Radiation research*, 165(4): 452–459.

- Park, Y., Li, Z., Cloutier, P., Sanche, L., et Wagner, J. R. (2011) DNA damage induced by low-energy electrons: Conversion of thymine to 5,6-dihydrothymine in the oligonucleotide trimer TpTpT. *Radiation Research*, 175(2): 240–246.
- Park, Y., Peoples, A. R., Madugundu, G. S., Sanche, L., et Wagner, J. R. (2013) Side-by-side comparison of DNA damage induced by low-energy electrons and high-energy photons with solid TpTpT trinucleotide. *The Journal of Physical Chemistry B*, 117(35): 10122–10131.
- Park, Y. S., Cho, H., Parenteau, L., Bass, A. D., et Sanche, L. (2006) Cross sections for electron trapping by dna and its component subunits i: Condensed tetrahydrofuran deposited on kr. *The Journal of chemical physics*, 125(7): 074714.
- Pimblott, S. M. et LaVerne, J. A. (2007) Production of low-energy electrons by ionizing radiation. *Radiation Physics and Chemistry*, 76(8-9): 1244–1247.
- Ptasińska, S., Denifl, S., Grill, V., Märk, T. D., Illenberger, E., et Scheier, P. (2005) Bond- and site-selective loss of  $h^-$  from pyrimidine bases. *Phys. Rev. Lett.*, 95: 093201.
- Ptasińska, S., Denifl, S., Grill, V., Märk, T. D., Scheier, P., Gohlke, S., Huels, M. A., et Illenberger, E. (2005) Bond-selective  $h^-$  ion abstraction from thymine. *Angewandte Chemie International Edition*, 44(11): 1647–1650.
- Ptasińska, S., Denifl, S., Scheier, P., et Märk, T. (2004) Inelastic electron interaction (attachment/ionization) with deoxyribose. *The Journal of chemical physics*, 120(18): 8505–8511.
- Ptasińska, S. et Sanche, L. (2006) On the mechanism of anion desorption from DNA induced by low energy electrons. *The Journal of Chemical Physics*, 125(14): 144713.
- Ptasińska, S. et Sanche, L. (2007) Dissociative electron attachment to abasic DNA. *Phys. Chem. Chem. Phys.*, 9: 1730–1735.
- Ptasińska, S. et Sanche, L. (2007) Dissociative electron attachment to hydrated single dna strands. *Phys. Rev. E*, 75: 031915.
- Rak, J., Kobylecka, M., et Storoniak, P. (2011) Single strand break in DNA coupled to the O—P bond cleavage. a computational study. *The Journal of Physical Chemistry B*, 115(8): 1911–1917.
- Raleigh, J. A., Whitehouse, R., et Kremers, W. (1974) Effect of oxygen and nitroaromatic cell radiosensitizers on radiation-induced phosphate release from 3'- and 5'-nucleotides: A model for nucleic acids. *Radiation Research*, 59(2): 453–465.
- Ray, S., Daube, S., et Naaman, R. (2005) On the capturing of low-energy electrons by dna. *Proceedings of the National Academy of Sciences*, 102(1): 15–19.
- Reed, A. B. (2011) The history of radiation use in medicine.

- Sanche, L. (2003) Low-energy electron damage to dna and its basic constituents. *Physica Scripta*, 68(5): C108.
- Sanche, L. (2009) *Low-energy electron interaction with DNA: Bond dissociation and formation of transient anions, radicals, and radical anions*. John Wiley & Sons Inc.
- Schürmann, R., Tsering, T., Tanzer, K., Denifl, S., Kumar, S. V. K., et Bald, I. (2017) Resonant formation of strand breaks in sensitized oligonucleotides induced by low-energy electrons (0.5–9 eV). *Angewandte Chemie International Edition*, 56(36): 10952–10955.
- Sevilla, M. D., Becker, D., Kumar, A., et Adhikary, A. (2016) Gamma and ion-beam irradiation of DNA: Free radical mechanisms, electron effects, and radiation chemical track structure. *Radiation Physics and Chemistry*, 128: 60–74.
- Shaik, R., Ellis, M. W., Starr, M. J., Amato, N. J., et Bryant-Friedrich, A. C. (2015) Photochemical generation of a c5'-uridiny radical. *ChemBioChem*, 16(16): 2379–2384.
- Shaw, A. et Cadet, J. (1988) Formation of cyclopyrimidines via the direct effects of gamma radiation of pyrimidine nucleosides. *International Journal of Radiation Biology*, 54(6): 987–997.
- Shaw, A. A., Voituriez, L., Cadet, J., Gregoli, S., et Symons, M. C. R. (1988) Identification of the products resulting from the direct effects of  $\gamma$ -radiation on thymidine. *J. Chem. Soc., Perkin Trans. 2*, pages 1303–1307.
- Simons, J. (2006) How do low-energy (0.1–2 eV) electrons cause DNA-strand breaks? *Accounts of Chemical Research*, 39(10): 772–779.
- Simons, J. (2007) How very low-energy (0.1–2 eV) electrons cause dna strand breaks. *Advances in Quantum Chemistry*, 52: 171–188.
- Smyth, M. et Kohanoff, J. (2012) Excess electron interactions with solvated DNA nucleotides: Strand breaks possible at room temperature. *Journal of the American Chemical Society*, 134(22): 9122–9125.
- Solomun, T., Seitz, H., et Sturm, H. (2009) DNA damage by low-energy electron impact: Dependence on guanine content. *The Journal of Physical Chemistry B*, 113(34): 11557–11559.
- Solomun, T. et Skalický, T. (2008) The interaction of a protein–dna surface complex with low-energy electrons. *Chemical Physics Letters*, 453(1): 101–104.
- Sonntag, C. (2006) *Free-radical-induced DNA damage and its repair: a chemical perspective*. Springer Science & Business Media.
- Swiderek, P. (2006) Fundamental processes in radiation damage of dna. *Angewandte Chemie International Edition*, 45(25): 4056–4059.

- Tretyakova, N., Villalta, P. W., et Kotapati, S. (2013) Mass spectrometry of structurally modified dna. *Chemical reviews*, 113(4): 2395–2436.
- Turner, J. E. (2008) *Atoms, radiation, and radiation protection*. John Wiley & Sons.
- Wang, J., Leszczynski, J., et Gu, J. (2010) Electron attachment-induced DNA single-strand breaks at the pyrimidine sites. *Nucleic Acids Research*, 38(16): 5280–5290.
- Zheng, Y., Cloutier, P., Hunting, D. J., Sanche, L., et Wagner, J. R. (2005) Chemical basis of DNA sugar-phosphate cleavage by low-energy electrons. *Journal of the American Chemical Society*, 127(47): 16592–16598.
- Zheng, Y., Cloutier, P., Hunting, D. J., Wagner, J. R., et Sanche, L. (2004a) Glycosidic bond cleavage of thymidine by low-energy electrons. *Journal of the American Chemical Society*, 126(4): 1002–1003.
- Zheng, Y., Cloutier, P., Hunting, D. J., Wagner, J. R., et Sanche, L. (2006a) Phosphodiester and N-glycosidic bond cleavage in DNA induced by 4–15 ev electrons. *The Journal of Chemical Physics*, 124(6): 064710.
- Zheng, Y., Cloutier, P., Wagner, J. R., et Sanche, L. (2004b) Irradiator to study damage induced to large nonvolatile molecules by low-energy electrons. *Review of Scientific Instruments*, 75(11): 4534–4540.
- Zheng, Y., Wagner, J. R., et Sanche, L. (2006b) DNA damage induced by low-energy electrons: Electron transfer and diffraction. *Phys. Rev. Lett.*, 96: 208101.